

(NASA-CR-140050) ANALYSIS OF DATA FROM
SPACECRAFT (STRATOSPHERIC HARMINGS) Final
Report, Sep. 1973 - Apr. 1974 (Lockheed
Missiles and Space Co.) 197 p HC \$13.00

N74-32779

CSCS 04A G3/13

Unclas
16945

Lockheed

MISSILES & SPACE COMPANY

A GROUP DIVISION OF LOCKHEED AIRCRAFT CORPORATION

SUNNYVALE, CALIFORNIA

LMSC/D420934
GCS/3548/6211
74 Apr 24

FINAL REPORT

**ANALYSIS OF DATA FROM SPACECRAFT
(STRATOSPHERIC WARMINGS)**

NASA CONTRACT NASW-2553

NASA HEADQUARTERS, WASH. D.C.

**CONTRACT MONITOR: H. D. CALAHAN
NASA HEADQUARTERS (CODE SG)
WASHINGTON, D.C. 20546**

**PROJECT LEADER: R. WEISS
LOCKHEED MISSILES & SPACE CO., INC.
SUNNYVALE, CALIF. 94088**

**PRINCIPAL CONTRIBUTOR: A. D. ANDERSON
ATMOSPHERIC PHYSICS BRANCH
RADIATION PHYSICS LABORATORY**

FOREWORD

This report was prepared by Lockheed Missiles and Space Company under NASA Contract NASW-2553. The period of performance of the research reported was September 1973 through April 1974. Technical direction for this contract originated from The Director, Physics and Astronomy (Code SG), NASA Headquarters, H. D. Calahan, Contract Monitor.

The contract was managed by Robert Weiss, Guidance and Control Systems organization of the LMSC Space Systems Division. Chief investigator and principal contributor to the report was A. D. Anderson, Atmospheric Physics Branch, Radiation Physics Laboratory, of the LMSC Research/Development Division.

This Final Report, LMSC Report D420934 (Guidance and Control Systems report GCS/3548/6211) documents and summarizes the results of the entire contract work, including conclusions and recommendations based upon the results obtained. It incorporates the material presented in the two Quarterly Progress Reports previously submitted:

QPR No. 1 LMSC/D384420, GCS/3475/6211, 73 Dec 12

QPR No. 2 LMSC/D387326, GCS/3529/6211, 74 Mar 12

This final report is divided into three parts. Part I, Definition of the Problem, contains a detailed description of the problem and of the Solar and Geophysical Indices used in the investigation. Part II, Analysis, presents an analysis of five stratospheric warming cases. Part III presents an hypothesis concerning the relationship between auroral electrojets and stratospheric warmings.

The authors wish to thank Drs. John Evans and Robert Varney of the LMSC Atmospheric Physics Branch for their helpful suggestions and guidance during the study.

SUMMARY

The primary objectives of the study are to establish the details of the stratospheric warming processes as to time, area, and intensity and to try to correlate the warmings with other terrestrial and solar phenomena occurring at satellite platform altitudes or observable from satellite platforms. The main purpose of the study is to find if there are links between the perturbed upper atmosphere (mesosphere and thermosphere) and the stratosphere that could explain stratospheric warmings.

Stratospheric warmings are large-area phenomena containing great amounts of energy. They probably have major influence on the weather over large areas, on observations from satellites and high-altitude platforms, on the dynamics of the upper and lower atmospheres, on atmospheric chemistry, on air pollution observations and on backgrounds for surveillance and earth resources observations. Little correlative data has been brought to bear on defining the relationship between energetic events above 50 km and the warmings at about 40 km. Current rocket and balloon-borne IR sounding instruments do not provide good coverage on a global basis. It is difficult to provide dynamic readings throughout a warming by means of ground based instrumentation. Satellite and other high altitude data, therefore, need to be applied to the problem.

Although meteorological analyses indicate that the warmings result from the transfer of energy from the troposphere to the stratosphere, the

initiating or trigger mechanism is unknown. In other words, no one has attempted to predict stratospheric warmings. The emphasis of this effort is to attempt to find clues to possible trigger mechanisms arising in the upper atmosphere or solar activity. Several steps are involved: (a) Determine from the literature possible correlations of warmings with geophysical events; (b) Find solar and geophysical indices that represent the pertinent events; (c) Define the stratospheric warming events (start, maximum, end) so that these indices may be applied to uncover the trigger mechanism(s).

Existing data and literature have been searched to find the identified cases of stratospheric warmings. Case histories of these events have been chosen by assembling correlative high altitude satellite, rocket and ground based measurements, geophysical characteristics and solar activity data. Existing data from NIMBUS spacecraft sensors such as the MRIR, SIRS, IRIS, and SCR were used to define the existence and characteristics of the warming in the 20-50 km-altitude regime. Data from various particle and radiation experiments on satellites were used to determine some of the energetic conditions existing in the upper atmosphere prior to and during the warming events.

The study of six different stratospheric warmings has indicated that the magnetic indices A_p , AE and D_{st} exhibit a marked increase 1 to 3 days preceding the onset of a warming at 10_{mb} (30 km), and a marked decrease on the day of onset and 4 days preceding. It is proposed that electrojet heating forms a "critical level" in the upper mesosphere, and that planetary waves propagating up from the troposphere interact with the critical level, releasing heat at that level. Waves reflected by the critical level release heat in the stratosphere by interference with upward-propagating waves seen as a warming.

The study is divided into three parts. In Part I, stratospheric warmings are described, the correlation problem is defined, and the various geophysical indices selected for the analysis are discussed. In addition, a bibliography on stratospheric warmings is included. In Part II, case histories for recent stratospheric warmings are given. The day-to-day detailed analyses of the warmings and geophysical indices are described. Conclusions are presented concerning the correlation between the geophysical indices and the onset of stratospheric warmings. Part III presents a brief hypothesis concerning the relationship between auroral electrojets and stratospheric warmings.

TABLE OF CONTENTS

PART I

	<u>Page</u>
SUMMARY	i
1. STRATOSPHERIC WARMINGS	1
2. THE PROBLEM OF DEFINING A GIVEN STRATOSPHERIC WARMING EVENT	5
3. POSSIBLE CORRELATION OF WARMINGS WITH GEOPHYSICAL EVENTS	7
4. SOLAR AND GEOPHYSICAL INDICES	14
Solar Flares	16
Daily Flare Index	19
Magnetic Condition	21
Sudden Ionospheric Disturbance (SID)	26
2800 MHz (10.7 cm) Solar Flux	32
He II Solar Flux	35
Solar Protons (Greater than 10 Mev)	36
The Magnetic Index A_p	40
The AE Index	42
The D_{st} Index	45
Solar X-Rays (1-8A)	46
5. SOLAR-TERRESTRIAL LINKS AND STRATOSPHERIC WARMINGS	49
Figures	54
References Cited in Part I	59
Literature Search - Stratospheric Warmings	61

TABLE OF CONTENTS

PART II

	<u>Page</u>
1. WARMING CASE STUDIES	
The Stratospheric Warming of April - May 1969	II-1
The Stratospheric Warmings of July - August 1969	II-2
Correlation of Geophysical Indices With SIRS A, Channel 8 Radiances, July - August 1969	II-4
The Stratospheric Warming of December 1969 - January 1970	II-6
Correlation of Geophysical Indices With 10-MB Temperature Increases, December 1969	II-13
The Stratospheric Warming of December 1970 - January 1971	II-16
Correlation of Geophysical Indices, December 1970 - January 1971	II-23
2. CORRELATIONS BETWEEN GEOPHYSICAL INDICES AND STRATOSPHERIC WARMINGS	II-30
The AE Index	II-30
Solar X-rays	II-32
Solar Flares	II-32
The A _p Index	II-33
The D _{st} Index	II-34
The He II Index	II-34
Solar Protons	II-35
The SID Index	II-36
Magnetic Condition	II-36
Summary	II-37
3. DISCUSSION AND CONCLUSIONS	II-40
4. TABLES	II-43
5. REFERENCES CITED IN PART II	II-79
6. FIGURES	II-82

TABLE OF CONTENTS

PART III

THE AURORAL ELECTROJETS	III-1
WINTER CIRCUMPOLAR VORTEX	III-2
PLANETARY WAVES AND THE CRITICAL LEVEL	III-2
AN HYPOTHESIS FOR THERMOSPHERIC-STRATOSPHERIC INTERACTION (WARMINGS)	III-3
IMPLICATIONS FOR OTHER ATMOSPHERIC PHENOMENA	III-7
REFERENCES TO PART III	III-8
FIGURES	III-11

PART I

ANALYSIS OF DATA FROM SPACECRAFT - STRATOSPHERIC WARMINGS

DEFINITION OF THE PROBLEM

TABLE OF CONTENTS

PART I

	<u>Page</u>
SUMMARY	i
1. STRATOSPHERIC WARMINGS	1
2. THE PROBLEM OF DEFINING A GIVEN STRATOSPHERIC WARMING EVENT	5
3. POSSIBLE CORRELATION OF WARMINGS WITH GEOPHYSICAL EVENTS	7
4. SOLAR AND GEOPHYSICAL INDICES	14
Solar Flares	16
Daily Flare Index	19
Magnetic Condition	21
Sudden Ionospheric Disturbance (SID)	26
2800 MHz (10.7 cm) Solar Flux	32
He II Solar Flux	35
Solar Protons (Greater than 10 Mev)	36
The Magnetic Index A_p	40
The AE Index	42
The D_{st} Index	45
Solar X-Rays (1-8A)	46
5. SOLAR-TERRESTRIAL LINKS AND STRATOSPHERIC WARMINGS	49
Figures	54
References Cited in Part I	59
Literature Search - Stratospheric Warmings	61

1. STRATOSPHERIC WARMINGS

A dynamic event in the stratospheric circulation which is principally characterized by a temperature increase in higher latitudes immediately above the stratopause level greater than 50°C over a period of ten days or less, accompanied by a disruption of the usual westerly zonal circumpolar flow of the stratospheric winter circulation, is called a Stratospheric Warming.

Stations centered under the warming region as it sweeps poleward provide a very dramatic record of the magnitude of events which must be in progress in the upper atmosphere. Temperature increases of from 300° to 900° over a period of a week are the rule, and stratospheric wind changes of the order of 100 meters/sec out of the west to 50 meters/sec from the east are common (Webb, 1966).

Figure 1 contains a sequence of rocket soundings from West Germinish, Germany, taken during a major warming in the winter of 1967-68 (Labitzke, 1971). Profile 1 indicates the beginning phase of the warming with the maximum warming at 60 km ($+11^{\circ}\text{C}$). In Profile 2, the maximum warming has descended to 46 km and increased to $+18^{\circ}\text{C}$. Profile 3 (21 Dec. 1967) the maximum warming is at 43 km and the temperature is $+40^{\circ}\text{C}$. Profile 4 represents a decreasing phase; the maximum warming at 44 km has decreased to -4°C . Profile 5 is an average atmospheric temperature profile from Groves (1970). Comparison of Profile 5 with the other profiles indicates that the warming affected a depth of atmosphere of approximately 34 km.

Stratospheric warmings are large-area phenomena containing large amounts of energy. They probably have major influence on the weather over large areas, on observations from satellites and high-altitude platforms, on the dynamics of the upper and lower atmospheres, on atmospheric chemistry, on air pollution observations and on backgrounds for surveillance and earth resources observations.

Little correlative data has been brought to bear on defining the relationship between energetic events above 50 km and the warmings at about 40 km. Current rocket and balloon-borne IR sounding instruments do not provide good coverage on a global basis. It is difficult to provide dynamic readings throughout a warming by means of ground based instrumentation. Satellite and other high attitude data, therefore, need to be applied to the problem.

Although stratospheric warmings have been studied extensively since their recognition in 1952, their characteristics are not well known or established. They occur mostly in winter and early spring seasons and show largest temperature changes in the northern and southern high-latitude regions. They start at 50 km or above and later sometimes appear at lower levels, penetrating to 25-35 km. The energy density of direct solar radiation on an element of atmosphere is smaller by many orders of magnitude than that required to explain the atmospheric temperature rise during a warming. Integration of this energy over time and area would be required to explain a warming in terms of direct heating. The heat input into a

square cm column of the stratosphere between 30 and 50 km altitude needed to raise the temperature 50°K amounts to some $5 \times 10^9 \text{ ergs cm}^{-2}$. Reported warmings may cover 10^{15} cm^2 so the total energy involved can be in excess of 10^{24} ergs. This energy might be compared with 5×10^{23} ergs reported in the solar storm of 11 February 1958 in the red arc aurora, and a computed total solar particle energy of 10^{25} ergs in such a storm. Muench (1965) considered the energy transformations during the stratospheric warming of 22-24 January 1958. His analysis indicated that the energy increase was caused almost entirely by a transfer of energy from the troposphere to the stratosphere. A report by Hirota (1967) on an observed upward propagation of stratospheric warming events supports this conclusion. Matsuno (1971) treated the interaction of vertically propagating planetary waves from the troposphere with the zonal flow in the stratosphere. His model produces many observed features present in stratospheric warmings. Trenberth (1972) used a model of this type to study stratospheric warmings. His model reproduced realistic stratospheric warmings in late winter. Although Trenberth neglected the chemistry, Clark (1970) had previously used a similar model (with somewhat fewer spherical harmonics and coarser vertical resolution) which did include the simple Chapman scheme of oxygen photochemistry. Clark was able to reproduce numerically the observed tendency for the large-scale motion field to shift the maximum of vertically integrated ozone poleward from the low-altitude source region. In such a model, the chemistry interacts with the dynamics via the heating rate Q , which will depend not only on infrared radiation and a parameterization of small-scale convection in the troposphere, but also the absorption of radiation by the variable amount of ozone.

A survey of recorded major and minor stratospheric warmings shows that in January of every year between 1966 and 1971 at least one event occurred in the Northern Hemisphere between 45° and 80° latitude. These same years produced events in the Southern Hemisphere in July and August.

2. THE PROBLEM OF DEFINING A GIVEN STRATOSPHERIC WARMING EVENT

A given stratospheric warming (SW) can be defined provided that the date and time of its start, maximum and end can be determined from the temperature at all altitudes that it affects. One major problem with characterization of SWs occurring in the past is that they occur at altitudes between about 20-65 km (Fig. 1). Until recently, the higher altitudes were only accessible to measurement with meteorological rockets. There are several disadvantages for defining warmings with rocket data. Although there are currently more than 20 meteorological rocket launch sites, these are mainly land-based in the Northern Hemisphere. Hence, the coverage is uneven. Also, the launches are made closer to a weekly than daily basis. However, even if daily launchings were made, this would be insufficient to characterize warmings, inasmuch as the warming centers probably would not lie over the rocket launch sites. In addition, the warming centers move.

The coverage and launch frequency of radiosondes carried by balloons is much better. There are at least 20 times as many radiosonde launch sites than rocket sites. The coverage is best in the Northern Hemisphere over land; the coverage is much poorer in the Southern Hemisphere because of the greater amount of water area. Also, the launch frequency (one to four times daily) is much greater than rockets. The main disadvantage is that only the lower altitudes at which SWs occur ~~are~~ accessible to the balloons (ceiling altitude about 30 km). The 10-mb surface (31 km) is the highest pressure altitude for which hemispheric charts, derived mainly from radiosonde data, are available from the National Weather Service on a daily

basis for the Northern Hemisphere warmings occurring during December 1969 - January 1970, December 1970 - January 1971, and January 1973 - February 1973.

The real hope for the future lies in satellite remote sensing techniques that scan worldwide twice daily. One example is the NIMBUS SIRS instrument data from which temperature profiles can be derived for the altitudes of interest on a worldwide basis. At present, there are some problems in obtaining data at the higher altitudes above 50 km. Therefore, at this time, the analysis of a given SW must be based on radiosonde, rocket-sonde, and satellite (radiance) data. The smallest time interval that can be used in characterization is about one day. It is not possible to specify warming start, maximum, or end at a given altitude in a time interval less than about one day. The definition must be incomplete for the warmings considered in this report because little data is available at the higher altitudes above 40-50 km. The radiance measurements made by the SCR on Nimbus 4 provide radiation information from the highest levels in the atmosphere so far obtained. Descriptions of the instrument can be found in the literature (Houghton and Smith, 1970) and the method used by the Oxford University Group to derive temperature profiles from the six radiances using a maximum probability technique has been described by Rodgers (1970). A series of daily charts for levels up to 1 mb (48 km) were constructed to cover the major northern hemisphere warming period in the middle of February 1972.

3. POSSIBLE CORRELATION OF WARMINGS WITH GEOPHYSICAL EVENTS

Stratospheric warmings favor the winter and early spring seasons; they exhibit the greatest change of temperature in the polar regions. They start at 50 km or above and later sometimes appear at lower levels. In some cases, the warmings do not penetrate downward as far as 30 km. These very high level relatively limited stratospheric warmings may represent the effects of comparatively limited penetration of the atmosphere by solar corpuscular emanations of only light to moderate intensity, which should be expected to occur not infrequently.

The major warmings of February 1952 and January 1963, which came well after the years of highest sunspot activity, both followed sudden bursts of strong geomagnetic disturbance with a moderate increase of sunspots, and in 1952 with a strong auroral display. The geomagnetically quiet years of 1953-1955 and 1964-1966 were apparently strikingly lacking in stratospheric warmings. The fact that of the sixteen years, 1951 to 1966 inclusive, the only six years lacking stratospheric warmings were also the six geomagnetically most quiet years would seem significant. With the exception of one weak warming at the beginning of March 1956, all 14 warmings, plus the two occurring in February 1952, originated during the months of January and February, when Northern Hemispheric auroral activity is very high, rising to a presumed early March peak frequency which may be even earlier in arctic latitudes. It is to be noted that none of them occurred during December, the month of the presumed winter solstice minimum of auroral frequency, and definitely the coldest month in the arctic stratosphere. During the period 1951-1966, all of the observed sudden

stratospheric warmings developed on the northern geomagnetic pole side of the geographic pole, i.e., essentially in the equatorward dip or trough of the zone of maximum auroral frequency.

The correlation of the time and space distribution of auroral activity with sudden changes of stratospheric temperature indicate a possible extraterrestrial control, perhaps solar corpuscular invasions of the upper atmosphere which produce auroras and strong geomagnetic disturbances. If solar corpuscular invasions are to cause and control the entire syndrome of associated auroral, and thermal phenomena, then they should possess the following properties and characteristics:

- 1) The energy contained in one of the strongest corpuscular invasions must be adequate, at whatever level of efficiency its conversion into thermal energy takes place, effectively to trigger the change of the temperature of the entire polar stratosphere in a relatively short time and in the virtual absence of sunlight from normal midwinter to normal midsummer conditions, such as occurred in the massive stratospheric warmings of January 1963. Less intense solar events (corpuscular invasions) will be restricted in their significant thermal effects to above the 50 km level.

- 2) There must exist some fairly effective means of downward transmission in the upper atmosphere of the direct thermal and magnetostrophic wind effects of strong solar corpuscular penetration of the higher atmosphere to at least the 50-km level.

3) Strong solar corpuscular penetration of the upper atmosphere should be favored, either as to frequency of occurrence or level of lowest penetration in the atmosphere, or both, on the geomagnetic pole side of the hemisphere in the general region where the zone of maximum auroral frequency extends to its lowest geographical latitude.

4) The initial burst phase of a massive warming of the middle or upper stratosphere should be roughly comparable in areal extent to that of a major auroral display (strong solar corpuscular penetration of the upper atmosphere).

Basically, it is the first two of the required characteristics of solar corpuscular invasions as noted above that are essential to their operation as a trigger of sudden massive stratospheric warmings. They must bring a large part of the necessary energy with them, and this energy must be transmitted effectively downward from the level of its direct absorption in the higher atmosphere (~ 70 - 100 km) to the middle or lower stratosphere.

The forms of corpuscular radiation which merit attention for present purposes are:

1) Electrons, in the energy range 1 - 100 keV, (and also in the range up to 1000 keV) which precipitate over the auroral zone.

2) protons, in the energy range 1 - 1000 MeV, originating in solar flares, and precipitating over the geomagnetic polar cap. Included in this latter group may be a proportion of α -particles, and possibly heavier elements.

Protons in the energy range 1-100 keV normally do not penetrate below 100 km, and hence are not considered as main phenomenon. All these phenomena tend to occur within the higher geomagnetic latitudes bounded by about magnetic latitude 45° , and mainly around $65-70^{\circ}$, but during major disturbances of the earth's magnetic field, extending a few degrees nearer the equator.

The depth of penetration of electrons into the atmosphere can be evaluated from known characteristics of energy loss, and by adoption of a model atmosphere. For example, a 10 keV electron may penetrate to a minimum altitude of 98 km, while a 400 keV electron will reach 64 km. There remains the question as to the fraction of total energy which is available for heating the atmosphere. Chamberlain has estimated a fraction of about 15% as appearing as heat. Dalgarno estimates the fraction as about 20%, but does not exclude a value of 50%. The heat input from electrons in auroral latitudes and at altitudes of 90-120 km is thus of the order of $1 \text{ erg cm}^{-2} \text{ sec}^{-1}$ for solar maximum and for zonal and long term average flux. After major solar flares, the corresponding zonal average is probably at least one order of magnitude greater for periods of a few days.

In contrast to the zonal character of auroral electron precipitation, the incidence of solar protons is distributed over the polar caps. Incoming protons are assumed to move in Störmer trajectories, and the magnetic rigidity necessary to permit entry at a given angle to the vertical and at a given latitude may be calculated provided the spatial character of the earth's field is known. As a rough guide, the precipitation of solar

protons may be considered as bounded by the auroral zones, but in major events, marked effects occur as low as 50° geomagnetic latitude.

The lowest observed ionization from solar protons has been found at 42 km in the southern polar region during winter darkness. Loss of energy from an incident proton is continuous along the trajectory, but is essentially concentrated over the last few kilometers of path. Reid has calculated that a 50 MeV proton will lose 90% of its energy between altitudes of 50 and 42 km, 50% between 44.5 and 42 km, and 10% between 42.1 and 42.0 km. Hence, in a particular solar proton event, the increment of energy released in a given altitude range depends upon the spectrum of the flux and the geomagnetic latitude. An upper boundary of about 100 km is typical for most events, with release of energy down to a probable lower limit of 30 km in the largest events.

The main effects of particle precipitation are those which have been used extensively to determine the morphology of the precipitation zones, viz., optical excitation and electron-ion pair production. The effects of interest are the heating produced directly by the particle flux, and the possibilities of indirect effects. Among the latter may be included the modification of minor constituent concentrations, and the initiation of atmospheric wave motion. The conversion of the kinetic energy of incident particles into heat has been discussed by Bates and Chamberlain and the values of conversion efficiency used are between 0.15 and 0.5.

The major temperature increases are naturally associated with the largest fluxes of electrons in aurorae. Electrons in the energy range of 1-10 keV affect the altitude range 150-100 km, and here the increases in temperature during more intense fluxes occur at rates up to 100K min^{-1} . In general, due to the many factors which enter into a quantitative discussion of temperatures of the higher atmosphere, and also due to the difficulties of observation of this matter, the effects on the mesosphere of particle heating are not well known.

The possibility that particle influx might produce changes in concentrations of minor atmospheric constituents, and that the return to equilibrium of these concentrations might be on a longer time scale than the duration of intense fluxes, has been considered by a few workers. The dissociation of molecular oxygen by auroral electron and proton impact has been investigated by Maeda in relation to the warming of the polar mesosphere. He found electrons with a differential spectral distribution of the form E^{-4} , or a little over $10^{-8}\text{ cm}^{-2}\text{ sec}^{-1}$ at 80-85 km altitude. Protons, distributed according to a differential spectrum of $E^{-2.8}$, gave similar results, though larger values than electrons below 80 km. This rate coefficient is nearly the same as that due to ultraviolet dissociation of O_2 in the Schumann-Runge continuum (1400-1750Å), and the height of maximum dissociation is nearly the same, viz., 90 km. Thus, the process of dissociation by particles may be significant during large fluxes, especially in polar winter darkness.

The generation of traveling atmospheric waves is one consequence of particle precipitation, presumably due to a combination of spatial and temporal changes, including pulsations, in the incident flux, with corresponding changes in local heating. King refers to the evidence for these waves, which in some modes of propagation proceed from the auroral zones towards mid-latitudes with velocities ranging between 400 and 700 m sec⁻¹. Other workers have considered the heating aspect of these waves. Thus, these disturbances, though clearly associated with the auroral zone initially, may be included in the general subject of atmospheric wave motion, and the heating induced thereby. Especially important is the Joule heating associated with the auroral electrojets discussed later.

4. SOLAR AND GEOPHYSICAL INDICES

There is a wealth of operational data on solar and geophysical indices. The main problem is determining which data are pertinent for correlation analysis involving the upper atmosphere and the warmings. In view of the fact that no direct correlations have been found between stratwarmings and the upper atmosphere phenomena represented by the indices, the selection of the indices to be used must be made on the basis of a possible connection and not a probable one. In other words, we are dealing with a strictly exploratory situation inasmuch as no connection may exist between stratwarmings and higher atmosphere phenomena. Although meteorological research to date indicates that stratospheric warmings are caused by a transfer of energy from the troposphere to the stratosphere (Matsuno, 1971), nevertheless the possibility has not been completely ruled out that such events are triggered or enhanced by certain conditions occurring in the upper atmosphere above 80 km.

The solar and geophysical indices used are listed in Table 1; in-house values are indicated by a X mark for the months containing warmings. These particular indices were selected on a preliminary basis because they all appear to be correlated with upper-atmospheric heating phenomena. All of the indices except the HeII flux and D_{st} are available from the Environmental Data Service, NOAA, National Geophysical and Solar-Terrestrial Data Center, Boulder, Colo., in the monthly publication "Solar-Geophysical Data." Each index in Table I will now be discussed in turn.

TABLE 1

INDICES USED FOR STRATWARM ANALYSIS

INDEX	Apr '69	May '69	June '69	July '69	Aug '69	Dec '69	Jan '70	Dec '70	Jan '71	Jan '73	Feb '73
Solar Flares	X	X	X	X	X	X	X	X	X	X	X
Daily Flare Index						X	X	X	X	X	X
S.I.D.	X	X	X	X	X	X	X	X	X	X	X
Magnetic Condition	X	X	X	X	X	X	X	X	X	X	X
2800 MHz Solar Flux	X	X	X	X	X	X	X	X	X	X	X
HeII Solar Flux	X	X	X	X	X						
A _p	X	X	X	X	X	X	X	X	X	X	X
D _{st}	X	X	X	X	X	X	X	X	X		
AE	X	X	X	X	X	X	X	X			
Solar X-Rays (1-8A)	X	X	X	X	X	X	X	X	X	X	X
Solar Protons(>10MeV)	X	X	X	X	X	X	X	X	X		

Solar Flares

The power emitted by the sun is $\sim 4 \times 10^{33}$ ergs sec⁻¹, of which $\sim 5 \times 10^{24}$ ergs sec⁻¹, or 5 million horsepower per sq mile, irradiates the atmosphere of the earth. Ionizing x-rays and ultraviolet radiation, which constitute only $\sim 10^{-3}$ percent of the solar flux ($\sim 5 \times 10^{19}$ ergs sec⁻¹) are absorbed in the outer atmosphere to produce the ionosphere. A considerably greater amount of energy, $\sim 10^{20}$ ergs sec⁻¹, arrives at the magnetosphere in the form of solar-wind plasma, even under solar-quiet conditions. When the sun is intensely active, the energy delivered in ionizing radiations, both electromagnetic and corpuscular, can increase by orders of magnitude. No comparable energy supplies are available elsewhere in the sun-earth system.

A great flare on the sun can release $\sim 10^{32}$ ergs in x-ray ultraviolet and energetic-particle radiation. Every link in the system from sun to earth reacts to such a catastrophic event. After interacting with the interplanetary medium, the magnetosphere, and the upper atmosphere, the last residue of energy from the sun's explosive gift to earth is a faint red airglow that suffuses all the sky from north pole to south pole. Although the glow is composed only of the single, characteristic emission line of oxygen at 6300A, following a great flare the full sky may radiate 10^{23} ergs of this monochromatic energy.

A flare is a short-lived sudden increase in the intensity of radiation emitted in the neighborhood of sunspots. It is best seen in H α , and usually occurs in the chromosphere. Flares are characterized by a

rise time of the order of minutes and a decay time of the order of tens of minutes. The total energy expended in a typical flare is about 10^{30} ergs; the magnetic field is extraordinarily high, reaching values of 10^2 to 10^4 gauss. Optical flares are usually accompanied by radio and x-ray bursts, or flares, and occasionally by high-energy particle emissions. The optical brightness and size of the flare are indicated by a two-character code called the importance. The first character, a number from 1 to 4, indicates the apparent area. For areas of less than 1, an "s" is used to designate a subflare. The second character indicates relative brightness; b for bright, n for normal, and f for faint. The most recent general discussion of solar flares is found in Smith and Smith (1963).

Hydrogen- α solar flare data are collected by numerous solar patrol stations over the globe. The February 1970 Solar-Geophysical Data Descriptive Text lists 53 stations. Data from these stations are found in the Solar-Geophysical Data bulletin and in the IAU Quarterly Bulletin on Solar Activity.

The Solar-Geophysical Data bulletin contains two listings of solar flare reports -- those published the month following the flare occurrence and those published 6 months after occurrence. The former list includes all reported flares of importance greater than one, giving the observatory, the date, the start time, the maximum and end times, the solar latitude and longitude, the McMath plage region, the duration in minutes, the importance, the observation condition and type, the area, and the maximum width of the $H\alpha$ intensity. A 1-month listing of subflares is also provided indicating

date, time, and location. A full discussion of these parameters is found in the Solar-Geophysical Data Descriptive Text which appears in February of each year.

The listing published in Solar-Geophysical Data 6 months after occurrence consists of those flare reports filtered according to a program used at the Observatoire de Paris, 92 Meudon, France, to produce the IAU Quarterly Bulletin on Solar Activity flare listing. The format of the 6-month listing is the same as that of the 1-month flare listing described above. The grouped flare data appearing in the 6-month listing are also available from WDC-A, Boulder, on punched cards and magnetic tape for the period 1955 to the present.

As the number and refinement of observations increases, it becomes impressively clear that there is no single, simple flare model but rather a large spectrum of flare events which we can only crudely characterize by our conventional categories of class 1, 2, 3, faint, normal, and bright, or by proton, hard x-ray, soft x-ray, white-light, and uv-continuum emissions, or by "fast burst", "gradual rise," "fluctuating," and other phenomenological features. Many long-held and presumably firmly established concepts of ionospheric behavior have become open to question as a result of improved observational powers both in space and on the ground.

It used to be that ionospheric disturbance phenomena were studied as a means of estimating solar-flare x-ray and uv fluxes. But flares have now become diagnostic probes for ionospheric processes because the flare spectrum is directly measurable from space and the aeronomic cross sections for ion production processes are becoming known with considerable accuracy.

Daily Flare Index

The significant influence of solar flares on terrestrial disturbances of various kinds suggests that a daily flare index, similar to daily sunspot number or to the geomagnetic activity index, would be widely useful. Some studies may require construction of a special daily measure, tailored to fit the needs of the particular analysis, but a general expression of flare activity may suffice for a number of other studies.

The index published currently at the High Altitude Observatory corresponds closely to the index I_f to be described here. We shall call the present index "the new H.A.O. index," as most of our discussion pertains to the original definition. For an individual flare, the integrated intensity in H α is defined as the product of four factors: relative brightness, apparent area, a factor depending on the fraction of area at maximum brightness, and duration. The sum of the integrated intensities of all the flares occurring on a given day is a quantitative estimate of the total excess solar energy due to flares. The clear physical interpretation of this index is augmented by other properties that are advantageous in many applications. Based on the apparent area and observed duration, this index gives a high weight to central flares. Its dependence on flare position is shared qualitatively by flare-associated radio and particle emission. The index also assigns a high weight to single large flares, as compared to numerous minor flares. This weighting also agrees with the probability of occurrence and the magnitude of sudden ionospheric disturbances. Thus, this index measures a definite physical quantity that is expected to bear a close relation to several interesting phenomena.

The daily flare index, calculated from the confirmed flares, is defined as

$$I_f = \frac{7600}{T^*} \sum A_d^2$$

where individual flare area A_d is measured in square degrees and T^* is the effective observing time in minutes. Only those confirmed flares of greater than 1 square degree in area, as included in the IAU Quarterly Bulletin on Solar Activity, are used in calculating the flare index. I_f corresponds closely to the flare index developed at the High Altitude Observatory to measure the integrated intensity of flare radiation. The flare areas are not corrected for geometric foreshortening, so the definition of I_f places great weight on large flares, located near the center of the sun's disk. Characteristics of the index I_f are discussed in more detail in the paper by C. Sawyer "A Daily Index of Solar Flare Activity" (J. Geophys. Res. 72, 385, 1967).

The table lists the date, index and actual hours of observation included in the calculation and follows the table of confirmed Solar Flares.

Magnetic Condition

The magnetosphere is disturbed with varying frequency and intensity by perturbation in the solar wind. Changes in the solar wind dynamic pressure, whether sudden (as in discontinuities) or gradual, result in a compression or expansion of the magnetosphere. The effects are transmitted inward as hydromagnetic waves and are manifested on the ground as an increase (for compression) or decrease (for expansion) in the magnetic field, representing a magnetospheric response of the simplest kind.

(1) Magnetospheric Substorms

Although the exact nature of the interaction between the solar wind and the magnetosphere at its boundary is not yet clear, there is increasing evidence that particles and other forms of energy are injected into the magnetosphere continuously or in bulk. It appears that when energy accumulated in the magnetosphere reaches a certain level, it is released rather abruptly in what is termed a magnetospheric substorm. The substorm involves a large-scale reorganization of the high-energy particle population, of the thermal plasma, and of the magnetic and electric fields in the magnetosphere; it also produces a severe magnetic disturbance on the surface of the earth at high latitudes, which is called a polar stat or magnetic substorm -- a complex phenomenon accompanied by other manifestations such as particle precipitation, auroral activity, infrasonic wave development, and generation of electromagnetic signals. Magnetospheric substorms often recur at intervals of 3 or 4 hours, suggesting that this duration is the time constant for the buildup and release of energy in the magnetosphere.

As just mentioned, a magnetospheric substorm has a variety of manifestations over the entire earth, each of which may provide an important clue to the basic processes involved. Recent studies indicate that the magnetospheric substorm is associated with a sudden growth of electric fields. These electric fields generate the auroral electrojet in the polar ionosphere and accelerate auroral particles, which, in turn, can produce visible auroras and x-ray bursts when they interact with the atmosphere.

The study of polar magnetic substorms alone is not sufficient to understand the whole phenomenon of magnetospheric substorms. Intensive interdisciplinary studies of polar upper atmospheric disturbance phenomena are also needed. Compact, transportable, geophysical observatories equipped with identical standard instruments are suggested for such studies. A major effort in the analysis of polar upper-atmospheric disturbance phenomena should be directed toward the establishment of a model for the distribution of electric fields consistent with various manifestations of the magnetospheric substorm. The next step is to infer how these electric fields are produced as a consequence of the interactions between the "disturbed" solar wind and the magnetosphere. Such studies may provide clues to important problems, including: How can solar wind energy enter the magnetosphere? How is this energy stored and finally converted into the energy for a magnetospheric substorm?

(2) Geomagnetic Storms

The magnetosphere is severely disturbed during magnetic storms, which often occur about two days after an intense solar flare, or sometimes following the passage of a boundary in the interplanetary plasma sector structure. Several hours after the onset of a magnetic storm, a rapid succession of severe magnetospheric substorms occurs and the geomagnetic field is globally depressed owing to a formation of a ring current in the magnetosphere. Physical processes that take place during a magnetic storm are extremely complex and many are not well understood. The major processes involved and their effects as observed in the magnetic field at the ground are shown schematically in Figure 2 (National Academy of Sciences, 1969).

A typical geomagnetic storm has three phases: initial, main, and recovery (see Figure 3). A compression of the magnetosphere, manifested by a sudden commencement, is the major feature of the initial phase. The main phase is characterized by the growth of an intense ring current belt and frequently by severe magnetospheric substorms. During the development of the main phase, as many as ten magnetospheric substorms may occur in close succession, as illustrated in Figure 3 (National Academy of Sciences, 1969). These substorms are observed from the ground as a repetition of rapid growth followed by decay of the polar magnetic substorms. The "AE" index has been derived to express the activity of these polar magnetic substorms and thus of magnetospheric substorms.

The ring current belt which develops during the main phase is predominantly composed of 5- to 50-kev protons. On the ground, the net effect of the ring-current system is a reduction of the horizontal component of the magnetic field in midlatitude and low latitude. An important aspect of the ring current belt is a large axial asymmetry during buildup. The " D_{st} " component represents the average intensity of the ring current field on the earth's surface, and "DS" gives the amplitude of the asymmetric component. There is some indication that the time variation of DS is similar to that of the AE index, suggesting that the asymmetric component of the ring current is closely associated with magnetospheric substorms. An east-west chain of geomagnetic stations is vital for examining the instantaneous distribution of the asymmetric part of the ring current.

Typically, about 6 hours after the onset of the main phase, the polar magnetic substorm activity begins to decay, while the main phase develops for an additional few hours. After the height of the main phase, the field begins to recover, sharply for a few hours and then more gradually with time. This can take several days or even longer.

In this report the indices D and S are used for magnetically-disturbed days and principal magnetic storms, respectively. The magnetically disturbed days (D) are selected in "Solar-Geophysical Data" in accordance with the general outline in Terrestrial Magnetism (48, 219, 1943). The method in current use calls for ranking the days of a month by their geomagnetic activity as determined from the following three criteria

with equal weight: (1) the sum of the eight K_p 's; (2) the sum of the squares of the eight K_p 's; and (3) the greatest K_p . (See the discussion of the Magnetic Index A_p on page I-40 for a definition of K_p).

A table in "Solar-Geophysical Data" presents the principal magnetic storms (S) for the month as reported by several observatories through cooperation with the International Association of Geomagnetism and Aeronomy.

Sudden Ionospheric Disturbances (SID)

Flares produce a variety of sudden ionospheric disturbances (SID), which can be resolved in height from the base of the D region to lower portions of the F region. Timing differences on a scale of a minute or less in the initiation of disturbances and in the rise to peak of the event can be highly diagnostic of the nature of the ionospheric production and loss processes when comparable data for ionizing fluxes are available directly from satellites.

Processes specific to the 60- to 75-km height range are:

1. Sudden phase anomalies (SPA), where the sky wave changes phase with respect to the ground wave as a result of an effective lowering of the reflection ceiling near the base of the D region, sometimes by as much as 16 km.

2. Sudden enhancement of atmospherics (SEA), manifested in improved reflection of very long radio waves (about 10,000 m) from the bottom of the D region. Distant tropical thunderstorms provide a steady background on a frequency of approximately 25 kHz, and signal strength may increase 100 percent during a large flare.

3. Sudden field-strength anomalies (SFA), observed as interference effects over medium distances between sky wave and ground wave when both are of nearly equal intensity. As the reflecting ceiling drops, the two waves vary in and out of phase, thus giving large variations in field strength at receiver.

In the 75- to 90-km range there occur sudden ionization increases which lead to:

4. Shortwave (5 to 20 MHz) radio fadeout (SWF), which is attributable to D region absorption. The phenomena is prompt to within a minute of flare outbreak as observed optically from the earth.

5. Increased absorption of cosmic radio noise from outer space observed by riometers at approximately 19 MHz (SCNA).

To explore the ionosphere above 90 km we can observe sudden frequency deviations (SFD). An SFD is an abrupt increase in the frequency of a high frequency radio wave reflected from the F region followed by a slower decay to the transmitted frequency. The frequency deviation characteristically may exhibit several peaks near maximum and may even show negative deviations during the decay phase. In contrast with the D region effects that accompany 1- to 10-A x-rays, the SFD's are highly impulsive -- the rise to maximum is roughly a minute, and the source radiation is probably in the EUV region from 10 to 1030A, most likely dominated by enhancement of the Lyman continuum radiation of hydrogen.

Observations of SFD in radio transmissions via the E and lower F regions have shown surprisingly fine temporal structure resolvable on a scale of only a few seconds. Without knowledge of the solar radiation flux, SFD's could serve as fast-resolving, broadband detectors of explosive flare outbursts. When combined with satellite flare measurements the SFD data can provide unique evidence of electron production rates and recombination coefficients. Recently it has become possible to record x-ray bursts with fine structure similar to SFD's, and it is remarkable that the SFD and

directly measured flux patterns are comparably sharp and can be matched to within 1 or 2 sec. From such comparisons it is possible to derive the concurrent solar evf continuum emission and to infer ionospheric reaction times far shorter than previously suspected.

SIDs are observed on the sunlit hemisphere and occur almost simultaneously with visual flare observations. SIDs and subsequent recovery of the ionosphere have a time duration somewhat longer than flare duration; generally from minutes to an hour, with rise more rapid than decay.

Several of the various SID observations are routinely identified and digitized. Samples of several types of original records as they appear before digitizing are nicely illustrated by Lincoln (1968). The types of SID are alphabetically listed below with brief descriptions of each. The SCNA, SEA, SES, SFD and SWF listings are available from the WDC-A for Upper Atmosphere Geophysics and have also been published in issues of Solar-Geophysical Data since 1963. Bursts and SFE are also listed in Solar-Geophysical Data.

Burst - A solar noise burst at riometer frequencies is seen as a sudden increase of signal strength on the riometer records. This is caused by solar radio noise emissions at riometer frequencies. This noise is affected by and can mask the ionospheric absorption that is present. The bursts are

of such short duration, however, that absorption changes during the burst can be estimated. In addition to riometer observations, solar noise is routinely observed at much higher frequencies than those used for riometer receivers.

Crochet - see SFE.

SCNA - Sudden Cosmic Noise Absorption, also referred to as CNA (Cosmic Noise Absorption) Type I (see below), is characterized on riometer recordings by a sudden daytime absorption increase of several db within a few minutes. Decay is somewhat slower than rise, and the riometer record is perturbed for a period of minutes to over an hour. SCNA involves absorption outside of auroral regions.

SEA - Sudden Enhancement of Atmospherics is observed as an increase in signal strength on wideband equipment operated to detect electromagnetic emissions from lightning. This equipment operates in the VLF (10 to 50 kHz) range with the most commonly used frequency near 27 kHz.

SES - Sudden Enhancement of Signal is observed on VLF frequencies (15 to 50 kHz). These observations are nearly identical to SEA except that the receivers are narrow-band receivers designed to pick up man-made VLF transmissions. As with SEA, signal strength increase is the SID indicator.

SFD - Sudden Frequency Deviation, caused by ionospheric disturbances, is observed by beating the received radio signal with a reference frequency that is near the received frequency. This technique allows small frequency changes to be observed. SFD is observed in the high-frequency range,

and the reference signal is obtained locally from a stable oscillator. Occurrence times and deviations in frequency are listed in data presentations.

SFE - Solar Flare Effect, or crochet, is observed as a small hook on magnetometer records. It is caused by the magnetic field response to increased current flow in the E region due to electron enhancement induced by flare x-rays.

SPA - Sudden Phase Anomaly is observed in the same manner as SFD, except that VLF frequencies are used and the reference signal is the ground wave. For observing SPA on transmitters more distant than possible for ground wave propagation (about 200 km), the ground wave reference signal is provided by telephone or a local reference signal source is used as in SFD observations.

SWF - Short Wave Fadeout is observed from signal strength records of any shortwave (3 to 30 MHz) receiver. Signals from sweep-frequency ionosondes (vertical or oblique incidence) may be completely absorbed. SWF is categorized as gradual (G), slow (Sl), or sudden (S), depending primarily on how rapidly the signal loss occurs.

CNA

In addition to SCNA discussed under SID, there are two other types of CNA. Data on these latter types are not generally available but are mentioned here to broaden perspective. Cosmic Noise Absorption is observed

on riometers that operate between 15 and 60 MHz, but most often near 30 MHz. Absorption is normalized to low nighttime absorption occurrences for that station. CNA can be divided into SCA (sudden commencement absorption), CNA Type I, also called SCNA (sudden cosmic noise absorption), and CNA Type II. CNA Type II is local nighttime absorption associated with active aurora. The absorption may persist for hours with irregular variation including individual peaks as high as 8 to 10 db persisting for several minutes. This is sometimes called auroral absorption.

SCA (Sudden Commencement Absorption) is characterized by sudden onset, occurrence in zones centered on the auroral zone (58° to 75° geomagnetic), and persistence for less than 1 hour. The SCA is similar to SCNA in rise time and duration. Type I and II CNA are somewhat local and irregularly distributed in longitude in contrast to the zonal occurrence of SCA. SCAs have been associated with geomagnetic storm sudden commencement x-ray fluxes.

2800 MHz (10.7 cm) Solar Flux

Within the past 20 years, radio observations have provided a new means of probing the temperature and electron distributions in the solar atmosphere with the resultant possibility of providing other indices of solar activity. In particular, it has been found that the intensity of radio emission from the whole disk above a certain minimum value varies from day to day and in the vicinity of 3000 MHz the variations correlate well with the Zurich relative sunspot numbers or the total area of sunspots present on the disk. Sudden enhancements in the emission or bursts occur and can be separated readily from the background daily level to provide a second radio indication of solar activity closely associated with flare appearances. It has been found that the intensity of the daily level and of the bursts changes slowly with frequency in the band from 1000 to 9000 MHz so that any observations made on a single frequency in the center of this band can be regarded as typical and provides most of the information. The routine observations of the sun at a wavelength of 10.7 cm (2800 MHz) were commenced in 1947 at Ottawa by the Radio and Electrical Engineering Division of the National Research Council and have provided observations suitable for establishing a radio index. It has been found that the single value obtained at local noon is sufficient for most applications.

The correlation between the orbital deceleration of an artificial satellite and the solar radio flux in the decimeter range has led to relationships between the atmospheric density at various heights and the 10.7- and 20-cm radio fluxes. Considering that the density variation is due to a temperature variation, it can be concluded that the solar extreme ultraviolet

radiation (EUV) is responsible for the heating of the upper atmosphere and that heat conduction is responsible for its cooling. A change in the ultraviolet radiation can be correlated with a change in the radio flux just as with the sunspot number, which is a well-known index of solar activity. The 10.7-cm and EUV should be correlated in some degree, inasmuch as many features of the sun vary with the solar cycle, including the number of sunspots, faculae, filaments, prominences, flares, and height of the chromosphere and shape of the corona. With regard to the radio waves represented and optical manifestations in the EUV regions, however, no exact causal relation between these groups of phenomena has been advanced.

Although it is true that both radiations issue from the upper chromosphere and lower corona, our knowledge of the details of their origin is very deficient. At present, there are no theoretical grounds for an exact relation (Anderson, 1965).

Daily observations of the 2800 MHz radio emissions which originate from the solar disk and from any active regions are made at the Algonquin Radio Observatory (ARO) of the National Research Council of Canada with a reflector 1.8 meters diameter. These are a continuation of observations which commenced in Ottawa in 1947. Numerical values of flux in the tables refer to a single calibration made near local noon at 1700 UT. When the flux changes rapidly, or there is a burst in progress at that time, the reported value is the best estimate of the undisturbed level and provides the reference level for measuring the burst intensity. The various types of outstanding events are listed separately in another table. The observed

flux values have variations resulting from the eccentric orbit of the earth in its annual path around the sun. Although these radio values are suitable to use with observed ionospheric and other data, an adjustment must be introduced when the observations are used in studies of the absolute or intrinsic variation of the solar radio flux. Thus, the tables show both the observed flux, S , and the flux adjusted to 1 A.U., S_a . The observations are made for a single North-South polarization but reduced for the assumption of two equal orthogonal polarizations. A graph showing the monthly highs and lows for the last two sunspot cycles is shown in Fig. 4. Relative errors over long periods of time are believed to be ± 2 percent, over a few days may be ± 0.5 percent. The characteristics of the observations are surveyed in "Solar Radio Emission at 10.7 cm" by A.E. Covington [J. Royal Astron. Soc., Canada, 63, 125, 1969]. Experiments conducted during the past few years indicate that a multiplying factor of 0.906 should be applied to the reported flux values in order to derive the absolute flux value.

HeII Solar Flux

Many workers have carried out the detailed calculations to determine how much of the incident solar UV energy is converted to heat in the thermosphere near 140 km, and how much dissociates and excites oxygen and nitrogen molecules. The mean free path in the thermosphere is so large that only a small amount of recombination and de-excitation occurs there. In order for these processes to occur, the atoms and excited molecules must diffuse down into the mesosphere. It is there that this energy is ultimately recovered and converted to heat. According to the latest estimates, about 70 percent of the solar UV energy is converted to chemical energy.

Most of the chemical energy is converted to heat in the altitude range 70 to 90 km, through two recombination processes: One process involves the production of O_2 and O_3 . The other process involves de-excitation.

The extreme ultraviolet line of HeII at 304A contains much of the energy involved in heating the atmosphere near 140 km. The measurements at 304A were obtained from Timothy and Timothy (1970) for April-August 1969. These data are a more accurate index than the 2800 MHz solar flux of the upper atmospheric EUV heating (Anderson, 1965).

Solar Protons (Greater than 10 Mev)

Significant numbers of charged particles, mainly electrons and protons, are accelerated at the sun during many solar flares. Some of these particles are subsequently detected within the interplanetary medium and at the earth. These particles serve as useful indicators of solar, terrestrial, and interplanetary conditions. Often, effects from these various regions are not separable, but in certain events they are.

A series of Solar Proton Monitoring Experiments (SPME), initiated by scientists at Johns Hopkins University /Applied Physics Laboratory and at NASA Goddard Space Flight Center, is intended to provide reliable flux and spectral measurements of solar protons over at least half a solar cycle and over a wide flux range. Each SPME consists of an array of solid-state detectors that measure the combined counting rate due to fluxes of protons and alpha particles in each of the three energy ranges: ≥ 10 Mev/nucleon, ≥ 30 Mev/nucleon, and ≥ 60 Mev/nucleon. The alpha particle component is usually very small and may be thought of as introducing an ambiguity of less than 10 percent into the proton count rate. Further discussions of this point and of the SPME in general can be found in the "Descriptive Text" of Solar-Geophysical Data (February 1970).

The SPME was successfully launched aboard the NASA satellites Explorers 34 (IMP-F, 1967-51A) and 41 (IMP-G, 1969-53A) on May 24, 1967 and June 21, 1969, respectively. Explorer 34 re-entered the earth's atmosphere on May 3, 1969 and Explorer 41 re-entered on December 23, 1972. Continuous data

from the SPME have been presented for the lifetimes of Explorers 34 and 41. Similar equipment was launched aboard Explorer 43 (IMP-I, 1971-19A) on March 13, 1971 and these data have been used to supplement the Explorer 41 data, and will continue in 1973.

The primary purpose of the SPME is to provide systematic monitoring of solar cosmic rays over at least half a solar cycle. The basic requirements set forth for such a monitoring program were:

- 1) to furnish simple reliable flux and spectral measurements,
- 2) to operate over a wide flux range and in particular provide coverage for very large events,
- 3) to provide a simple and easily reproducible detector system to form the basis of an operational monitoring program.

All data from the SPME published as monitoring data satisfy the following requirements:

- 1) final orbit determinations have been made,
- 2) final time corrections have been made,
- 3) all data quality flags indicate that the individual data point is "good."

Data that satisfy these requirements are then used to construct hourly averages of the respective energy channels. The ≥ 60 Mev and ≥ 30 Mev channels are sampled for 19.2 seconds once every 2 minutes 43.8 seconds. The ≥ 10 Mev channel is sampled twice every 2 minutes 43.8 seconds at 19.2 seconds per sample. Thus, the maximum number of points in an hourly average

is 22 for the ≥ 60 Mev and ≥ 30 Mev channels and 44 for the ≥ 10 Mev channel. If the number of "good" data points is less than 5, the hourly average is not constructed.

These hourly averages are then tabulated in a grid where the hours of the day run to the right and the days of the month run from top to bottom. The day is identified as both day of the month and day of the year. The tabular entries are nominally four characters each. The decimal point will be automatically shifted to the right as the intensity increases until it finally disappears when the intensity is ≥ 1000 protons $\text{cm}^{-2}\text{sec}^{-1}$. If the intensity becomes $\geq 10,000$ protons $\text{cm}^{-2}\text{sec}^{-1}$, the blank space between columns is utilized so that intensities up to $99,999$ protons $\text{cm}^{-2}\text{sec}^{-1}$ may be accommodated. The entries all begin with a low intensity format of 0.XX. The following is an example of how the entries appear for an intensity increasing from 0.55 protons $\text{cm}^{-2}\text{sec}^{-1}$ to $55,000$ protons $\text{cm}^{-2}\text{sec}^{-1}$.

0.55
5.50
55.0
550.
5500
55000

The hourly averages are also plotted vs. time in monthly blocks. The response of the ≥ 10 Mev channel in the radiation belts is very noticeable since this channel also responds to electrons of energy ≥ 515 kev. This low an electron energy threshold makes this channel respond to the radiation belt

for a much larger radial extent (at times out to 10 earth radii) than channels 1 and 2 whose electron thresholds are several Mev in energy. The actual time profiles, due to the radiation belts, displayed by the ≥ 10 Mev channel on the hourly plots are highly variable due to the great variations in these trajectories through the trapping regions.

The Magnetic Index A_p

Types of solar-terrestrial correlations and more recent space observations demonstrate, when viewed in total, that magnetic activity on the earth is very closely related to solar phenomena. This has already been discussed to some extent in the section "Magnetic Condition."

To facilitate correlations with other phenomena, both terrestrial and solar, and to have simple criteria for relating changes in magnetic activity from hour to hour, day to day, month to month, etc., various indices of magnetic activity have been proposed and used. Two of the oldest are: C, the daily character figure on a scale of 0 to 2, which is a simple numerical, but qualitative, estimate of the day's activity at each observatory, and U which is a measure of the change in the average value of the horizontal component from day to day.

In the past two decades considerably more use has been made of an index called K, when given for a single observatory, and K_p, when given for a select group of observatories which we will describe below. K_p, in particular, has been used extensively in space studies both for characterizing solar-terrestrial conditions and for correlating in detail magnetic activity with numerous types of space measurements ranging from magnetospheric neutral particle densities to cosmic rays. Thus, it is important that we have some understanding of the meaning of K_p.

The K-index of a station is a quasi-logarithmic measure of the local magnetic activity obtained in 3-hour intervals of the Greenwich day. It

is related to the maximum range in the 3-hour interval of the most disturbed component of the magnetic field. The index assumes values between 0 and 9 corresponding to the quietest and most disturbed conditions, respectively. Since the degree of magnetic activity as measured by the range in gammas is strongly latitude-dependent, the different magnetic observatories must apply appropriate scaling factors to convert the gamma-range to K-index in order that the frequency distribution of K-indices be the same for all observing stations. Thus, a K of 9 would represent a range of at least 300 gammas at low latitudes and 2500 gammas in the auroral zone. More than 80 stations currently provide K-indices.

The planetary index K_p is the average of 3-hourly K-indices from 12 selected observatories located in middle geomagnetic latitudes from 47° to 63° . All but one of the stations are located in the northern hemisphere. The index is commonly used as a measure of the global average magnetic activity. However, it must be borne in mind that conditions in polar and equatorial regions may not conform with the planetary K_p .

A linear scale of disturbance values a_p has been adopted corresponding to the quasi-logarithmic values K_p . Each Greenwich day has 8 a_p -values corresponding to the 8 K_p -values. The daily average of a_p is called the daily planetary amplitude and is denoted A_p . High values of this index are definitely associated with upper atmosphere heating although the heating mechanism is not completely understood (Anderson, 1973).

The 3-hourly K_p and daily A_p values for each month are published (with a 2-month lag) in the Solar-Geophysical Data (Prompt Reports), Part I, CRPL-FB 135⁺, U.S. Dept. of Commerce, Boulder, Colo., USA 80302.

The AE Index

Although the A_p index is capable of describing the general state of planetary geomagnetic activity, it contains contributions from at least two major sources, the auroral electrojet and the ring current. To study auroral-zone activity it is desirable to maximize the auroral electrojet contribution. This has been accomplished by the development of the AE index. To obtain this index of geomagnetic activity, only slightly sub-auroral-zone stations are employed for the most part, and they are chosen so as to provide uniformly spaced coverage around the auroral zone. In some cases this necessitates the use of southern hemisphere stations to take advantage of the apparent conjugacy of magnetic variations of a sub-storm nature.

The AE index is constructed by using only the H component of the perturbation field. The H component at each observatory is scaled at 2.5-min intervals; the average quiet-time baseline is used as a reference level. These baseline levels are assumed to be within ~ 10 gamma of the undisturbed H component, and thus the actual scaled values of ΔH include S_q contributions in addition to those from the auroral current system.

All the scaled values from the various observatories are superimposed in a magnetogram format. This composite drawing is enclosed by upper and lower envelopes representing the maximum positive and negative values of ΔH for all observatories at each given time. The amplitude of the upper envelope at any instant is denoted by AU, and the amplitude of the lower envelope is designated by AL. If the station distribution were

closely enough knit, AU and AL would represent the maximum positive and negative deviations occurring along the auroral zone.

Physically speaking, AU gives a good representation of the maximum magnetic perturbation generated by the eastward electrojet usually found in the afternoon sector. Similarly, AL represents the maximum magnetic perturbation generated by the westward electrojet in the morning and midnight sectors. At the present time it appears as though the eastward and westward electrojets may fluctuate independently of one another, and it may be useful to treat AU and AL as independent indices. However, at the present time it is customary to combine these indices to give a direct measure of the total maximum amplitude of the eastward and westward electrojet currents. Hence, the index AE is defined by $AE = AU - AL$. Thus, AE represents the difference in levels (measured in gammas) between the upper and lower envelopes at any given instant in time.

Although AE is generally calculated at 2.5-min intervals and is available in this form from the World Data Center, hourly average values of AE are also available for the period 1957-1964, inclusive (University of Alaska Reports UAGR-192, UAGR-200). More recent AE index values through 1970 are available from the National Space Science Data Center, Goddard Space Flight Center, Greenbelt, Md. 20771.

Observations of traveling ionospheric disturbances emanating from polar regions have led to the suggestion that auroral energy may be coupled to atmospheric wave motions through heating produced by ohmic dissipation

of electric currents, Joule heating. Cole's (1962) pioneer work has established that Joule heating in the region 100-200 km could lead to large temperature changes, through heat flux by thermal conduction in the vicinity of 150 km and above. However, below 150 km it appears that the relaxation time, i.e., the time it takes an initial temperature impulse T_1 to fall to $e^{-1}T_1$, is at least one day and is independent of T_1 . On this basis, short period gravity waves (~ 1 hr) should transfer energy more efficiently than conduction below about 150 km, if the vertical scale of the propagating waves is approximately greater than the local scale height and if the coupling of auroral heating into gravity wave energy is efficient. Blumen and Hendl (1969) have investigated Joule heating in the vicinity of the auroral electrojet (100-150 km).

The D_{st} Index

The D_{st} index provides a planetary magnetic index on a hourly basis that has been used extensively in studies of geophysical disturbances, particles and plasma in the magnetosphere, solar-terrestrial relationships, and cosmic rays (Sugira and Cain, 1969).

Equatorial D_{st} is a measure of the mean departure from normal of the horizontal component, H , of the Earth's magnetic field observed at a group of low-latitude stations, whereas a_p is based on 3 hr ranges of the field at stations in higher latitudes.

The strength of D_{st} lies in its ability to detect all magnetic storms. This stems from the fact that the ring current is world wide in nature, and thus there is little or no possibility of D_{st} not reacting to the growth of the ring current. Furthermore, within about two hours, the D_{st} index should be able to identify the onset and termination of the main phase of a magnetic storm (during which time the major portion of the energy of the storm is dissipated in the magnetosphere). Thus, the D_{st} index gives a good qualitative description of the gross level of magnetospheric activity at any time, although it cannot be used to reveal the presence of individual substorms.

The values of D_{st} used in this analysis came from Goddard Space Flight Center reports (see for example, Sugiura and Poros, 1971).

Solar X-Rays (1-8A)

This index is used to indicate the magnitude of the x-ray flux between 1-8A which can cause atmospheric heating between 55-105 km. Solar x-ray emissions, like solar radio emissions, originate from both thermal and nonthermal processes that take place primarily in the solar corona. Solar x-ray emissions can be divided into three components: the quiet sun component, the slowly varying component, and the burst component. Nonthermal x-ray emissions occur only in the hard x-ray emissions (photon energies greater than about 10 kev or wavelengths less than about 1A) accompanying solar flares. Solar x-ray astronomy has been reviewed by Krimigis and Wende (1970).

Solar x-rays are directly observed with satellite-born detectors and indirectly observed through their effects on the ionosphere. The occurrences of solar x-ray bursts are indicated by the sudden ionospheric disturbances (SID). Patrol types of solar x-ray measurements must be carried out using instruments flown on satellites. Because solar x-ray instrumentation must be flown on satellites, the data quite often contain periodic and significant time intervals when no data were obtained due to the satellite's being eclipsed.

Ion chambers, proportional counters, Geiger tubes, and scintillators are used to measure the integral solar x-ray flux within specific wavelength or energy passbands. A review of such instrumentation is given by Neupert (1969).

Solar x-ray fluxes, integrated over the entire solar disk in units of $\text{ergs cm}^{-2} \text{sec}^{-1}$ over a specified passband, have been obtained from several satellites. The x-ray fluxes are useful and sensitive indicators of the level of solar activity.

The data used in this report consist of tables of hourly averages of x-ray flux in the 1 to 8A band. The primary source of the data is the Naval Research Laboratory's SOLRAD 9 and 10 satellites. Each satellite stores 0.5 to 3A, 1 to 8A, and 8 to 20A data in the satellite memory with a one minute time resolution. Therefore, a continuous record of the x-ray emission from the sun, except for gaps due to satellite night and charged particle interference, is available for these three bands. A complete description of the SOLRAD 10 experiments is given in NRL Report No. 7408 titled "The SOLRAD 10 Satellite, Explorer 44, 1971-058A." A complete description of the SOLRAD 9 experiments is given in NRL Report No. 6800 titled "The NRL SOLRAD 9 Satellite, Solar Explorer B, 1968-17A."

The data from the 1 to 8A ionization chamber are converted to a 1 to 8A energy flux based on a 2×10^6 K gray-body solar emission spectrum (Kreplin, R.W., Annales de Geophysique, 17, 151, 1961). The averages include data obtained during solar flares but data contaminated by charged particle interference are excluded wherever possible. When SOLRAD 10 data for an hour are missing, SOLRAD 9 data are used. Measurements by the SOLRAD 9 and SOLRAD 10 1 to 8A ionization chambers are virtually identical so normalization is not required. For identification purposes only, the SOLRAD 9 data are followed by the symbol <. The values given for each

hourly average are in units of 10^{-3} ergs/cm² sec, and the time scale is UT. The tabular entries are made with a shifting decimal point. Therefore, the values which may be expressed in the four spaces assigned to each entry range from .001 to 9999 times the basic unit, 10^{-3} ergs/cm² sec.

5. SOLAR-TERRESTRIAL LINKS AND STRATOSPHERIC WARMINGS

Before physical theories can be invented to explain certain suspected solar-weather relations, including stratospheric warmings, several links must be filled in. Some of the principal missing links in the development of such theories are as follows:

Thorough knowledge of incident solar flux - Long-term accurate measurements are needed at all wavelengths, including Lyman-alpha (1216\AA), EUV ($100\text{--}900\text{\AA}$), and x-rays ($< 100\text{\AA}$). Most of the Lyman-alpha is absorbed below 100 km. Its flux varies from about 6 to 3 $\text{ergs cm}^{-2}\text{sec}^{-1}$ between high to low solar activity. Changes during flare periods are not significant geophysically. The x-rays should be measured globally, since the greatest variation in solar photon output occurs in the x-ray region (up to 3 orders of magnitude with periods of minutes to hours). It is necessary to separate out the ionizing effect of the x-rays from that of longer wavelengths. The main action of x-rays is to create ionization between 120 km (100\AA) and 55 km (1\AA). However, they are not the sole ionizing agent in this altitude range nor is their contribution to heating the major one.

Appropriate data on the primary photon interactions - Quantitative data on the rate coefficients of various types of transitions for all the important constituents at all important wavelengths so that the consequential effects of the primary photon interactions, such as ionizations of atoms and molecules, dissociation of molecules, etc., can be assessed.

Heat budget of the mesosphere near 80 km - What are the altitude, latitude, temporal, diurnal, and seasonal variations of mesospheric temperatures? How are the temperatures related to the intensity and variations of the solar Lyman-alpha and x-rays? Are there other important heat sources for the mesosphere, such as particle influx, and how do they contribute to the temperature structure? What is the energy balance of the mesosphere as a function of height, and what are its global variations? A difficult aspect of this problem is the transfer of energy as a result of radiative processes and various circulation processes. The altitude at which energy is absorbed need not in general correspond to the altitude at which it is converted into thermal energy.

Circulation in the Mesosphere - It is necessary that the temperature, density or pressure, and composition of the mesosphere be measured as functions of altitude, location, and time, in sufficient detail to disclose the general patterns and systematic variations that occur with (a) time, (b) season, (c) sun-spot cycle, (d) location, and (5) the condition of other parameters (meteorological, auroral, geomagnetic, etc.). The limits and characteristics of random variations that cannot be associated with other geophysical parameters should also be determined. Thus, it is necessary to establish the inherent variability of the mesosphere, both short term (to determine possible effects due to x-rays) and long term (to find possible effects due to Lyman-alpha).

What are the vertical distributions of the chemically active atmospheric species? - What processes control those distributions? The most important species are ozone, nitric oxide, carbon dioxide, hydrogen and its compounds, atomic oxygen, argon, methane, and excited atoms and molecules. These minor constituents need to be measured as function of latitude and time. Water vapor and methane dissociate in the 60-100 km region, and the dissociation and recombination rates are so poorly known that a direct measurement of their concentration is needed. Accurate measurements of the vertical profile of some or all of these species will be interpretable in terms of the large-scale circulation in the mesosphere.

Laboratory measurements of reaction rate coefficients - While some of the chemistry of the mesosphere is understood, there are serious gaps in our knowledge of the chemical processes involved, and many of the needed rate coefficients are missing.

How is turbulence generated in the mesosphere? - If waves are responsible, what are their origins, and are their amplitudes sufficient to cause nonlinearities?

How does eddy diffusion affect the distribution of atmospheric gases and the transport of heat? - This is an important question near 80 km. It is necessary to determine the value of the eddy diffusion coefficient as a function of height and time from 60-100 km.

What are the physical mechanism(s) responsible for interaction(s) between the mesosphere and lower atmosphere (troposphere and stratosphere)?-

How does their relative importance vary with altitude, location and time?

Statistical studies indicating correlation between upper and lower atmospheric phenomena have little validity unless backed up by physical mechanisms. For example, the statistical correlation between the international magnetic character index C (which is correlated with solar activity) and lower atmosphere circulation systems may result from dynamic interconnections between lower and upper atmosphere circulation systems rather than of solar emission.

Hydrodynamic theory of atmospheric perturbations - This theory needs to be developed in order to find the influence of upper atmospheric solar heating, etc., upon the circulation in the atmosphere. How is the general circulation influenced by irregular changes in the sun's emissivity or by variations of the reflectivity of the earth-atmosphere system? The physical basis for changes in lower atmosphere circulation patterns is not fully understood.

Development of techniques to evaluate the significance of weak relationships or relationships exposed from a small number of cases -

Only about .01 percent of the solar radiation is in the wavelengths considered. Even if this energy absorbed near 80 km does influence the earth's lower atmosphere, how could this be detected?

Figure 5 indicates the many types of perturbations affecting the stratosphere and the connections among them.

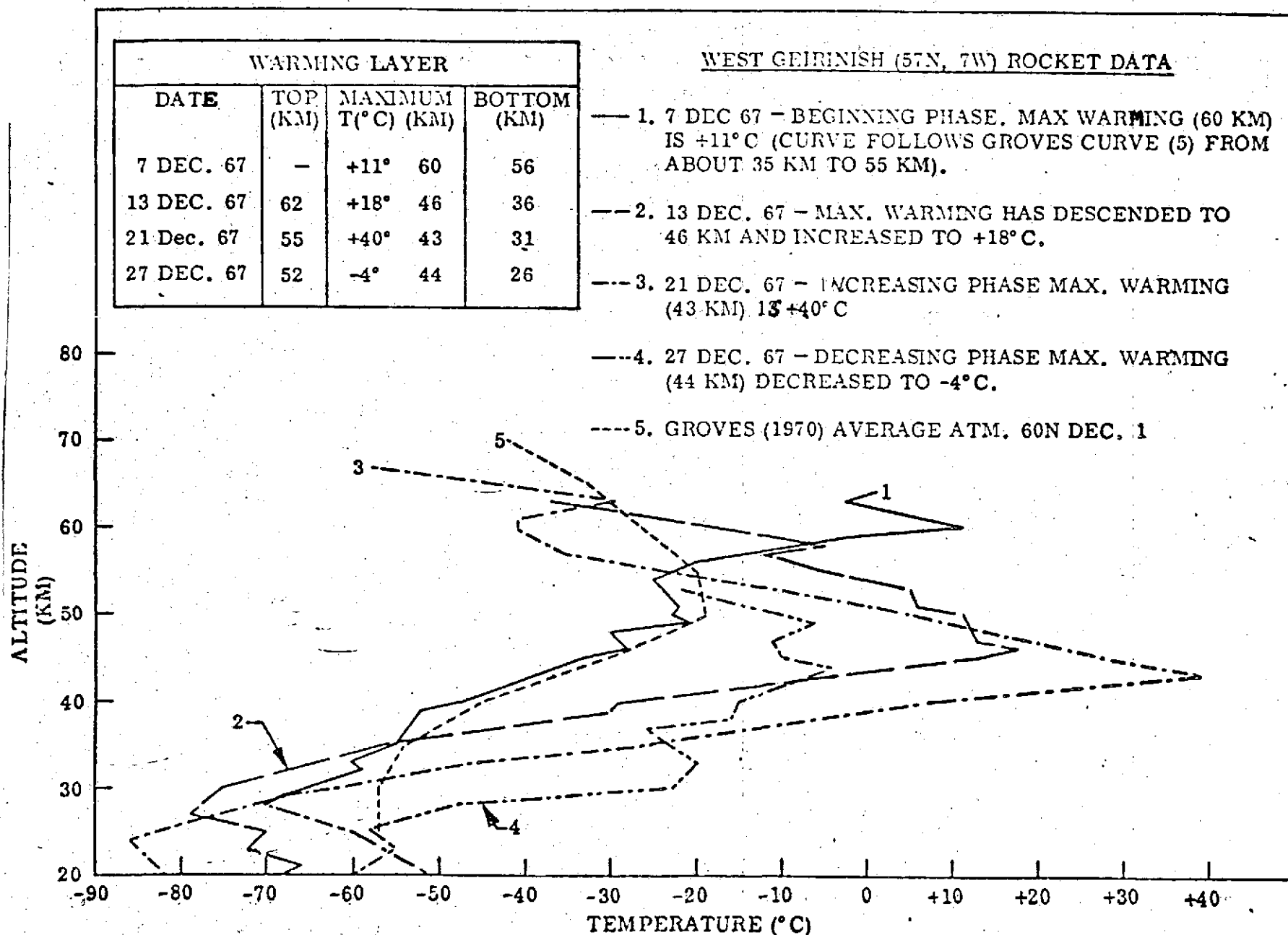


FIGURE 1 WEST GEIRINISH ROCKET DATA DURING WARMING (Labitzke 1971)

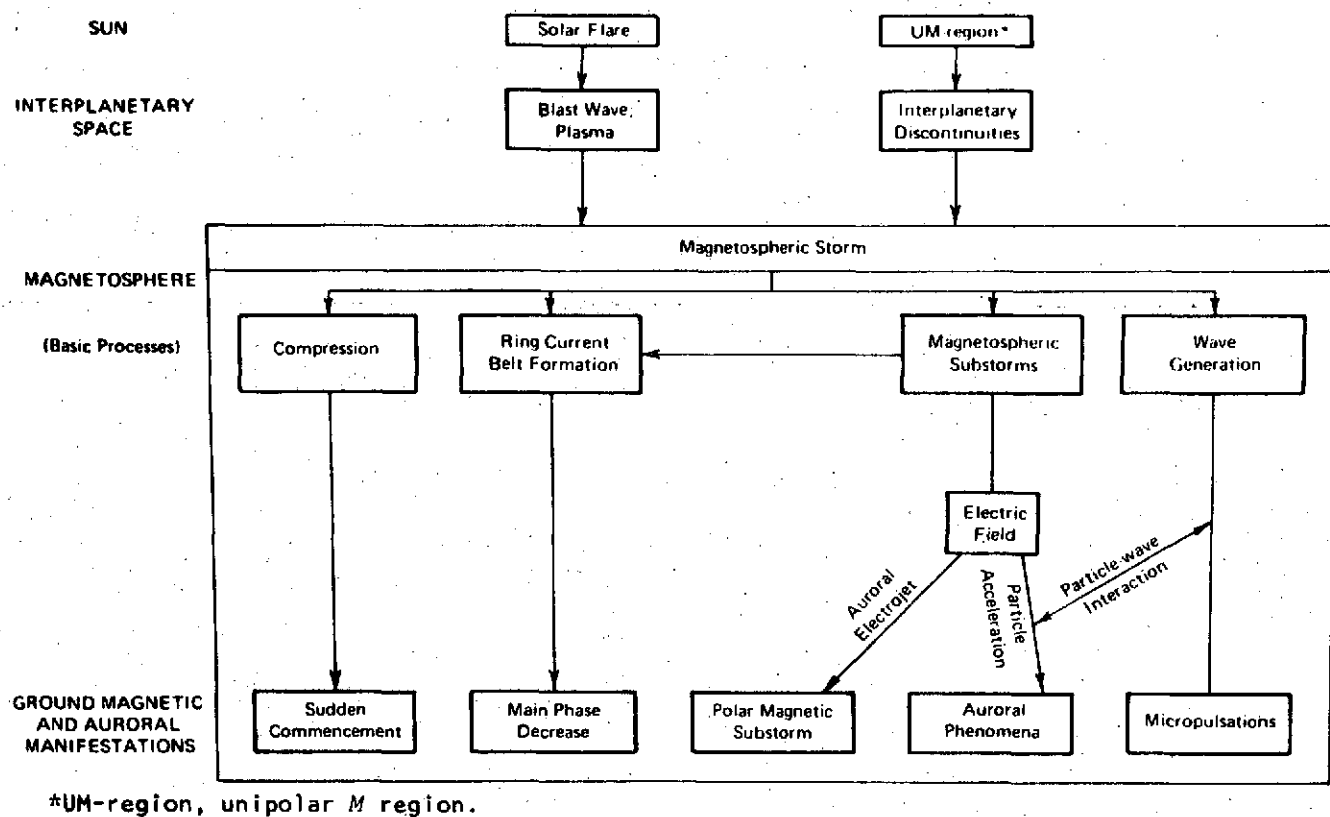


FIGURE 2 Schematic of major processes and their effects during a magnetic storm.
(National Academy of Sciences, 1969)

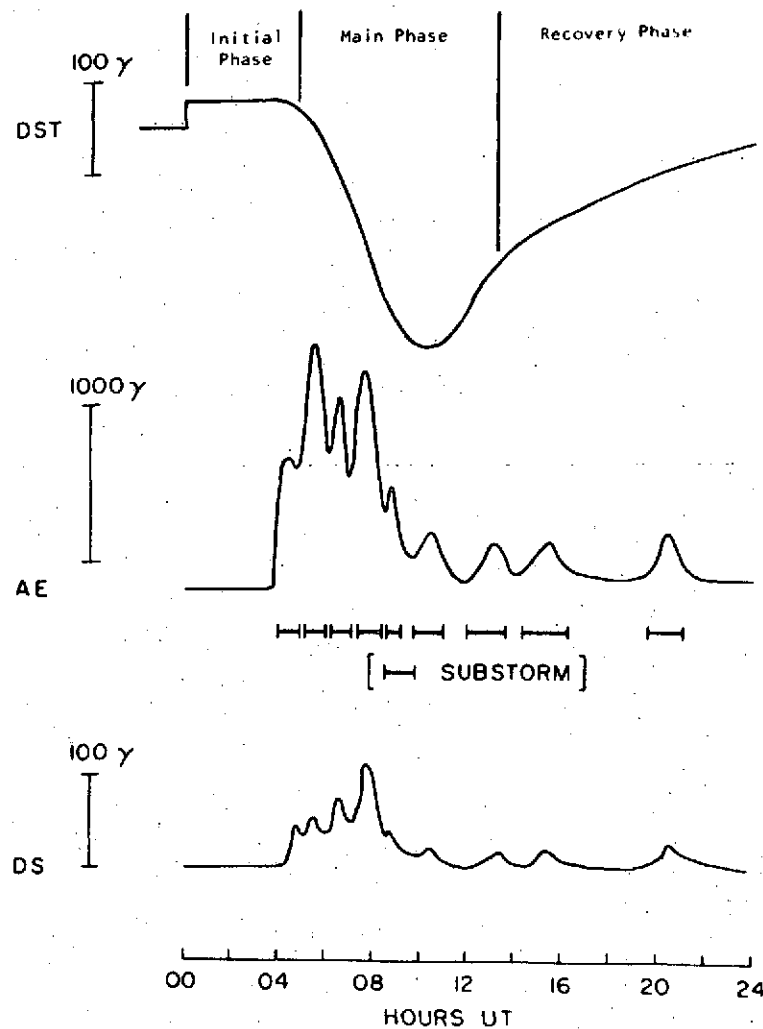


FIGURE 3 An example of a typical geomagnetic storm showing the three characteristic phases and the relationship between the Dst, AE, and DS indices. The Dst index is a measure of the magnetic field intensity of the ring current and also of the total kinetic energy of the ring current belt. The AE index is a measure of the intensity of magnetospheric substorms. The DS index is a measure of the magnitude of the asymmetry of the ring current field.

REPRODUCIBILITY OF THE
ORIGINAL PAGE IS POOR

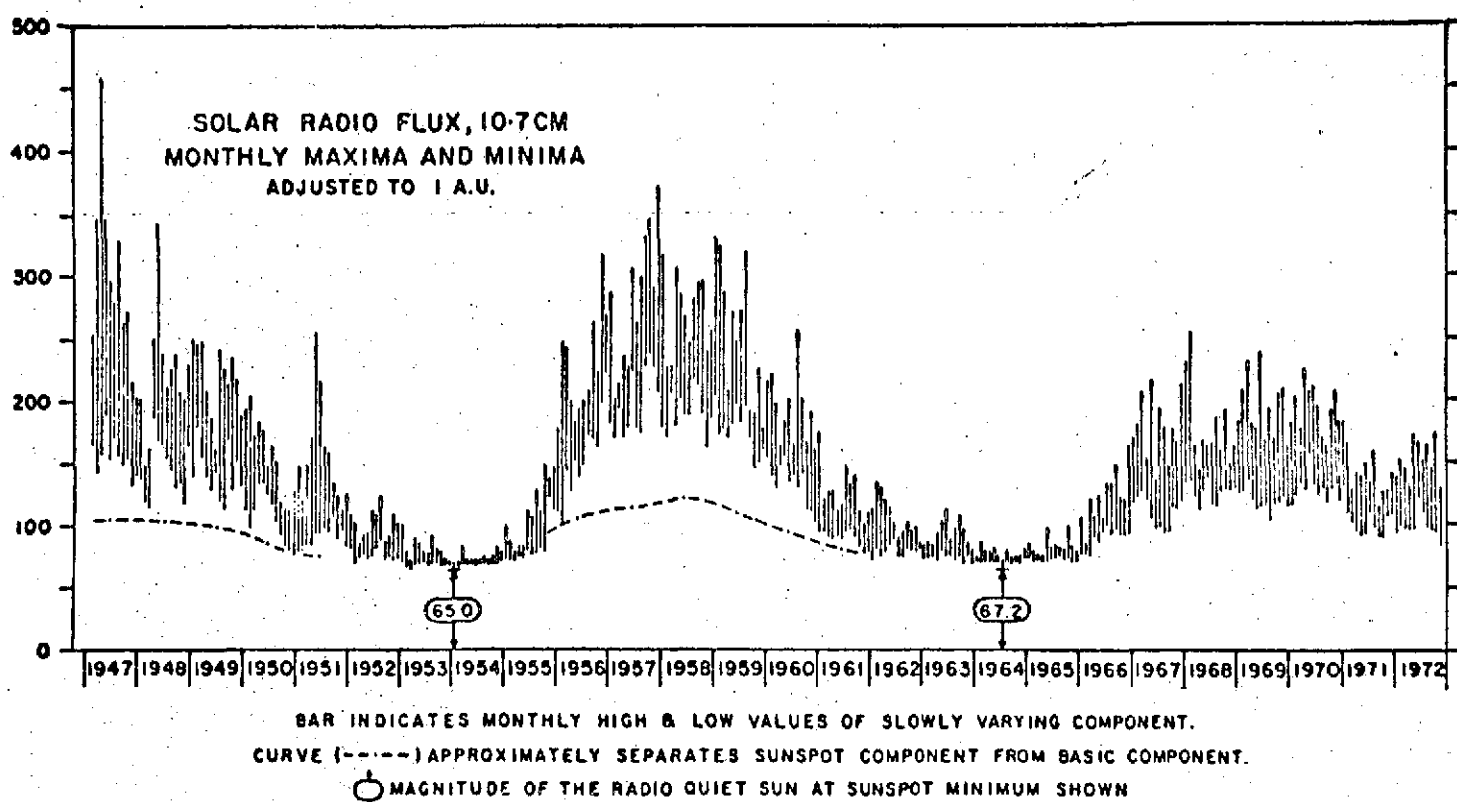


FIGURE 4 Monthly Maxima and Minima of 2800 MHz (10.7 cm) Solar Flux, 1947-1972.
(Covington, 1969)

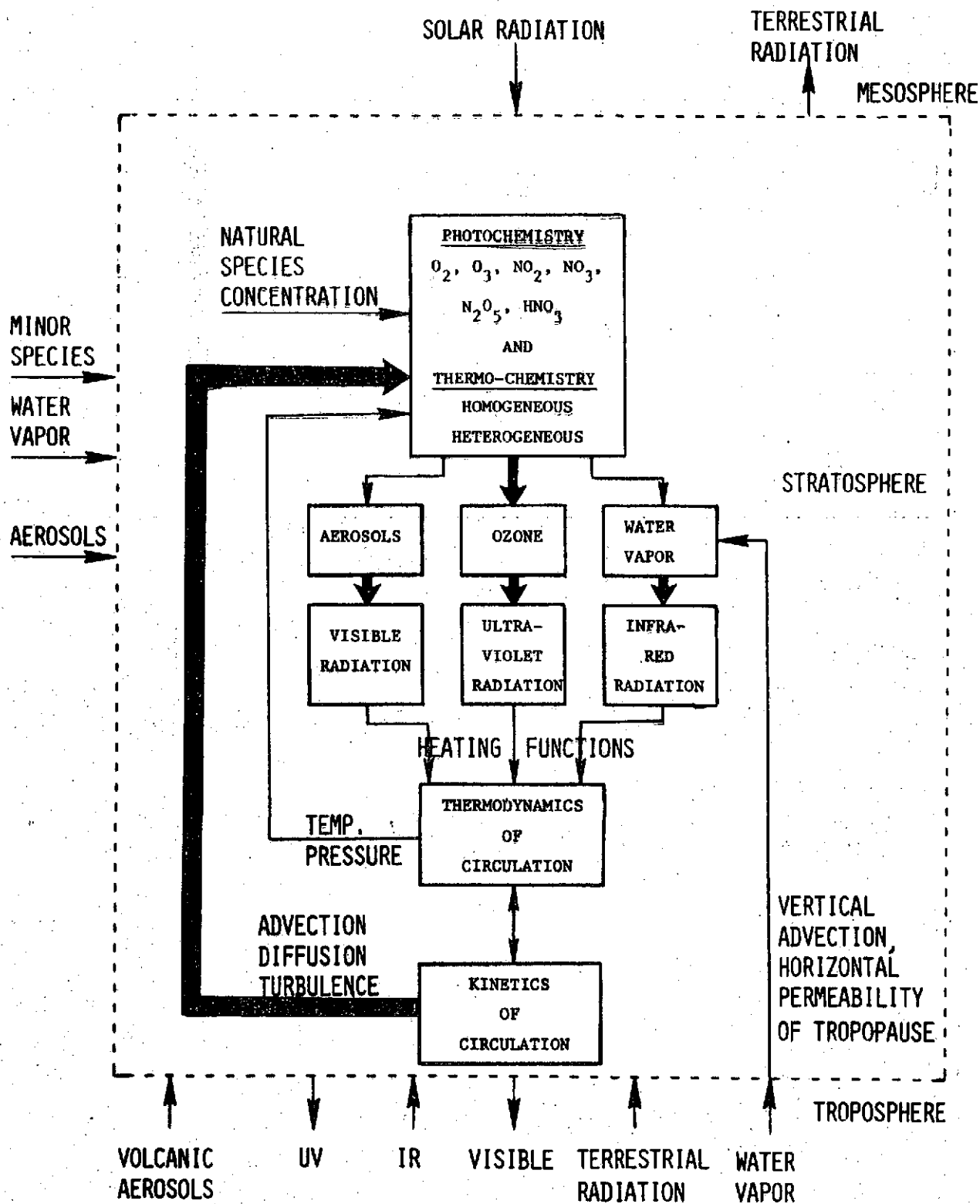


FIGURE 5 Perturbations Affecting the Stratosphere
(Systems Control, Inc., 1973)

REFERENCES CITED IN PART I

- Anderson, A.D; "The correlation between low-altitude neutral density variations near 400km and magnetic activity indices," Planet Sp.Sci. 21, 2049, 1973.
- Anderson, A.D.; "Long-term (solar cycle) variation of the extreme ultraviolet radiation and 10.7-centimeter flux from the sun," J. Geophys. Res. 70, 3231, 1965.
- Blumen, W. and R.G. Hendl; "On the role of joule heating as a source of gravity-wave energy above 100 km," J. Atmos. Sci. 26, 210, 1969.
- Clark, J.; Monthly Wea. Rev. 98, 443, 1970.
- Cole, K.D.; "Joule heating of the upper atmosphere," Australian J. Phys. 15, 223, 1962.
- Covington, A. E., "Solar Radio Emission at 10.7 cm", J Roy Astron Soc, Canada, 63, 125, 1969
- Groves, G.V.; "Seasonal and latitudinal models of atmospheric temperature, pressure, and density, 25 to 110 km," AFCRL-70-0261, 1970.
- Hirota, I.; "The vertical structure of the stratospheric sudden warming," J. Meteor. Soc. Japan 45, 422, 1967.
- Houghton, J.T. and S.D. Smith; "Remote sounding of atmospheric temperature from satellites," Proc. R. Soc. London A 320, 23, 1970.
- Krimigis, S.M. and C.D. Wende; Solar Eclipses and the Ionosphere, ed. M. Anastassiades, Plenum Press, New York, 1970.
- Labitzke, K.; "Synoptic-scale motions above the stratosphere," NCAR 71-139, 1971.
- Lincoln, J.V., Reporting of sudden ionospheric disturbances, Ann. IQSY, 1, 1969.
- Matsuno, T.; "A dynamical model of the stratospheric sudden warming," J. Atmos. Sci. 28, 1479, 1971.
- Muench, H.S.; "Stratospheric energy processes and associated atmospheric long-wave structure in winter," AFCRL Environmental Res. Paper 95, 1965.

References (Cont'd)

- National Academy of Sciences, Physics of the Earth in Space, National Research Council, Washington, D. C., 1969.
- Neupert, W. M.; "X-rays from the sun," Ann. Rev. of Astron. and Astrophys. 7, 121, 1969.
- Rodgers, C. D.; "Remote sounding of the atmospheric temperature profile in the presence of cloud," Quart. J. Roy. Met. Soc. 96, 654, 1970
- Smith, H. J. and P. Smith; Solar Flares, Macmillan Co., New York, 1963.
- Sugiura, M. and S. J. Cain, NASA Goddard Space Flight Center Rep. X-612-69-20, 1969.
- Sugiura, M. and D. Poros; "Hourly values of Equatorial D_{st} for years 1957 to 1970," Goddard Space Flight Center Rep. X-645-71-278, 1971
- Systems Control, Inc., "Climatic Impact Assessment Program Error Variance Analysis," SCI 5101-2, Sept. 1973.
- Timothy, A. F. and J. G. Timothy; "Long-term intensity variations in the solar Helium II Lyman Alpha Line," J. Geophys. Res. 75, 6950, 1970.
- Trenberth, K. E.; "Dynamical coupling of the stratosphere with the troposphere and sudden warmings," MIT, Dept. Meteorology, Ph.D. Thesis, Jan. 1972.
- Webb, W. L.; Structure of the Stratosphere and Mesosphere, Academic Press, New York, 1966.

LITERATURE SEARCH

STRATOSPHERIC WARMINGS

- (Abel 1970), Abel, P. G., Ellis, P. J., Houghton, J. T., Peckham, G., Rodgers, C. D., Smith, S. D., and Williamson, E. J., "Remote Sounding of Atmospheric Temperature from Radiometer for Nimbus D," Proc. Roy. Soc. London, Series A, Vol. 320, Nov. 1970, pp 35-55.
- (Bandeem 1963), Bandeem, W. R., Conrath, B. J., and Hanel, R. A., "Experimental Confirmation from The TIROS VII Meteorological Satellite of The Theoretically Calculated Radiance of The Earth Within The 15-Micron Band of Carbon Dioxide," Journal of the Atmospheric Sciences, Vol. 20, Nov. 1963, pp 609-614.
- (Bandeem 1965), Bandeem, W. R., Halev, M., and Strange, I., "A Radiation Climatology in The Visible and Infrared from The TIROS Meteorological Satellites," NASA TN-D-2534, June 1965.
- (Barnett 1971b), Barnett, J. J., "1.8 The Filter Wedge Spectrometer (FWS) Experiment," The Nimbus 4 Data Catalog, Volume 6, Allied Research Associates, Inc., August 1971, Goddard Space Flight Center.
- (Barnett 1971a), Barnett, J. J., Harwood, R. S., Houghton, J. T., Morgan, C. G., Peckham, G., Rodgers, C. D., Smith, S. D., Williamson, E. J., "Stratospheric Warming Observed by Nimbus 4," Nature, Vol. 230, March 5, 1971, pp 47-48.
- (Barnett 1972), Barnett, J. J., Cross, M. J., Harwood, R. S., Houghton, J. T., Morgan, C. G., Peckham, G. E., Rodgers, C. D., Smith, S. D., and Williamson, E. J., "The First Year of The Selective Chopper Radiometer on Nimbus 4," Quart. J of the Royal Meteorological Soc., Vol. 98, No. 415, pp 17-37 (1972).
- (Blamont 1969), Blamont, J. E., Heinsheimer, T. F., and Pommereau, J. P., "New Experimental Description of the Geographical Temperature Distribution in The Southern Hemisphere Near The 100-Millibar Level During Winter and Spring," Journal of Geophysical Research, Vol. 74, No. 28, Dec. 20, 1969, pp 7038-7043.
- (Charney 1961), Charney, J. G., and Drazin, P. G., "Propagation of Planetary-Scale Disturbances from The Lower into The Upper Atmosphere," Journal of Geophysical Research, Vol. 66, No. 1, Jan. 1961, pp 83-109.
- (Clark 1970), Clark, J. H. E., "A Quasi-Geostrophic Model of the Winter Stratospheric Circulation," Monthly Weather Review, Vol. 98, No. 6, June 1970, pp 443-461.
- (Cole 1970), Cole, A. E., "Extreme Variations in Temperature and Density Between 30 and 90 KM," paper presented at the American Meteorological Society's Fourth National Conference on Aerospace Meteorology, May 4-7, 1970, Las Vegas, Nev.
- (Conrath 1972), Conrath, B. J., "Vertical Resolution of Temperature Profiles Obtained from Remote Radiation Measurements," Journal of Atmospheric Sciences, Vol. 29, No. 7, Oct. 1972, pp 1262-1271.

- (Conrath 1970), Conrath, B. J., Hanel, R. A., Kunde, V. G., Prabhakara, C., "The Infrared Interferometer Experiment on Nimbus 3," Journal of Geophysical Research, Vol. 75, No. 30, Oct. 20, 1970, pp 5831-5857.
- (Craig 1962), Craig, R. A., and Lateef, M. A., "Vertical Motion During The 1957 Stratospheric Warming," Journal of Geophysical Research, Vol. 67, No. 5, pp 1839-1854.
- (Dickenson 1968), Dickinson, R. E., "Planetary Rossby Waves Propagating Vertically Through Weak Westerly Wind Wave Guides," Journal of the Atmospheric Sciences, Vol. 25, Nov. 1968, pp 984-1002.
- (Dickinson 1973), Dickinson, R. E., "Photochemical, Radiative and Dynamic Modeling of The Stratosphere," AIAA Paper No. 73-527 presented at the AIAA/AMS International Conference on the Environmental Impact of Aerospace Operations in the High Atmosphere, Denver, Colo., June 11-13, 1973.
- (Elliott 1970), Elliott, D. D., "Research on the Earth's Upper Atmosphere" Aerospace Report No. TR-0059(6260-10)-1, AF Report No. SAMS0-TR-70-300, 70 Jul 31.
- (Ellis 1970), Ellis, P. J., Peckham, G., Smith, S. D., Houghton, J. T., Morgan, C. G., Rodgers, C. D., and Williamson, E. J. "First Results from the Selective Chopper Radiometer on Nimbus 4," Nature, Vol. 228, Oct. 10, 1970, pp 139-143.
- (EXAMETNET 1971), "Experimental Inter-American Meteorological Rocket Network (EXAMETNET) - The First Five Years, 1966-1970," June 1971.
- (Falbel 1972) Falbel, G., "Design and Performance Characteristics of the Vertical Temperature Profile Radiometer (VTPR) for Atmospheric Temperature Soundings," presented at the 8th Remote Sensing Symposium, Oct. 4, 1972.
- (Finger 1969), Finger, F. G. and McInturff, R. M., "Needs and Uses of Stratospheric Observations in the Stratwarm Programme," in Upper Air Instruments and Observations, Proceedings of the WMO Technical Conference, Paris, 8-12 Sept. 1969, pp 113-131.
- (Finger 1970), Finger, F. G. and McInturff, R. M., "Meteorology and the Supersonic Transport," Science, Vol. 167, pp 16-25.
- (Finger 1964), Finger, F. G. and Teweles, S., "The Mid-Winter 1963 Stratospheric Warming and Circulation Change," Journal of Applied Meteorology, Vol. 3, No. 1, Feb. 1964, pp 1-15.
- (Finger 1967), Finger, F. G. and Woolf, H. M., "Southern Hemisphere Stratospheric Circulation As Indicated by Shipboard Meteorological Rocket Observations," NASA TM X-1346, March 1967.
- (Fritz 1970a), Fritz, S., "Earth's Radiation to Space at 15 Microns: Stratospheric Temperature Variations," Journal of Applied Meteorology, Vol. 9, Oct. 1970, pp 815-823.

- (Fritz 1972a), Fritz, S. and McInturff, R. M., "Stratospheric Temperature Variations in Autumn - Northern and Southern Hemispheres Compared," Monthly Weather Review, Vol. 100, No. 1, Jan. 1972, pp 1-7.
- (Fritz 1970b), Fritz, S. and Soules, S. D., "Large-Scale Temperature Changes in the Stratosphere Observed from Nimbus III," Journal of the Atmospheric Sciences, Vol. 27, Oct 1970, pp 1091-1097.
- (Fritz 1972b), Fritz, S. and Soules, S. D., "Planetary Variations of Stratospheric Temperatures," Monthly Weather Review, Vol. 100, No. 7, July 1972, pp 582-589.
- (Gelman 1970), Gelman, M. E., "The Stratospheric Warming of December 1969 - January 1970," paper presented at the AMS/AGU Meeting April 20-24, 1970.
- (Gelman 1972), Gelman, M. E., Miller, A. J., Woolf, H. M., "A Regression Technique for Determining Temperature Profiles in the Upper Stratosphere from Satellite-Measured Radiances," Proc. AMS International Conference on Aerospace and Aeronautical Meteorology of the AMS, May 26-27, 1972, Wash. D. C., pp 109-112.
- (Girard 1969), Girard, A., and Lamaitre, M. P., "Profils Expérimentaux de l'Horizon Infrarouge de la Terre. Expérience TACITE 2," paper presented at the 13th Plenary meeting of COSPAR, Prague, May 19-24, 1969, (Also ONERA Report T.P. 709).
- (Godson 1969), Godson, W. L., "Problems of and Requirements for High Altitude Balloon Sounding," in Upper Air Instruments and Observations, Proceedings of the WMO Technical Conference, Paris, 8-12 Sept. 1969, pp 95-111.
- (Hanel 1969), Hanel, R. and Conrath, B., "Interferometer Experiment on Nimbus 3: Preliminary Results," Science, Vol. 165, 19 Sept. 1969, pp 1258-1260.
- (Hanel 1970b), Hanel, R. A. and Conrath, B. J., "Thermal Emission Spectra of the Earth and Atmosphere from the Nimbus 4 Michelson Interferometer Experiment," Nature, Vol. 228, Oct. 10, 1970, pp 143-145.
- (Hanel 1970a), Hanel, R. A., Schlachman, B., Clark, F. D., Prokesh, C. H., Taylor, J. B., Wilson, W. M., and Chaney, L., "The Nimbus III Michelson Interferometer," Applied Optics, Vol. 9, No. 8, Aug. 1970, pp 1767-1774.
- (Hanel 1972), Hanel, R. A., Conrath, G. J., Kunde, V. G., Prabhakara, C., Revah, I., Salomonson, V. V., and Wolford, G., "The Nimbus 4 Infrared Spectroscopy Experiment 1. Calibrated Thermal Emission Spectra," Journal of Geophysical Research, Vol. 77, No. 15, May 20, 1972, pp 2629-2641.
- (Heath 1969), Heath, D. F., "Observations of the Intensity and Variability of the Near-Ultraviolet Solar Flux from the Nimbus III Satellite," Journal of Atmospheric Sciences, Vol. 26, Sept. 1969, pp 1157-1160.
- (Heath 1973), Heath, D. F., "Space Observations of the Variability of Solar Irradiance in the Near and Far Ultraviolet," Journal of Geophysical Research, Vol. 78, No. 16, June 1, 1973, pp 2779-2792.

(Hirota 1967), Hirota, I., "The Vertical Structure of the Stratospheric Sudden Warming," Journal of the Meteorological Society of Japan, Vol. 45, No. 5, Oct. 1967, pp 422-435.

(Hirota 1968), Hirota, I., "Planetary Waves in the Upper Stratosphere in Early 1966," Journal Meteorological Society of Japan, Vol. 46, No. 5, Oct 1968, pp 418-430.

(Houghton 1970), Houghton, J. T., and Smith, S. D., "Remote Sounding of Atmospheric Temperature from Satellites - I Introduction," Proc Roy. Soc. London, Series A, Vol. 320, Nov. 1970, pp 23-33.

(Hoxit 1972), Hoxit, L. R. and Henry, R. M., "Diurnal and Annual Temperature Variations in The 30-60 km Region as Indicated by Statistical Analysis of Rocketsonde Temperature Data," presented at the American Meteorological Society International Conference on Aerospace and Aeronautical Meteorology, May 22-26, 1972, Wash. D. C., Proceedings, pp 149-157.

(Johnson 1970b), Johnson, D. S., "Global Atmospheric Research Program," Astronautics and Aeronautics, Oct 1970, pp 28-32.

(Johnson 1969), Johnson, K. W., "A Preliminary Study of the Stratospheric Warming of December 1967 - January 1968," Monthly Weather Review, Vol. 97, No. 8, Aug 1969, pp 553-564.

(Johnson 1968), Johnson, K. W. and Gelman, M. E., "Temperature and Height Variability in the Middle and Upper Stratosphere during 1964-1966 as Determined from Constant Pressure Charts," Monthly Weather Review, Vol. 96, No. 6, June 1968, pp 371-382.

(Johnson 1970a), Johnson, K. W. and McInturff, R. M., "On the Use of SIRS Data in Stratospheric Synoptic Analysis," Monthly Weather Review, Vol. 98, No. 9, Sept. 1970, pp 635-642.

(Johnson 1969), Johnson, K. W., Miller, A. J., and Gelman, M. E., "Proposed Indices Characterizing Stratospheric Circulation and Temperature Fields," Monthly Weather Review, Vol. 97, No. 8, August 1969, pp 565-570.

(Julian 1967), Julian, P. R., "Midwinter Stratospheric Warmings in the Southern Hemisphere: General Remarks and A Case Study," Journal of Applied Meteorology, Vol. 6, June 1967, pp 557-563.

(Koshelkov 1968), Koshelkov, J. P. and Tarasenko, P. A., "Stratospheric Warming in February 1966," (Translation dated 29 May 1970, NLL-M-9039).

(Kuhn 1969), Kuhn, W. R. and London, J., "Infrared Radiative Cooling in the Middle Atmosphere (30-110 km)," J. Atmos Sciences, Vol. 26, No. 2, March 1969, pp 189-204.

(Labitzke 1965a), Labitzke, K., "On The Mutual Relationship between Stratosphere and Troposphere during Periods of Stratospheric Warmings in Winter," Journal of Applied Meteorology, Vol. 4, Feb. 1965, pp 91-99. Also paper presented at the WMO-IUGG Symposium on Research and Development Aspects of Long Range Forecasting, June 29 - July 3, 1964, Boulder, Colo.

- (Labitzke 1968a), Labitzke, K., "Midwinter Warmings in the Upper Stratosphere in 1966," Q. Journ. Royal Meteorological Soc., Vol. 94 (1968), pp 279-291.
- (Labitzke 1971), Labitzke, K., "Synoptic Scale Motions Above the Stratopause," National Center for Atmospheric Research masters thesis NCAR MS No. 71-1.9. Presented at the XV General Assembly of IUGG, Moscow, July 30 - Aug. 14, 1971 - in the Symposium on Energetics and Dynamics of the Mesosphere and Lower Thermosphere.
- (Labitzke 1972a), Labitzke, K., "Temperature Changes in the Mesosphere and Stratosphere Connected with Circulation Changes in Winter," Journal of Atmospheric Sciences, Vol. 29, May 1972, pp 756-766.
- (Labitzke 1972b), Labitzke, K., "The Interaction Between Stratosphere and Mesosphere in Winter," Journal of Atmospheric Sciences, Vol. 29, No. 7, Oct. 1972, pp 1395-1399.
- (Labitzke 1973), Labitzke, K. and Barnett, J. J., "Global Time and Space Changes of Satellite Radiances Received from the Stratosphere and Lower Mesosphere," Journal of Geophysical Research, Vol. 78, No. 3, Jan. 20, 1973, pp 483-496.
- (Labitzke 1965b), Labitzke, K. and Van Loon, H., "A Note on Stratospheric Midwinter Warmings in the Southern Hemisphere," Journal of Applied Meteorology, Vol. 4, April 1965, pp 292-295.
- (Labitzke 1968b), Labitzke, K. and Schwentek, H., "Midwinter Warmings in the Stratosphere and Lower Mesosphere and the Behavior of Ionospheric Absorption," Zeitschrift für Geophysik, Vol. 34, pp 555-566. Presented at the XI COSPAR meeting in Tokyo, May 9-21, 1968.
- (Larsen 1971), Larsen, T. R., "Short Path VLF Phase and Amplitude Measurements during a Stratospheric Warming in February 1969," Journal of Atmospheric and Terrestrial Physics, Vol. 33, pp 1251-1256, 1971.
- (Lebedinsky), Lebedinsky, A. I., Andrianov, Yu. G., Barkova, G. N., Boldyrev, V. G., Karavaev, I. I., Lelyakina, T. A., Polyakova, T. G., Safronov, Yu. P., and Tulupov, V. I., "The Angular and Spectral Distribution of the Earth's Infrared Radiation into Space According to the Results of Measurements from Artificial Earth Satellites," Space Research VIII, pp 1044-1062.
- (Lienesch 1967), Lienesch, J. H. and Wark, D. Q., "Infrared Limb Darkening of the Earth from Statistical Analysis of TIROS Data," Journal of Applied Meteorology, Vol. 6, Aug. 1967, pp 674-682.
- (Lovill 1972), Lovill, J. E., "Characteristics of the General Circulation of the Atmosphere and the Global Distribution of Total Ozone as Determined by the Nimbus III Satellite Infrared Interferometer Spectrometer," Colorado State University, Dept. of Atmospheric Science, Atmospheric Science Paper No. 180, COO-1340-30, Feb. 1972.
- (Matsuno 1970), Matsuno, T., "Vertical Propagation of Stationary Planetary Waves in the Winter Northern Hemisphere," Journal of Atmospheric Sciences, Vol. 27, Sept. 1970, pp 871-883.

- (Matsuno 1971), Matsuno, T., "A Dynamical Model of the Stratospheric Sudden Warming," Journal of the Atmospheric Sciences, Vol. 28, Nov. 1971, pp 1479-1494.
- (McInturff 1969), McInturff, R. M. and Finger, F. G., "Atmospheric Circulation and Variability at Proposed SST Flight Levels," Canadian Aeronautics and Space Journal, Vol. 15, No. 7, Sept 1969, pp 255-259.
- (McInturff 1972), McInturff, R. M. and Fritz, S., "The Depiction of Stratospheric Warmings with Satellite Radiance Data," Proceedings of the International Conference on Aerospace and Aeronautical Meteorology of the American Meteorological Society, May 22-26, 1962, Wash. D. C., pp 113-114.
- (Miller 1970b), Miller, A. J., "The Transfer of Kinetic Energy from the Troposphere to the Stratosphere," Journal of Atmospheric Sciences, Vol. 27, No. 3, May 1970, pp 388-393.
- (Miller 1970c), Miller, A. J., "A Note on Vertical Motion Analyses for the Upper Stratosphere," Monthly Weather Review.
- (Miller 1971), Miller, A. J., "Rocketsonde Repeatability and Stratospheric Variability," Journal of Applied Meteorology, Vol. 10, No. 2, April 1971, pp 320-327.
- (Miller 1972), Miller, A. J., Brown, J. A., and Campana, K. A., "A Study of the Energetics of An Upper Stratospheric Warming (1969-1970)," Quart. Journal Royal Meteorological Society, Vol. 98, Oct. 1972, pp 730-744.
- (Miller 1969), Miller, A. J. and Finger, F. G., "Synoptic Analysis of the Southern Hemisphere Stratosphere," NASA TM X-1814, Aug. 1969.
- (Miller 1970d), Miller, A. J., Finger, F. G., and Gelman, M. E., "30-MB Synoptic Analyses for the 1969 Southern Hemisphere Winter Derived With the Aid of Nimbus III (SIRS) Data," NASA TM X-2109, Dec. 1970.
- (Miller 1970a), Miller, A. J. and Johnson, K. W., "On the Interaction between the Stratosphere and Troposphere during the Warming of December 1967 - January 1968," Quart. Journal Royal Meteorological Society, Vol. 96, No. 407, pp 24-31.
- (Moe 1963), Moe, K. "Statistical Properties of the Fluctuations in Density at 700 Kilometers," Space Technology Labs Report, Sept 1963.
- (Nordberg 1969), Nordberg, W., "Observation of Meteorological Parameters with Research Satellites," Upper Air Instruments and Observations. Proceedings of the WMO Technical Conference, Paris, 8-12 Sept. 1969, pp 433-445.
- (Nordberg 1965), Nordberg, W., Bandeen, W. R., Wernecke, G., and Kunde, V., "Stratospheric Temperature Patterns Based on Radiometric Measurements from the TIROS 7 Satellite," Space Research VII, North Holland Publishing Co, Amsterdam, 1965, pp 782-809.
- (Nordberg 1966), Nordberg, W., McCulloch, A. W., Foshee, L. L., and Bandeen, W. R., "Preliminary Results from Nimbus II," Bulletin of the American Meteorological Society, Vol. 47, No. 11, Nov. 1966, pp 857-872.

- (Phillpot 1969), Phillpot, H. R., "Antarctic Stratospheric Warming Reviewed in the Light of 1967 Observations," Quart. Journal Royal Meteorological Society, Vol. 95 (1969), pp 329-348.
- (Quiroz 1966), Quiroz, R. S., "Mid-Winter Stratospheric Warming in the Antarctic Revealed by Rocket Data," Journal of Applied Meteorology, Vol. 5, Feb. 1966, pp 126-128.
- (Quiroz 1968), Quiroz, R. S., "Synoptic Density Maps of the Upper Atmosphere," Journal Applied Meteorology, Vol. 7, No. 6, Dec. 1968, pp 969-976.
- (Quiroz 1969a), Quiroz, R. S., "Meteorological Rocket Research Since 1959 and Current Requirements for Observations and Analysis Above 60 Kilometers," NASA CR-1293, Upper Air Branch, National Meteorological Ctr., Weather Bureau, Feb. 1969.
- (Quiroz 1969b), Quiroz, R. S., "The Warming of the Upper Stratosphere in February 1966 and the Associated Structure of the Mesosphere," Monthly Weather Review, Vol. 97, No. 8, Aug. 1969, pp 541-552.
- (Quiroz 1970), Quiroz, R. S., "Modification of the Atmospheric Density Field in Response to Stratospheric Warmings," paper presented at the American Meteorological Society's Fourth National Conference on Aerospace Meteorology, May 4-7, 1970, Las Vegas, Nev.
- (Quiroz 1971), Quiroz, R. S., "The Determination of the Amplitude and Altitude of Stratospheric Warmings from Satellite-Measured Radiance Changes," Applied Meteorology, Vol. 10, No. 3, June 1971, pp 555-574.
- (Quiroz 1973), Quiroz, R. S., "The Abnormal Stratosphere Studies with the Aid of Satellite Radiation Measurements," presented at the AIAA/AMS International Conference on Environmental Impact of Aerospace Operations in the High Atmosphere, June 11-13, 1973, Denver, Colo.
- (Quiroz 1972), Quiroz, R. S. and Gelman, M. E., "Direct Determination of the Thickness of Stratospheric Layers from Single Channel Satellite Radiance Measurements," Monthly Weather Review, Vol. 100, No. 11, Nov. 1972, pp 788-795.
- (Reed 1963), Reed, R. J., Wolfe, J. L., and Nishimoto, H., "A Spectral Analysis of the Energetics of the Stratospheric Sudden Warming of Early 1957," Journal of the Atmospheric Sciences, Vol. 20, July 1963, pp 256-275.
- (Ryazonova 1965), Ryazonova, L. A. and Khvostikov, I. A., "Processes in the Stratosphere Based on Rocket Sounding Data," Meteorologicheskije Issledovaniya, No. 9 pp 58-63. Translated as NASA TT-F-399, Dec. 1965.
- (Scherhag 1970), Scherhag, R., Labitzke, K., and Finger, F. G., "Developments in Stratospheric and Mesospheric Analyses which Dictate the Need for Additional Upper Air Data," Meteorological Monographs, Vol. 11, No. 33, Oct 1970, pp 85-90
- (Shen 1968), Shen, W. C., Nicholas, G. W., and Belmont, A. D., "Antarctic Stratospheric Warmings During 1963 Revealed by 15 μ TIROS VII Data," Journal of Applied Meteorology, Vol. 7, Apr. 1968, pp 268-283.

- (Smith 1971), Smith, J. W., "The Genesis of Sudden Stratospheric Warmings and the Quasi-Biennial Cycles," NASA TN D-6522, October, 1971.
- (Smith 1970b), Smith, W. L., "Iterative Solution of the Radiative Transfer Equation for the Temperature and Absorbing Gas Profile of an Atmosphere," Applied Optics, Vol. 9, No. 9, Sept. 1970, pp 1993-1999.
- (Smith 1970a), Smith, W. L., Woolf, and Jacob, W. J., "A Regression Method for Obtaining Real Time Temperature and Geopotential Height Profiles from Satellite Spectrometer Measurements and Its Application to Nimbus 3 SIRS Observations," Monthly Weather Review, Vol. 98, No. 8, Aug. 1970, pp 582-603.
- (Smith 1972), Smith, W. L., "Satellite Techniques for Observing the Temperature Structure of the Atmosphere," presented at the AMS International Conference on Aerospace and Aeronautical Meteorology, May 22-26, 1972, Washington, D. C. Also: Bull Am Met Soc., Vol 53, No. 11, Nov. 1972, pp 1074-1082.
- (Smith 1969b), Smith, W. L. and Fritz, S., "On the Statistical Relation Between Geopotential Height and Temperature Pressure Profiles," NESCTM 18, November 1969.
- (Smith, 1969a), Smith, W. L., and Wark, D. Q., "Atmospheric Soundings Derived From Nimbus III Spectrometer Measurements," Upper Air Instruments and Observations Proceedings of the WMO Technical Conference, Paris, 8-12 Sept. 1969, pp 475-492.
- (Staff 1968), Staff, Upper Air Branch, NMC, NOAA, Weekly Synoptic Analyses, 5-, 2-, and 0.4 Millibar Surfaces for 1968.
- (Teweles 1963), Teweles, S., "A Spectral Study of the Warming Epoch of January-February 1958," Monthly Weather Review, Oct-Dec 1963, pp 505-519.
- (Theon 1970), Theon, J. S., and Smith, W. S., "Seasonal Transitions in the Thermal Structure of the Mesosphere at High Latitudes," Journal of Atmospheric Sciences, Vol. 27, January 1970, pp 173-176.
- (Van Loon 1972), Van Loon, H., Labitzke, K., and Jenne, R. L., "Half-Yearly Wave in the Stratosphere," Journal of Geophysical Research, Vol. 77, No. 21, July 20, 1972, pp 3846-55.
- (Wark 1970), Wark, D. Q., "SIRS: An Experiment to Measure the Free Air Temperature From A Satellite," Applied Optics, Vol. 9, No. 8, Aug. 1970, pp 1761-1766.
- (Wark 1969), Wark, D. Q. and Hilleary, D. T., "Atmospheric Temperature: Successful Test of Remote Probing," Science, Vol. 165, 19 Sept. 1969, pp 1256-1258.
- (Willett 1968), Willett, H. C., "Remarks on the Seasonal Changes of Temperature and of Ozone in the Arctic and Antarctic Stratospheres," Journal of the Atmospheric Sciences, Vol. 25, No. 3, May 1968, pp 341-360.
- (Yates 1969), Yates, H. W., "Present and Future Capabilities of the Sensor Systems on the ESSA Operational Satellites," Upper Air Instruments and Observations, Proceedings at the WMO Technical Conference, Paris, 8-12 Sept. 1969, pp 447-473.

PART II

ANALYSIS OF DATA FROM SPACECRAFT - STRATOSPHERIC WARMINGS

ANALYSIS

TABLE OF CONTENTS

PART II

	<u>Page</u>
1. WARMING CASE STUDIES	
The Stratospheric Warming of April - May 1969	II-1
The Stratospheric Warmings of July - August 1969	II-2
Correlation of Geophysical Indices With SIRS A, Channel 8 Radiances, July - August 1969	II-4
The Stratospheric Warming of December 1969 - January 1970	II-6
Correlation of Geophysical Indices With 10-MB Temperature Increases, December 1969	II-13
The Stratospheric Warming of December 1970 - January 1971	II-16
Correlation of Geophysical Indices, December 1970 - January 1971	II-23
2. CORRELATIONS BETWEEN GEOPHYSICAL INDICES AND STRATOSPHERIC WARMINGS	II-30
The AE Index	II-30
Solar X-rays	II-32
Solar Flares	II-32
The A _p Index	II-33
The D _{st} Index	II-34
The He II Index	II-34
Solar Protons	II-35
The SID Index	II-36
Magnetic Condition	II-36
Summary	II-37
3. DISCUSSION AND CONCLUSIONS	II-40
4. TABLES	II-43
5. REFERENCES CITED IN PART II	II-79
6. FIGURES	II-82

1. WARMING CASE STUDIES

The study began with the selection of a set of cases for study. The original set of cases were identified through an extensive survey of the literature on Stratospheric Warmings. Through detailed study of these cases and additional data acquired during the study, the case histories were expanded. A number of data sources were used in the study of each case. Routine 10-mb analyses on a daily basis are available in microfilm form for the northern hemisphere from the Environmental Data Service, National Weather Records Center. These maps were augmented by a number of additional analyses of warmings kindly loaned the investigators by Mr. Roderick S. Quiroz, Upper Air Branch, National Meteorological Center. Extensive use was made of published materials from journals. These data were derived from rocket sondes, balloon sondes, and satellite analytic soundings and radiance measurements. The bulk of the data used for southern hemisphere analysis was loaned to the investigators by Dr. Sigmund Fritz, National Environmental Satellite Service and consisted of daily digital global maps of SIRS radiance. This data was augmented by a small number of Nimbus 3 MRIR plots of radiance from Channel 3 (14.5-15.5 μ m) obtained from National Space Science Data Center. Attempts to obtain vertical temperature profiles through an identified warming from the Environmental Data Service were unsuccessful. Also unsuccessful were attempts to obtain any data from Clarendon Laboratory, University of Oxford, the principal investigators of the Selective Chopper Radiometer on Nimbus.

The Stratospheric Warming of April - May 1969

Fritz (1970) describes a stratospheric warming present in early May over the Indian Ocean near 45°S. Figure 1 presents a march of the maximum zonal radiance (SIRS A, Channel 8) for 40°S, 50°S, 60°S, 70°S, and 80°S from 15 April - 14 May 1969.

This data was derived from digital plots of SIRS radiance obtained from Dr. Sigmund Fritz, National Environmental Satellite Service. The warming is evident in early May from 40-60°S. However, from 70-80°S, the maximum radiance occurs on 24 April. Figure 2 displays the maximum radiance at latitudes of 40°S or greater. Five peaks are apparent; the two major peaks occur at 30 April and 5 May. Unfortunately, the lack of radiance data for days earlier than 15 April does not allow an accurate selection of the date of the start of this warming. Therefore, no detailed analysis will be attempted; however, some of the data from this warming will be used in later general analysis.

The Stratospheric Warmings of July - August 1969

Three distinct stratospheric warmings occurred between 3 July 1969 and 19 August 1969, with peaks near 13 July, 6 August, and 16 August (Figs. 3 and 4). With regard to the July warming, Fig. 5 (Fritz and Soules, 1970), displays the change in radiance in the CO₂ band centered at 669.3 cm⁻¹ measured by the Nimbus 3 SIRS instrument from 25 June - 10 July 1969. Fig. 6 (Wark, 1970) indicates that this band (channel 8) is most representative of temperatures near 10 mb (31 km). In Fig. 5, cooling (C) occurred everywhere from 20°S-40°N, while large-scale warming took place over much of the region south of 20°S. The 669 cm⁻¹ radiance field on 8 and 9 July 1969 is presented in Finger and McInturff (1970). A 30-mb (24 km) temperature field for 9 July 1969 is shown in Miller et al. (1970).

The starting and ending dates of the July warming may be determined from Fig. 3, where the solid curve is derived from the daily maximum radiance (ergs cm⁻² s⁻¹ ster⁻¹ cm⁻¹) values at latitudes 40°S or greater from SIRS A, Channel 8 world-wide digital printouts, displaying radiance values at intervals of 10 degrees of latitude and 30 degrees of longitude. The maximum radiance values were between 40-60°S latitude. The dashed curves represent the 10-mb (31 km), 30-mb (24 km)

temperatures from Mirny, Antarctica (Finger and McInturff, 1969; Smith et al., 1970). From Fig. 3 the start of the warming at 31 km is (solid curve) at 5 July; the maximum at 13 July, and the end at 21 July. The 10-mb and 30-mb curves indicate that the warming started 3 July. The 10-mb curve indicates that the peak of the warming near the South Pole at 31 km was near 16-17 July. Close agreement is not expected between the solid and dashed curves since the respective locations differ appreciably.

From Fig. 4, solid curve, the second warming starts on 1 August, peaks on 6 August, and ends on 11 August. The third warming starts on 11 August, peaks on 16 August, and ends on 19 August. For these latter two warmings, the Mirny 10-mb and 30-mb temperatures agree within about one day for the start, peaks and ends of the warmings. Fig. 7 presents a 30-mb temperature field for 17 August 1969, near the peak of the third warming (Miller et al., 1970). Two warm centers are shown.

Correlation of Geophysical Indices with SIRS A, Channel 8 Radiances, July - August 1969

Table 1 lists the indices vs. day of the month from 1-17 July 1969. No daily flare index was available for this period. If the start of the warming was 3 July (10-mb and 30-mb curves, Fig. 3), then possible heating candidates are solar x-rays and/or electrojet heating. Solar flare of importance 2 or greater occurred on July 1, 3, 4, 5, 6, and 7. On 3 July, there was an SID of importance 3 and a strong x-ray flux (1-8A). Table 2 shows the 1-8A solar x-ray bursts (Explorer 37) from 1-16 July 1969. The 3 July flux of $0.19 \text{ ergs cm}^{-2} \text{ s}^{-1}$ was not only the strongest x-ray burst measured during this period but it also was of long duration (40 minutes). The AE maximum of 294 on 1 July indicates that joule heating associated with the auroral electrojet must be considered also as a trigger mechanism. On 5 July, there was a flare of importance 3, SID of importance 2⁺, and maxima in solar x-rays, He II flux and AE. If the heating started on 5 July, as indicated by the solid curve of Fig. 3, then EUV heating (He II flux) (140 km) and electrojet (AE) (100 km) are possibilities. Fig. 3 (Solid curve) indicates a broad warming maximum from 8-15 July. This broad maximum could result from enhancements indicated by indices for x-rays, He II flux, Ap, D_{st}, and AE. The x-ray fluxes (Table 2) do not appear strong enough during this period. Again, electrojet heating offers the best possibility since it occurs lower (100 km) than the EUV heating (140 km).

Table 3 lists the indices vs. day of the month from 29 July - 14 August 1969. Fig. 4, solid curve, indicates that the start of the second warming was 1 August; it was followed by a very steep rise in radiance

to the peak on 6 August. A solar flare and SID of importance 3 occurred on 29 July. Also, an x-ray maximum occurred on this date, but the x-ray bursts were not very strong. On 30 July, a principal magnetic storm occurred together with maxima in Ap and AE. On 31 July, a Dst maximum occurred. The most likely cause of the start of the second warming was electrojet (AE) heating.

The third warming started on 11 August and peaked on 16 August (Fig. 4). Both the solar x-rays and He II flux had maxima on 11 August. However, the associated fluxes were not particularly strong. On 7 August, there was an importance 2 solar flare and a weak maximum in x-rays. On 9 August, Ap had a maximum. On 10 August, Dst and AE had moderate maxima.

The Stratospheric Warming of December 1969 - January 1970

A mid-winter warming affecting a deep layer of the Northern Hemisphere stratosphere occurred in December 1969 - January 1970. While limited circulation changes were observed, meteorological rocketsonde data indicated a warming of significant proportions, with temperature increases of up to 80°C near 40 km. At the 10-mb level (approx. 31 km), unusually warm temperatures were first noted over southern Europe after mid-December. According to Gelman (1970), the warm area expanded and the center moved north-eastward along the direction of wind flow to central Siberia, where temperatures warmer than -10°C were observed at 10 mb around 27 December. At West Gelrinish, Scotland, extreme conditions were observed, with a temperature of $+38^{\circ}\text{C}$ and winds in excess of 300 kt. at 43 km. An intense anticyclone centered over Alaska had developed during the course of the warming. At the end of December the warm air at 10 mb was displaced poleward from center Siberia in the southerly flow between this anticyclone and the elongated polar vortex. By January 3, the warm air had reached the polar region with the moderated cold air being displaced southward, thus reversing the normal wintertime temperature gradient.

Miller et al. (1972) constructed high-altitude analyses of the warming event, up to the 2-mb level (43 km). The Satellite Infrared Spectrometer (SIRS) aboard the Nimbus 3 satellite yielded large amounts of radiation temperature data (Quiroz, 1971). The use of rocketsonde and satellite data combined with high-altitude radiosonde observations allowed hemispheric synoptic analyses at the 10-, 5-, and 2-mb levels to be constructed.

Unfortunately, it was not possible to construct the high-altitude analyses on a daily basis. Consequently, analyses were done for the seven selected days: December 17, 24, 29, 31 and January 3, 7 and 14.

Figure 8 depicts the height and temperature analyses at 2-mb for 24 December. At this time the polar cyclone was the prominent circulation feature with ridge development near Japan. The cold centre associated with the polar low is located over Canada, with warm air centers over the USSR and southeast United States. Comparison of the positions of these warm and cold areas with those at 5-mb (not shown here) indicates a general westward slope with height.

By 29 December, Fig. 9, the Eastern Hemisphere warm air center had intensified considerably and moved westward with time. As an example of the change in intensity, a rocket observation at the United Kingdom's West Geirinish station on 23 December measured a 2-mb temperature of -23°C ; but on the 27th, the observed temperature was $+23^{\circ}\text{C}$, a rise of 46°C . In addition, the general height pattern developed a more wave 2 type configuration, with a general elongation of the polar cyclone.

Figure 10 illustrates the analyses for 3 January. It is obvious that tremendous changes have taken place in the height field in the 5-day period from 29 December. The most striking feature on this chart is the segmentation of the height field. Remnants of the polar cyclone were located mainly over the Northern Pacific and Atlantic Ocean areas, while relative highs

were situated over the North American and Eurasian continents, including a ridge across the polar regions. The temperature fields had continued their westward retrogression with the warm air, about $+20^{\circ}\text{C}$, mainly over North America and the cold cell associated with the deepest cyclonic segment located with the coldest air over the Alaskan-Siberian area. This series of maps clearly points out the rapidity with which the warming and circulation breakdown took place.

The last analysis of this series, Fig. 11, shows that by the middle of January, the warming in northern latitudes had run its course and cooling was taking place. The height field, however, was still considerably perturbed and the wintertime polar cyclone had not yet returned to the Arctic region. The circulation changes in lower levels of the stratosphere (at and below about 30 mb) were not nearly as pronounced as those described above. Although warm air was noticeable over the Siberian-Alaskan region, the polar cyclone remained strong and primarily in its seasonal Arctic location.

Figure 12 shows the change in temperature at 2 mb (43 km) from 24 December 1969 to 3 January 1970. This map was derived by subtracting the temperature field in Fig. 8 from that of Fig. 10. The maximum temperature increase is 80 degrees with center located at 258° longitude. The maximum decrease is around 30° with center at 182° longitude.

A description of the major radiance changes during December 1969 - January 1970 has been given by Quiroz (1971). The analysis was based on Nimbus 3 SIRS maps. The features of greatest interest include:

- 1) Development of a strong bi-cellular pattern of high radiance with eastward displacement of the system centered over northwest Africa.
- 2) Apparent wave reinforcement over Siberia (Fig. 13) resulting in a radiance maximum > 70 ergs/ in channel 8, around 27-28 December.
- 3) Translation of high radiance system across the polar area to the western hemisphere, with maximum local increase of 38 ergs/ near 75°N , 10°E , from 24 December to 4 January.
- 4) Dampening of this system, with generation of westward-traveling waves across North America to Asia.
- 5) Displacement of polar low-radiance system (central value 31.5 ergs/ on 24 December (Fig. 13) to Canada, thence westward to Asia (Fig. 14) and return to pole by 9 January.

The down-pointing NIMBUS SIRS instrument has a field of view of about 200 km by 200 km. (The angle of view is $\pm 6^{\circ}$.) The orbit is sun-synchronous and is therefore always shifting westward as the satellite proceeds northward to 81°N , then southward on the opposite side of the globe to 81°S . The longitude separation between successive orbits is 27° . The instrumental accuracy is high. Observations were made every 8 sec along the orbit, yielding some ten measurements every 4° of latitude. The radiance data which were used are generally averages of up to five of these measurements, taken within squares defined in the numerical prediction grid used by the National Meteorological Center, about 380 km on the side. All orbital data that met basic calibration criteria, taken in a 24-hr period centered on 1200 GMT, were used.

Map printout was obtained at 2-day intervals in a 60-day period centered on 26 December 1969 near the time of maximum warming. Analyzed channel 8 radiance maps for two selected dates are shown in Figs. 13 and 14.

For a typical warm-layer thickness (20-25 km), Quiroz (1971) has shown that the central altitude and the amplitude of warming can be satisfactorily discriminated through the use of two simple parameters including the ratio of radiance change in NIMBUS SIRS channels 7 ($\sim 678 \text{ cm}^{-1}$) and 8 ($\sim 669 \text{ cm}^{-1}$). A nomogram is developed for specifying warming altitude and amplitude from observed radiance changes and is tested during the December 1969 - January 1970 warming event.

A distinct pattern is revealed in the ratio of change in channels 7 and 8, with decreasing values poleward for the period 20-28 December and from the pole to the North Atlantic in the next 8-day period.

The ratio varies from more than 1.00 in the "rear" portion of the system of large increase, to less than 0.30 in the forward part. On the basis of the Quiroz model, this ratio pattern together with the actual radiance increases in channel 8 implies warming of approximately 60°C centered near an altitude of 25 km in the rear portion; and of $70\text{-}80^\circ\text{C}$ centered just above 40 km in the forward portion.

Northern Hemisphere 10-mb (31 km) charts were available from the Numerical Weather Prediction Unit, National Weather Service, for 1200 GMT each day in December 1969 and January 1970. These series of maps offer the best opportunity to define many of the SW characteristics in detail. Inasmuch as the warmings proceed from above, these charts can be used to determine the latest dates at which the warmings start. Also, they probably give the best information on the end of the warmings. Figure 15 shows the chart for 26 December 1969; the maximum warming center (266°K) is located at 100°E and 57°N . Figure 16 illustrates the movement of this center from 23 December (140°E , 50°N) to 30 December (90°E , 60°N). Several other warming centers were also present at 10 mb during the same period, but they were not as intense. The circles on Fig. 16 indicate the location of warming centers at 2 mb (43 km) for 24 and 29 December 1969. It is obvious that the maximum warming centers on these dates do not coincide at 10 mb and 2 mb. Figure 17 is a plot of the daily maximum temperature at 10 mb (31 km) occurring in the higher latitudes of the Northern Hemisphere. The maximum temperatures on 21 December 1969 and 7 January 1970 are the same, as indicated by the straight line. It appears that the start of the warming occurred on about the 17 December and the end by the 5 of January at 31 km altitude. The dashed line on Fig. 17, indicating the maximum 2 mb (43 km) temperature, is based on 5 values from Fig. 8-11 and Miller et al. (1972) (indicated by crosses on Fig. 17). It appears that the highest maximum temperature at 2 mb occurred on Dec. 27. There was little change between 29 Dec. 1969 and 3 Jan. 1970, during the same period when the 10 mb maximum temperatures are decreasing markedly. Although some of the difference occurring between

10 mb and 2 mb may be explained by the scarcity of 2 mb data, it is difficult to explain all the difference on this basis. Rather, it appears likely that warming center locations (Fig. 16) and magnitude (Fig. 17) differ considerably at the two altitudes for the same date.

Hence, it can be concluded from 2 mb, 10 mb, and radiance data (Quiroz, 1971) that the maximum warming occurred between 26-29 December 1969 at altitudes 25-43 km. It is more difficult to determine the start or end of the warming. The warming certainly has started by 24 December, although the 10 mb data (Fig. 17) indicates that it could have started as early as 17 December. Likewise, the end is difficult to pinpoint. Figure 11 and Fig. 17 indicate that the warming had run its course by 14 Jan. 1970 at 2 mb; it definitely appears to end at 10 mb by 5 Jan. (Fig. 17). Nothing can be stated concerning the altitudes above 45 km.

Correlation of Geophysical Indices with 10-MB Temperature Increases,
December 1969

Maxima in the daily flare index, SID's and x-rays are expected to occur on the same day as solar flares. This is not necessarily true of the 2800 MHz flux unless the EUV associated with the flare is very strong. Likewise, maxima of solar protons, A_p , Dst, and AE should occur about two days later than a flare. This information may give clues that can be used to distinguish among possible heating from the various solar effects. For example, we should expect x-ray heating to occur immediately after a solar flare, while proton heating would occur approximately two days later. Also, x-ray heating (electromagnetic) should occur on the dayside of the earth only. Protons precipitate on both the day and night sides with a marked preference for the auroral zones.

Table 4 lists the indices vs. day of the month from 11-27 December 1969. On 17 December, the 10-mb (31 km) maximum temperature was 238°K it increased 10 degrees to 248°K on the 18th of December and dropped down to 241°K on 19 December. The warming center was located near 35°N, 20°E. According to Groves (1970), the average temperature at 35°N during December is about 237°K. Assuming for the moment that this marked temperature rise was due to an extra terrestrial (solar) cause, what is a possible candidate?

Note in Table 4 that an importance 3 solar flare occurred on 14 December. This flare occurred at 0345 UT in McMath plage region 10477. On this same day the daily flare index and solar x-rays (1-8A) experienced relative maxima of 115 and 9×10^{-3} ergs cm⁻² s⁻¹, respectively. About

two days later (Dec. 16), the solar protons greater than 10 MEV exhibited an hourly maximum of $1596 \text{ cm}^{-2} \text{ s}^{-1}$. Also, relative maxima were exhibited on 16 December for A_p , Dst, and AE. On 17 December, an importance 2 flare occurred; the daily flare index was 457 or almost four times as high as on 14 December. Also, an SID of importance 2 and solar x-ray maximum ($26 \times 10^{-3} \text{ ergs cm}^{-2} \text{ s}^{-1}$) occurred on 17 December. The proton maxima, recurring at 2-3 day intervals, are probably due to the earth's radiation belt. Therefore, if the flare of December 17 was responsible for the temperature maximum of 248K occurring on the 18th of December, the most likely mechanism was heating of the atmosphere below 100 km by solar x-rays (1-8A) occurring on 17 December. Table 5 indicates that the x-rays on 17 December were more intense and longer lasting than on 14 December. If this were true, then it took about a day for the heating between 60-100 km to reach the 10-mb surface at 31 km.

If the heating is associated with the flare of 14 December, then the AE index maximum of 190 on 16 December indicates that the most likely avenue was Joule heating associated with the auroral electrojet near 100 km. The maximum hourly value of the AE index (521) occurred on 16 December at 1700 UT. The AE index was above the December 1969 monthly mean of 110, 71 percent of the hours on December 16 (Table 6). Thus, if electrojet heating was the cause, it took about two days for the heating to reach the 10-mb surface at 31 km. One problem with electrojet heating is that it is restricted to higher latitudes near the auroral zone, at least initially. However, the warming center on the 18 December was located near 35°N .

The 10-mb (31 km) temperature (Table 4) increased 10 degrees from December 24 to December 25 and 5 degrees from December 25 to December 26, reaching a maximum of 263°K on December 26. On December 23, there were maxima in x-rays, protons, A_p and AE. All maxima except the x-rays evidently originated from the solar flare (importance 2) that occurred on 21 December with a daily flare index maximum of 142. In this case, the heating could have been caused by x-rays, or the electrojet, or a combination of these. Table 5 does not indicate an especially strong flux of x-rays on December 23. On the other hand, the AE index was above normal 75 percent of the time on December 23 (Table 6), about two days before the marked 10-mb temperature change of 10 degrees.

The Stratospheric Warming of December 1970-January 1971

This major midwinter warming is a typical example of the so-called "European-type" warming. For the first time such an event could be followed at regular intervals at high altitudes up to 42 km with available Nimbus 4 data. In April 1970, Nimbus 4 carried into space, in addition to SIRS B, the Selective Chopper Radiometer, which measures the thermal emission in selected channels (Houghton and Smith, 1970). The radiometer has six channels, each accepting infrared radiation emitted by carbon dioxide in the atmosphere below the satellite at wavelengths of approximately 15 μm . The radiation measured by channel A originates in a layer approximately 20 km thick centered at the 2 mb (42 km) level, while that measured by channel B originates in a layer of similar thickness centered at 20 mb (26 km). Figs. 18a and c are northern hemisphere maps of channel A radiance, while Figs. 18b and d are northern hemisphere maps of channel B radiance (Barnett et al., 1971). Table A gives the black body temperature equivalent to infrared radiance for channels A and B. The interpretation in terms of atmospheric temperature is explained in Ellis et al., (1970); as a rough guide it may be considered that these temperatures are those occurring in the region of the 2mb and 20 mb levels, respectively.

Figs. 18a and b show the situation on December 30, 1970. On channel A (Fig. 18a), a warm region with a maximum radiance of $95 \text{ mW/m}^2\text{-sr-cm}^{-1}$ was developing at $45^\circ\text{N } 65^\circ\text{E}$; 3 days earlier this warm region had been at $25^\circ\text{N } 20^\circ\text{E}$ with a maximum radiance of $85 \text{ mW/m}^2\text{-sr-cm}^{-1}$. A corresponding warm region was present on channel B (Fig. 18b) with a maximum at $35^\circ\text{N } 50^\circ\text{E}$, implying a northward tilt of the warm anomaly.

Table A
 Equivalent Temperature as a Function of
 Radiance for a Black Body
 Nimbus 4 Selective Chopper Radiometer

<u>Radiance $\text{mW/m}^2\text{-sr-cm}^{-1}$</u>	<u>Equivalent temperature ($^{\circ}\text{K}$)</u>
30	201.0
40	213.7
50	224.7
60	234.5
70	243.6
80	251.9
90	259.8
100	267.2
110	274.2
120	281.0

By January 4, 1971, a great change had occurred in the temperature distributions observed by both channels. The warm area described above had intensified and at the 2 mb level (Fig. 18c) had moved north to 70°N 90°E with a radiance at the center of $120 \text{ mW/m}^2\text{-sr-cm}^{-1}$. At this time the difference in equivalent temperature near the 2 mb level between the hottest and coldest region was more than 60 K. The whole northern hemisphere was dominated by a wave number one pattern with little contribution from the higher wave numbers apparent on December 30. The pattern was similar at the 20 mb level, but the amplitude of wave number one was less and the phase is about 25° farther eastward. This implies a westward tilt of the warm anomaly of 1.5° longitude per km height. Subsequently, the warm region increased little in intensity, but moved westward. On January 9, the warm region had moved to 75°N 40°E with a westward slope of 3° longitude/km;

thereafter the warm region at the 2mb level moved farther westward and decayed in intensity.

On channel A on December 30 (Fig. 18a), there was a warm region at 65°N 120°E and a corresponding warm region on channel B (Fig. 18b) at 65°N 170°E ; this was what remained of a warming which had a maximum intensity on December 26 at 70°N 125°E at the 2 mb level. On December 30 this warm anomaly had a westward tilt of 3° longitude/km while the cold anomaly over North America had a westward tilt of approximately 4.5° longitude/km. By January 2, this warm anomaly had disappeared.

The increase of amplitude of the warming and the westward phase tilt with height are to be expected if temperature variations are caused by upward propagating planetary waves (Dickinson, 1968).

The Nimbus SIRS instrument was described in the section containing the Stratospheric Warming of December 1969-January 1970. Labitzke (1972) uses both the SCR and SIRS data to describe the warming of December 1970-January 1971. The set of maps in Fig. 19 shows the intense development over Asia on 6 and 7 January 1971. In Fig. 19a, the 30-mb temperatures are compared with the radiances of channel 8 of SIRS. The northwestward displacement of highest radiances from the warm region of the Aleutian high is very pronounced indicating a strong development in the upper stratosphere, since conditions in the lower stratosphere (100 and 50 mb) are known to be similar to those at 30 mb. The lowest radiances are also found somewhat west of the cold pole. The pronounced wavenumber 1 should be noted.

On 6 January (Fig. 19b), the highest radiances of channel A have reached polar latitudes and are found west of the center of warmest air at the 45-km level, though this, of course, can be stated only tentatively because of the few rocket observations. Comparing the position of the lowest temperatures with the lowest radiances, we note that the distribution is not the same as in early winter and that it differs from that of the lower stratosphere in Fig. 19a. The center of lowest radiances in Fig. 19b is found east of the lowest temperatures which reflects an eastward tilt with height of the axis of the cold pole. This agrees with the temperatures at 60 km (Fig. 19c), where one part of the cold pole is found over the Barents Sea.

The axis of warmest air slopes with height across the polar region and at the 60 km level (Fig. 19c), it is found over Canada, right above the cold pole of the upper stratosphere. Cooling took place at 60 km over Asia, Europe and Alaska, i.e., above the intense warming area where the stratopause descended to about 40 km; and the northerly winds over Canada and Alaska indicate that the Aleutian high moved toward northern Siberia, dominating the circulation over the whole arctic, while the center of the polar vortex was displaced toward Iceland.

Fig. 20 is a plot (solid line) of the daily maximum temperature at 10 mb (31 km) occurring at the higher latitudes in the Northern Hemisphere from 15 December 1970 to 24 January 1971, derived from NWP maps. The dashed line connects the daily zonal means of channel A of the SCR on Nimbus 4 converted into equivalent blackbody temperatures for an average value for 60° and 80° N. latitude. (Labitzke and Barnett, 1973) This represents the best estimate

available of the high latitude temperature at 2 mb (43 km). From Fig. 20, the 2-mb temperature is greater than the 10-mb temperature from 22 Dec. 70 to 24 Jan. 71. The 2-mb temperature rises continuously from 17 December to 27 December. Both the 10- and 2 -mb temperatures show maxima near 28 Dec. 70 and 10 Jan. 71. The 10-mb curve indicates strong maxima at 4, 8, and 11 Jan. 71; the smoother 2-mb curve does not indicate these peaks. However, this is not surprising in view of the type of averaging employed (zonal averaging). Evidently, the start of the warming is 17 December.

Fig. 21 shows the location of the warming centers (maximum temperatures) at 3-day intervals on the 10-mb (31 km) NWP Unit charts for 1-13 January 1971. The crosses indicate the location; the dates are beneath the crosses. Two main centers are apparent on January 1 at widely separated locations; one center near 40° N, the other near 60° N. These centers merge near 80° N by 13 January.

The December 1970 - January 1971 warming represents the first occasion in which it is possible to determine in some detail the three dimensional structure of a stratospheric warming up to 60 km. The period selected (Jan. 6-7, 1971) is near the middle of the major warming interval (Fig. 20). Northern hemisphere isotherm patterns were derived at every 5 km from 25 to 60 km by using the maps of Fig. 19 (Labitzke, 1972) and the temperature profiles in Fig. 22 for January at 30° N, 50° N, and 70° N (Groves, 1970). The dashed curve in Fig. 22 represents the warming profile for January 6, 1971 at 60° N, derived from the maps in Fig. 19 and the 10-mb NWP Unit chart. Hence, the 25-60 km maps were derived by graphical addition and subtraction,

using Fig. 19 and extrapolation, using Fig. 22, the solid curves of Fig. 22 for the cold low areas and the dashed curve for the warming areas. Fig. 23 shows the location of the centers of the warm areas (crosses) and cold areas (circles) from 25-60 km on 6 Jan. 71. The altitude in kilometers is indicated below the circles and crosses. The closed cold isotherm center appears at all altitudes from 25-60 km, while the warm center appears only between 30-50 km. The cold center has a decided slope with increasing altitude, while the warm center has only a slight slope. In addition to these two features, there was another warm center from 35-55 km located near 25°N , 240°E , which was about 5 degrees warmer at the same altitude, from 40-50 km, ~~than~~ the higher-latitude warm center (Table 7). The 10-mb NWP Unit charts were not used in this analysis in order to maintain internal consistency. The two triangles on Fig. 23 indicate the location of two warm centers appearing on the 10-mb (31 km) chart; the square indicates the 10-mb low center position.

Although the information in Table 7 is useful, perhaps a more meaningful way of depicting the December 1970-January 1971 stratospheric warming is to find those areas of the atmosphere where the temperature differed from normal and the magnitude of the difference. In order to accomplish this, the "normal" situation must be defined first. To do this, mean monthly 10-mb and 5-mb maps for January 1966 (Labitzke, 1968) were used inasmuch as no major warming occurred during this month. At 60 km, the map for 27 January 1971 in Fig. 10c of Labitzke (1972) was used since the warming has disappeared by this date and the temperature field has returned to normal. The maps at every 5 kilometers from 25-60 km were derived by

graphical addition, subtraction and extrapolation in the same way as the "warming" maps above. Finally, temperature change maps were derived at every 5 kilometers from 25-60 km and 5 degree isotherm intervals by graphically subtracting at each altitude the "normal" map from the "warming" map. Fig. 24 shows the temperature change map at 25 km for 6 January 1971. Table 8 displays the location above 40° N of the temperature change centers at every 5 km from 25-60 km. The maximum increase ($+45^{\circ}$) occurs from 40-50 km near 80° N between $70-125^{\circ}$ E. There are two temperature increase centers at 35 km and 55 km. There is only one temperature decrease center above 40° N; it exists between 50-60 km. Fig. 25 indicates the location of the centers on a Northern Hemisphere map, where a cross denotes a center of temperature increase and a circle is a center of temperature decrease. A comparison with Fig. 23 points out that a maximum temperature increase or decrease is not located at the same place as a warm or cold center. However, evidently there is some correlation; for example, the movement of the temperature decrease center from 50-60 km (Fig. 25) appears to be related to the movement of the cold center (Fig. 23). Fig. 26 is a plot illustrating how the maximum $+\Delta T$ changes with altitude at the same location (78° N 70° E; Table 8). The data points, selected from the ΔT charts from 25-60 km, are fitted with two straight lines meeting at 45 km. Fig. 27 shows how the gradient of $+\Delta T$ varies from the center at 78° N 70° E along the 70° E meridian. The gradient can be represented by two straight lines fitted to data points selected from the 45 km ΔT chart. One line indicates a constant ΔT of 45° K from 78° N to 66° N. The other line shows that ΔT decreases linearly to 28° N.

Correlation of Geophysical Indices, December 1970-January 1971

Highlights for 08-15 December 1970: Nineteen events of class M or greater were observed during the past seven days - fourteen small class M (class M3 or less), one each of class M5, M7, and M8, and two class X1. In addition, a minor proton enhancement and a major geomagnetic storm were observed. McMath regions 073 (N15W54, L = 034) and 077 (N10W17, L = 357, includes region 079 which was combined with 077 on 14 December) accounted for 15 of the events. Region 077 produced the following major events - class M5 imp 1N at 09/0758Z with minor radio frequency emission and significant ionospheric disturbances; class X1 imp 1B at 11/1016Z with a 630 flux unit burst at 2700 MHz and significant SID; class X1 imp SB at 12/0856Z with minor radio emission and major SID; and class M7 imp Sn at 12/2348Z with minor radio emission and moderate SID. Region 073 produced the class M8 imp 2N event near N16W00 at 11/2215Z.

Highlights for the period 16-22 December 1970: Only three events of M intensity have been reported the past seven days:

18/0118Z	M1	No optical counterpart
22/1245Z	M6	Optically 1B, N22W44
22/1516Z	M5	Optically 1B, N24W44. Accompanying 10 cm burst of the order of 100 flux units.

In addition, a major radio burst with no optical counterpart was observed by three different observatories at 17/0549Z. The peak flux values at 21 and 11 cm as observed at Carnarvon, Australia were 249 and 5300 flux units, respectively. Moreover, Solrad-9 observed no x-ray burst corresponding to

this radio burst. Both energetic flares on 22 December arose within McMath region 084. The associated spot group made its initial appearance on 18 December near N24, L = 290 and grew rapidly to a type/area D/180 by 19 December. **Another** spot group within McMath plage 084 attained a class/area of D/490 but produced no energetic events. Proton counting rates near earth have remained at background.

It was shown (Fig. 20) that the 2-mb zonal temperature rose continuously from 17-27 December. From this, it was estimated that the warming started about 17 December 1970. Table 9 presents the indices vs. date from 8-24 December 1970. The solar proton maxima are due to electrons from the earth's radiation belt. The only solar flare of importance 2 or greater during this period was on 11 December, 2215 UT. This flare was accompanied by a major radio burst of 1020 flux units at 2700 MHz and moderate SID. The ATS-1 satellite observed a proton enhancement with a gradual beginning at about 12/0500Z. The 21-70 Mev energy range peaked at two particles per sq cm per sec (about four times background) near 12/1700Z. Peaks occurred in the 5-21 Mev flux (250). Nighttime absorption of 0.6 db was observed on the Thule 30 MHz riometer. The 14/0200Z peak in the lower energy particle flux had a very sharp onset and rapid decay and coincided with a geomagnetic sudden commencement at 14/0156Z.

In Table 9, on 12 December there were maxima in the daily flare index, solar x-rays, and 2800 MHz solar flux. On 14 December, a magnetic storm occurred. On this day, there were very pronounced maxima in A_p , Dst, and AE.

If the start of the warming ~~were~~ associated with the flare of 11 December, then the large AE maximum of 416 on 14 December indicates that the most likely avenue was Joule heating associated with the auroral electrojet near 100 km. The maximum hour value of the AE index (527) occurred on 14 December at 2300 UT. The AE index was above the December 1970 monthly mean of 134, 91 percent of the hours on 14 December and 75 percent of the hours on 15 December. Thus, if electrojet heating ~~were~~ the cause, it took about two days to reach the 2-mb surface near 43 km. The start of the warming at 10-mb is estimated to be 18 December. The daily 10-mb NWP charts for December 1970 plainly indicate that a small 243°K isotherm center located at 42N 215E on 18 December expanded greatly as it moved North to 60°N, so that it covered most of Siberia on 27 December.

Highlights for the period 23-29 December 1970: Solar activity was at an extremely low level throughout the past seven days. One class M5 west limb event was observed from McMath region 084 (N18 L = 290) at 26/0840Z. Although the x-ray burst was of M5 intensity its total duration was only about 10 minutes. The associated radio burst was about 75 flux units at 2700 MHz. A minor sudden ionospheric disturbance was reported. A small satellite level proton enhancement began at 24/0740Z. The peak fluxes observed by ATS-1 occurred at 24/2200Z and were of the order of 40 (5-21 Mev) and eight (21-70 Mev) particles per sq cm per sec. The specific cause of this proton enhancement is unknown; the nearest energetic events were the class M9 (22/1516Z) and M6 (22/1245Z) events near N22W44 in region 084. The particle enhancement may have resulted from coronal storage of particles energized by the above events or from an event behind the west limb. The fluxes are still very slightly enhanced as of 29/1700Z. The geomagnetic field was relatively quiet throughout the period.

Highlights for the period 30 December 1970-05 January 1971: No energetic flares were observed during the 7-day period. On the average 6 small regions were visible each day; no one disk feature exceeded 200 millionths in area. A sector-like magnetic disturbance began about 02/0445Z followed by a 120 gamma bay roughly 4 hours later. No sudden commencement marked the storm's onset, however, the co-rotating proton stream was detected by ATS-1.

Highlights for the period 06-12 January 1971: Solar activity continued at a very low level with an average of only ten subflares per day. The most energetic event was a class M1 subnormal flare at 10/1728Z in McMath region 111 (S04W32, L=003). This region dominated the solar disk throughout the week with a large (E/800 millionths) but magnetically simple sunspot group. It was probably the source of a 20-200 MHz radio noise storm which has been in progress since 07 January. The geomagnetic field was also very quiet.

Table 10 lists the indices vs. day of the month from 25 December 1970 to 10 January 1971. The E-W and N-S average daily wind components in the meteor region above College, Alaska (Hook, 1972) are presented at the bottom of the table. A significant change in prevailing winds at the 75-100 km level at College was observed by Hook during this warming. These winds for the upper mesosphere and lower thermosphere were derived from radar measurements of the drift of meteor trails. The normal prevailing wind at College in the wind is eastward and usually poleward. During the stratospheric warming, both the meridional and zonal prevailing flow reversed from about December 31 to January 7, as indicated by the minus values in Table 10. A reversal

in the wind was not evident at 130 km. Hence, the upper limit of the circulation breakdown does not appear to have extended above approximately 100 km at College for this warming event. This wind data by Hook is important because it indicates for the first time the vertical extent of a fully developed stratospheric warming. The highest map of Figure 19 goes up to 60 km; the Hook wind data extends the warming effect upward another 40 km.

Hook (1972) defines the warming by means of a Temperature Index Parameter (TIP), which indicates the mean temperature gradient from the pole to 60°N, and a circulation index, called the Height Index Parameter (HIP), at 60°N (Johnson et al., 1969). Hook concludes that the warming, indicated by the minus wind components, started approximately 10 days before the warming at the 10-mb level, indicated by plus values of TIP starting about 10 January. From this, he states that the circulation breakdown during this warming affected the meteor region before it affected the mid-stratospheric level. However, the daily 10-mb maximum temperatures in Table 10 indicates a minor peak in the warming on 27-28 December. The 2-mb zonal temperature has maxima on these same days. Based on this, some warming apparently occurred before the wind reversal pointed out by Hook. Thus, Hook's conclusion that the warming affected the meteor region before the mid-stratosphere is questionable. Also, the value of TIP and CIP is questionable for indicating the start of a stratospheric warming. As pointed out previously, the daily 10-mb NWP charts for December 1970 plainly indicate that a small 243°K isotherm center located at 42N 225E on 18 December expanded greatly as it moved north to 60N so that it covered most of Siberia on 27 December. It is not easy to pinpoint the start of the warming, but

it was indicated previously from 2-mb data that it started near 17 December (Figure 20).

No flare of importance 2 or greater occurred during the period covered in Table 10. The daily flare indices were all below 85. The low level of solar activity is also exhibited in the small solar x-ray flux. The 2800 MHz solar flux, representing the EUV, varied in a fairly regular manner. The solar proton maxima occur at regular intervals, indicating the influence of the trapping region. The maxima in A_p , Dst, and AE on December 28 seem to have little influence on the 2-mb and 10-mb temperature maxima of the same date, inasmuch as these latter maxima did not change from the previous day. Both temperatures decrease from 28 to 29 December. Table 10 indicates that nothing occurred on 25 or 26 December that could result in the temperature maxima on 27-28 December. Table 9 shows on 22 December an SID with importance of 2 and maxima in the daily flare index and solar x-rays. On 24 December, a "disturbed" day, a small solar proton enhancement was observed. Also, maxima occur in A_p , Dst, and AE. Since the 2-mb temperature exhibited a 3-degree increase from 25 to 26 December, and the 10-mb temperature showed a 5-degree increase from 26 to 27 December, electrojet heating is not ruled out as the cause for the minor warming peak on 27-28 December.

Table 10 (including Hook's wind data) show that the stratospheric warming involved the whole atmosphere from about 30 km (10-mb) to 100 km from about 31 December 1970 to 9 January 1971. Although it is not possible to seek a trigger mechanism during this period, it is possible to look for enhancements. For example, the 10-mb charts show maximum temperatures on 4,

8, and 11 January 1971. On the other hand, the 2-mb zonal temperatures indicate a fairly steady rise from 243°K on 31 December to a maximum of 268°K on 10 January. Therefore, no clues based on enhancement are to be sought here. Unfortunately, the AE index was not available for January 1971, so no check could be made on the possible effect of joule heating.

2. CORRELATIONS BETWEEN GEOPHYSICAL INDICES AND STRATOSPHERIC WARMINGS

A statistical analysis was made to compare average values of the indices for warming and nonwarming days with that for total days considered. Also, comparisons were made with average values of the indices for 0 to 4 days preceding the date of start of warmings, and date of major and minor warming peaks. The daily flare index was not included because it was not available in April - August 1969. Also, the 2800 MHz solar flux index was left out, since the He II index is a more accurate index for EUV. The following dates were selected as the start and end of the warmings 1969-1971:

15 April - 10 May 1969

3 July - 21 July 1969

1 August - 11 August 1969

11 August - 19 August 1969

17 December 1969 - 4 January 1970

17 December 1970 - 21 January 1971.

The AE Index

AE indices were selected during the above warming months. There were 98 "warming" days and 134 "nonwarming" days. AE averages for both warming and nonwarming days did not differ significantly. Table 11 displays the AE index versus the elapsed days from start of the warmings above, for up to 4 days preceding the warming. The April - May 1969 warming was not included inasmuch as the start time could not be determined accurately.

In all five cases, AE had a large maximum one to three days preceding the start of the warming. Table 12 shows the relative variation of AE from the average value of each 5-day period vs. elapsed days from start of warming. There is marked variation in the day-by-day values of AE in the days immediately preceding the start of the warmings. The average value of AE for the two days preceding the start of all warmings was 46 percent above the averages for the five-day intervals considered; it was 37 percent below average on the day the warmings started. The relative AE variations are even greater for all individual warmings, except for that starting 11 August 1969. The others show variations ranging from 59 percent to 183 percent above average at 1-3 days preceding the start of the warmings. It is not unusual to find variations of the type indicated in Table 12 during any five-day interval. However, it may be significant that the daily variations line up in the fashion described, where on 0 day, all AE indices are below normal, the -1 day, one is below normal, the -2 day, none, -3 day, three are below normal, and the -4 day, four are below normal.

The relationship of the AE index to warming was explored further with regard to the major and minor warming peaks. Table 13 exhibits the AE index vs. elapsed days from date of ten major warming peaks. The AE relative maxima are marked with an asterisk. It is noted that there are twice as many relative maxima on either -1 and -2 as on 0 and -3 days. The average AE value is a maximum at -2 days (222). The Grand AE average (198) is 14 percent above normal. Table 14 shows the AE index vs. elapsed days from date of 12 minor warming peaks. Again, as in Table 13, the maximum AE average occurs at -2 days. Over twice as many relative maxima in AE occur

on -2 day as on either 0 or -4 days. The average AE (149) for 0-4 days preceding minor warming peaks is below normal. In Table 13, the average AE for 0-4 days (total 50 days) preceding major peaks (198) is one-third higher than the same average for the minor peaks (total 60 days). This may be significant since it was found previously that there was no significant difference between the AE average for warming days versus nonwarming days.

Solar X-Rays

The average maximum hourly value (24 hour interval) of the 1-8A solar x-ray flux is 7.9×10^{-3} ergs $\text{cm}^{-2} \text{s}^{-1}$. The average value is less during the 119 warming days than during the 144 nonwarming days. Table 15 shows the x-ray flux values versus elapsed days from start of warming. The average flux occurring during days 0 to -4 is less than average. The average flux is greater than average on day 0; also, there are three relative maxima. Tables 16 and 17 exhibit the solar x-ray flux vs. elapsed days from date of major and minor warming peaks, respectively. In both tables, the average x-ray flux occurring 0 to 4 days preceding major and minor peaks is below average. Nothing unusual is noted in the distribution of the relative maxima.

Solar Flares

Forty percent of the flares of importance 2 or greater out of a total of 69 occurred during warming days. Since 45 percent of the total days considered (total 264) were warming days, apparently, there is no significant

difference in the occurrence of flares (importance ≥ 2) between warming and nonwarming days. Only 2 out of 10 importance 3 flares occurred during warming days.

Table 18 displays the solar flare importance (2 or 3) versus elapsed days from start of warming. The number of flares occurring 0 to 5 days preceding the start of the warming is not significantly different from the average. However, in 2 out of 5 cases, flares of importance 3 occurred at -3 days. Tables 19 and 20 show the solar flare importance versus elapsed days from dates of major and minor warming peaks, respectively. In both tables, the number of flares occurring 0 to 5 days preceding major and minor peaks are not significantly different from the average. Nothing unusual is noted in the flare distribution.

The A_p Index

The average value of A_p for the interval considered (264 days) was 10.0. The average (9.0) for 119 warming days is less than the average (10.8) for the 145 nonwarming days. Table 21 shows the A_p indices vs. elapsed days from start of warming. Above average values of A_p occur at -2 and -3 days. All the relative maxima of A_p occur at -1 to -3 days. The average A_p for 0 to 4 days preceding the start of the warmings is below normal. Tables 22 and 23 exhibit A_p vs. elapsed days from date of major and minor warming peaks, respectively. The average A_p for 0 to 4 days preceding the peaks is below normal in both tables. Both tables show a relative maximum at -2 days. This maximum is above normal (28 percent) for major peaks and below normal for minor peaks.

The D_{st} Index

Figure 3 (Part I) shows the relationship between D_{st} and AE. The main feature to be noted is that the main phase of a magnetic storm has high positive AE values but large negative D_{st} values. Hence, in the following analysis, "maxima" in D_{st} are taken to be the largest negative values. The average D_{st} index (261 days) is -0.6. The average for 119 warming days (+0.7) is below normal; the average for 142 nonwarming days (-2.2) is above normal. Table 24 displays the D_{st} index vs. elapsed days from start of warming. D_{st} is above normal at -1 to -3 days. The relative "maximum" is at -1 days. The average from 0 to 4 days preceding the start of warming is below normal in 4 out of 5 cases. Tables 25 and 26 show the elapsed days from date of major and minor peaks, respectively. Both tables show that the average D_{st} 0 to 4 days preceding the peaks is below normal. The relative maximum in Table 25, major peaks, occurs at -2 days, while it occurs at -3 days, Table 26, minor peaks.

The He II Index

This index, representing the 304A solar flux, is a more accurate indication of the EUV upper-atmosphere heating than the 2800 MHz solar flux (Anderson, 1965). However, it is available only for the months of April - August 1969. During this period, the He II index ranged from 68 to 96 photons $\text{cm}^{-2} \text{s}^{-1} \times 10^8$. There was no significant difference between the average for the 64 warm days (85.8) and the average for the 75 nonwarm days (84.3). The average for all days considered was 84.9. In Table 27, He II index vs. elapsed days from start of warming, the relative maximum

occurs at 0 days. The average He II index for 0 to 4 days preceding the start of the warming is 80, a below-normal value. Tables 28 and 29 exhibit the He II index vs. elapsed days from date of major and minor warming peaks, respectively. In both tables, the average of the He II index for 0 to 4 days preceding the peaks is close to normal.

Solar Protons (greater than 10 Mev)

Every three to four days a large maximum appears in the solar proton flux, evidently due to passage of the measuring spacecraft through the radiation belt (see, for example, Table 10). Therefore, it is meaningless to attempt to analyze the proton flux like, say, the x-ray flux (Table 15). However, a check was made to try to find any influence, if any, of the radiation belt particles on stratospheric warmings (start, major and minor peaks). None was found.

The SID Index

An equal number (24) of warming and nonwarming days were associated with an SID index of 2- or greater. Nineteen percent of the days had an SID 2- or greater. Table 30 shows the SID index vs. elapsed days from start of warming. Twenty percent of the days 0 to 4 days preceding the start of warming had an SID 2- or greater; hence, there is nothing unusual about this distribution.

Tables 31 and 32 display the SID index vs. elapsed days from date of major and minor warming peaks, respectively. In Table 31, only 9 percent of the days 0 to 4 days preceding the date of major warming peaks have an SID index of 2- or greater. In Table 32, 28 percent of the days have such an index. Consequently, about three times as many SID indices 2- or greater are found in the 0 to 4 days preceding minor warming peaks than in the same period for major warming peaks.

Magnetic Condition

A magnetically-disturbed day is denoted by the indices D (disturbed) or S (principal magnetic storm). Nineteen percent of the warming days had a D or S index, while 19 percent of the nonwarming days had such an index. Nineteen percent of the days considered (253) had either a D or S index. Table 33 shows the magnetic condition index vs. elapsed days from start of warming. The number of disturbed days is about average. Tables 34 and 35 exhibit the magnetic index vs. elapsed days from dates of major and minor warming peaks, respectively. The number of days in both tables having a

magnetic index 0 to 4 days preceding a peak is 17 percent, or almost average. In Table 35, 91 percent of the days having an index occur within 2 days preceding the minor warming peak.

Summary

The preceding analysis indicated no strong correlation of solar flares, SID, x-rays, He II and magnetic condition with stratospheric warmings. However, some definite correlations with stratospheric warmings were indicated for the magnetic indices AE, A_p and D_{st} . These magnetic indices are correlated somewhat with each other; for example, the A_p index contains contributions from at least two major sources, the auroral electrojet (AE) and the ring current (D_{st}). (See Figure 3, Part I and Figure 2a, b, Coffey and Lincoln, 1973.) (These indices are described in greater detail in Part I.)

Table 36 summarizes the statistical information concerning AE, A_p and D_{st} . It shows the average value of the indices vs. warming, non-warming days, total days, and for 0-4 days preceding the start of warming, major warming peaks and minor warming peaks. The symbols in parentheses after the averages refer to whether or not the index average is above-normal (A), below-normal (B), or normal (N).

In Table 36, there is no significant difference between the AE index average for warming days and nonwarming days. Although the average AE for 0 to 4 days preceding the start of warming is 24 percent below normal in all 5 cases considered, AE has a large maximum 1-3 days preceding the start of warming ranging from 20 percent to 100 percent above average. The average AE for all cases at 2 days preceding the start of warming is 46 percent above normal, while at 0 and -4 days it is 37 percent below normal and 24 percent below normal, respectively. The average AE for 0 to 4 days preceding 10 major warming peaks is 14 percent above normal. The maximum average AE is at 2 days preceding the major peaks, where it is 27 percent above normal. The average AE for 0 to 4 days preceding 12 minor warming peaks is 15 percent below normal. The maximum average AE is at 2 days preceding the minor peaks.

Although the average A_p for 0 to 4 days preceding the start of warming is 13 percent below normal (Table 36), the average values at 2 and 3 days preceding the start of warming are 20 percent and 70 percent above normal, respectively. The average A_p for warming days is lower than for nonwarming days. The average A_p at 0 and 4 days are 66 percent below normal and 54 percent below normal, respectively. The average A_p for 0 to 4 days preceding 13 major peaks is 9 percent below normal. The maximum average A_p is at 2 days preceding the major peaks, where it is 28 percent above normal. The average A_p preceding 13 minor warming peaks is 27 percent below normal. The maximum average A_p is at 2 days preceding the minor peaks.

In Table 36, the average D_{st} for warming days is lower than for nonwarming days. The average D_{st} for 0 to 4 days preceding the start of the warming is "below" normal for 4 out of the 5 cases considered. The average D_{st} is "above" normal at 1 to 3 days preceding the start of warming, with the maximum average at -1 day. The average D_{st} for 0 to 4 days preceding both the major and minor warming peaks is below normal. The maximum average value occurs at -2 days for major peaks and -3 days for minor peaks.

Thus, there appears to be a significant relationship between the AE index 1-3 days preceding the data of the start of the warmings and dates of the major and minor warming peaks. The relationship is strongest for start of the warmings and weakest for minor warming peaks. The analysis of the A_p index results in the same conclusion. The analysis of the D_{st} index does not give as strong results. It is of interest to note that none of the indices in Table 36 had above-normal averages for warming days.

3. DISCUSSION AND CONCLUSIONS

Five different stratospheric warmings, three different associated phenomena (start, major and minor peaks) and three different magnetic indices all indicate the same thing; namely, the average value of the magnetic indices (AE , Ap , D_{st}) display a marked increase 1 to 3 days before the warming phenomena and a marked decrease at 0 and -4 days. Although the temperature of the thermosphere above 100 km is definitely enhanced during magnetic storms (Anderson, 1973), no direct evidence has been presented that the mesosphere and lower atmosphere is affected. Statistical studies have established that correlations exist between lower atmospheric behavior and variations in the intensity of geomagnetic fluctuations (Shapiro, 1972; Roberts and Olson, 1973; Wilcox et al., 1973). King (1974), based on a comparison between meteorological pressures and the strength of the geomagnetic field, suggests a possible influence of the Earth's magnetic field on the height of the 500 mb level in regions surrounding the magnetic poles. These statistical studies have indicated that indirect correlations exist between magnetic variations and lower atmosphere circulation. However no direct (cause and effect) correlations can be established unless a physical theory is advanced to explain how the connections work. Hines (1973) points out that the observed magnetic fluctuations are undoubtedly to be associated with solar plasma mechanisms. The existence of fluctuating winds in the ionospheric dynamo region and of associated magnetic variations at ground level is equally beyond question. The main question is: are these dynamo winds influenced by the lower atmosphere circulation? In other words, does the lower atmosphere circulation cause

changes in the ionospheric winds so that magnetic variations ensue or vice versa?

The major stratospheric warmings from 1951 to 1966 all occurred during years of strong solar and geomagnetic disturbance, or following active bursts of disturbance (Willet, 1968). The only six years lacking stratospheric warmings were also the six geomagnetically quiet years. The definite correlation of the warming phenomena with magnetic activity, especially the AE index indicates that the auroral electrojets near 100 km may be the primary source of the auroral zone heating that influences the circulation at 50 km and below.

The auroral electrojets are intense electric currents, associated with polar magnetic disturbances, that flow in the auroral oval (Akasofu et al., 1965). The westward auroral electrojet grows to approximately 10^6 amperes during a magnetic substorm due to an increase in the conductivity of the E-layer of the ionosphere in the midnight to dawn sector of the auroral oval. The eastward flowing electrojet has a strength of about 10^3 amperes in the late evening sector. Cole (1962) has estimated that $5 \text{ ergs cm}^{-2} \text{ s}^{-1}$ could be deposited in the auroral zone by means of joule heating associated with the electrojet at moderately disturbed times and an order of magnitude more during large geomagnetic storms. Whether or not the electrojets are the primary cause or trigger the heating from below (Hirota, 1967; Matsuno, 1971; Trenberth, 1972) cannot be determined without a detailed energy transfer analysis, which cannot be performed at present because of lack of data in the mesosphere.

Conclusions

This detailed study of five different stratospheric warmings (1969-1971) has established that the magnetic indices AE, A_p , and Dst display a marked increase 1 to 3 days before warming phenomena and a marked decrease at 0 and -4 days. The definite correlation of the warming phenomena with the AE index indicates that the auroral electrojet joule heating near 100 km may be the original source of the heating that influences the atmosphere at 50 km and below. If this is true, then whether the electrojet heating is the primary cause or triggers the heating by releasing energy in the troposphere cannot be determined without mesospheric data above 50 km.

TABLE

Indices vs. Date (1 - 17 July 1969)

Date Index	1	2	3	4	5	6	7	8	9	10	11	12	13	14	15	16	17	Units
Solar Flare	2		(2)	2	(3)	2	2											Importance
SID	2 ⁺		(3)		(2)													Importance
Solar X-Rays (1-8A)	2	3	(39*)	4	(6*)	1	1	2*	1	3*	1	7*	3	3	3	2	1	Max.Hr.Value 10^{-3} ergs $\text{cm}^{-2}\text{s}^{-1}$
He II Flux	77	82	86	(90*)	(90*)	86	83	88	91*	89	87	89*	89*	85	85	85	84	10^8 photons $\text{cm}^{-2}\text{s}^{-1}$
2800 MHz Solar Flux	144	157	162	(164*)	161	160	161*	160	163*	159	153	147	150*	139	122	122	120	10^{-22} Wm^{-2} MHz^{-1}
Solar Protons	2778*	1	1	13089*	1	1	1	8*	1	1	12812*	1	1	1	437*	1	1	Max.Hr.Value Protons cm^{-2} s^{-1} (>10MeV)
Magnetic Condition	S											S						
A _p	(17*)	6	3	3	2	4	(6*)	5	7*	7*	6	12	14*	13	5	10*	4	Daily Avg.
D _{st}	7	4*	12	19	24	29	24	19	8	5*	14	7	2	0*	6	6	6	Max.Hr.Value
AE	(294*)	169	97	90	(110*)	98	(146*)	139	299*	235	208	291*	278	246	129	229*	120	DailyAvg. Gammas
Max. Radiance SIRS-A, Channel 8		57.7	(57.9*)	57.0	57.0	56.5	58.3	60.5	60.5	60.5	61.0	60.7	61.4*	60.3	60.1	58.8	58.2	Ergs $\text{cm}^{-2}\text{s}^{-1}$ $\text{ster}^{-1}\text{cm}^{-1}$

* Relative Maximum

TABLE 2

1-8A Solar X-Rays (Explorer 37)

Day (July 1969)	Flux (10^{-4} ergs $\text{cm}^{-2} \text{s}^{-1}$)	Start (UT)	Peak (UT)	End (UT)	Duration (Min)
1	96	1125	1128	1135	10
1	130	1627	1629	1636	9
2	89	0349	0352	0400	11
2	44	0408	0412	0416	8
3	1900	1523	1524	1603	40
4	61	0006	0014	0032	26
4	38	1200	1206	1206	6
5	210	1229	1237	1244	15
7	53	1636	1648	1648	12
8	46	2218	2227	2234	16
10	38	0649	0653	0658	9
12	86	1430	1435	1517	47
13	38	0341	0348	0354	13
13	71	0400	0410	0416	16
13	46	1513	1515	1517	4
13	39	2229	2245	2245	16
13	58	2320	2324	2328	8
14	43	0244	0246	0249	5
14	61	1437	1437	1438	1
14	40	1730	1736	1741	11
15	57	1717	1720	1728	11
16	37	1903	1910	1914	11

TABLE 3

Indices vs. Date (29 July - 14 August 1969)

Date Index	29	30	31	1	2	3	4	5	6	7	8	9	10	11	12	13	14	Units
Solar Flare	(3)							2		(2)				2				Importance
SID	(3)		2											3				Importance
Solar X-rays (1-8A)	(4*)	2	2	(7*)	6	3	2	3*	1	(6*)	1	1	2	(10*)	2	2	2	Max. Hr. Value 10^{-3} ergs cm^{-2} s^{-1}
He II Flux	71	71	70	80	83	86	93*	88	88	88	(90*)	90*	90*	(90*)	87	85	82	10^8 photons $\text{cm}^{-2} \text{s}^{-1}$
2800 MHz Solar Flux	133	143	162	171	187*	183	188*	182	167	159	146	142	136	132	125	121	114	$10^{-22} \text{ W m}^{-2} \text{ MHz}^{-1}$
Solar Protons	1	1	8035*	1	1	1	6*	1	1	45470*	1	1	34*	4	1	1	2221*	Max. Hr. Value Protons cm^{-2} $\text{s}^{-1} (>10 \text{ MeV})$
Magnetic Condition		(S)				D				S				(S)	S			
A_p	2	(13*)	6	3	5	14*	13	7	5	8	9	(11*)	6	4	21*	7	6	Daily Avg.
D_{st}	-1	12	(-1*)	6	21	9	-13*	-4	4	16	4	-1	(-6*)	15	-3	-4*	0	Max. Hr. Value
AE	67	(191*)	131	102	93	294*	291	178	116	215*	210	203	(219*)	65	315*	174	192*	Daily Av. Gammas
Max. Radiance SIRS-A, Channel 8	57.5*	57.4	57.0	56.9	58.0	59.3	60.5	61.4	64.2*	63.4	63.6*	61.9	59.6	57.2	58.0	59.1	59.4	Ergs $\text{cm}^{-2} \text{s}^{-1}$ ster $^{-1} \text{cm}^{-1}$

* Relative Maximum

TABLE 4
Indices vs. Date (11-27 December 1969)

Date	11	12	13	14	15	16	17	18	19	20	21	22	23	24	25	26	27	Units
Solar Flare				(3)			(2)		2		(2)							Importance
Daily Flare Index	3	11	70	(115*)	80	32	(457*)	39	176*	114	(142*)	16	36	45	22	49	54	
SID	3 ⁻	2			2		(2)					2 ⁻	2			2 ⁺		Importance
Solar X-rays (1-8A)	4	9*	2	(9*)	3	2	(26*)	2	10*	2	2	2	6*	1	3	7*	3	Max.hrly. value 10^{-3} ergs $\text{cm}^{-2}\text{s}^{-1}$
2800 MHz Solar Flux	118	122	130	133	136	137	144	144	147	154	160	163*	156	153	154*	151	147	$10^{-22} \text{ w m}^{-2} \text{ MHz}^{-1}$
Solar Protons	1	1	4262*	1	1	1596*	1	2	1	1705*	1	1	2631*	1	1	2101*	1	Max.hrly. value Protons $\text{cm}^{-2}\text{s}^{-1}$ (>10 Mev)
Magnetic Condition													(D)					
A _p	11*	5	3	4	5	(11*)	4	3	4	3	3	7	(11*)	9	9	10*	9	Daily Avg.
D _{st}	-5*	-1	8	13	10	(-6*)	0	10	14	20	17	19	3	-1	-2*	4	-5*	Max.hrly. value
AE	140*	88	46	62	99	(190*)	78	47	39	32	35	107	(236*)	155	189*	147	145	Daily Avg., Gammas
10-mb Max. Temp.	234	238	240*	238	236	236	238	248*	241	243	238	243	243	248	258	263*	258	°K.

* Relative maximum

TABLE 5

1-8A Solar X-Rays (Explorer 37)

Day(Dec. 1969)	Flux (10^{-4} ergs $\text{cm}^{-2} \text{s}^{-1}$)	Start (UT)	Peak (UT)	End (UT)	Duration (Min)
14	87	0257	0305	0321	24
14	260	0338	0351	0444	6
17	260	0038	0052	0230	112
17	770	0658	0700	0726	28
17	470	0950	0956	1017	27
23	91	0649	0654	0750	61
23	62	0850	0900	0922	32

TABLE 6
AE Index (Gammas) (11-27 December 1969)

Date	Mean Value	Maximum Hourly Value	Percent Hours/7110
11 Dec. 1969	140*	284	58
12	88	221	25
13	46	109	0
14	62	260	9
15	99	278	42
16	190*	521	71
17	78	176	25
18	47	113	9
19	39	86	0
20	32	55	0
21	35	83	0
22	107	364	42
23	236*	527	75
24	155	372	42
25	189*	324	67
26	147	413	54
27	145	429	58

* Relative maximum

Table 7

LOCATION AND TEMPERATURE OF NORTHERN HEMISPHERE
COLD AND WARM CENTERS, 25-60 KM, JAN. 6, 1971

Altitude (km)	Cold Center			Warm Centers								
	Lat. (°N)	Long. (°E)	Temp. (°K)	Lat. (°N)	Long. (°E)	Temp. (°K)	Lat. (°N)	Long. (°E)	Temp. (°K)	Lat. (°N)	Long. (°E)	Temp. (°K)
25	70	10	198	60	150	233	30	15	218			
30	70	10	203	62	155	243	30	15	228			
35	78	320	228	58	145	253	30	15	243	25	240	243
40	60	240	233	65	140	268				25	240	273
45	57	245	243	65	140	278				25	245	283
50	60	250	248	65	140	288				25	240	293
55	70	220	248							30	250	278
60	79	10	238									
	65	200	233				55	250	278			

Table 8

LOCATION AND MAGNITUDE OF NORTHERN HEMISPHERE
TEMPERATURE CHANGE CENTERS, 25-60 KM, JAN. 6, 1971

Altitude (km)	Lat. (°N)	Long. (°E)	Change (°)	Lat. (°N)	Long. (°E)	Change (°)	Lat. (°N)	Long. (°E)	Change (°)
25	70	220	+15						
30	70	230	+25						
35	70	175	+35	70	310	+20			
40	78	70	+45						
45	78	70	+45						
50	82	125	+45				50	230	-10
55	70	100	+20	60	320	+20	55	205	-15
60				60	280	+30	55	195	-20

TABLE 9

Indices vs. Date (8 - 24 December 1970)

Date	8	9	10	11	12	13	14	15	16	17	18	19	20	21	22	23	24	Units
Solar Flare				(2)														Importance
Daily Flare Index	34	79	250*	111	(155*)	99	140	16	10	6	61*	52	16	5	(68*)	50	2	
SID															(2)			Importance
Solar X-rays (1-8A)	40*	22	2	35	(68*)	5	5	2	2	1	4	2	2	2	(18*)	2	1	Max.Hr.Value 10^{-3} ergs cm^{-2} s^{-1}
2800 MHz Solar Flux	167	172	171	173	(178*)	164	155	154	147	147	152	152	156*	146	137	132	124	10^{-22} $\text{W m}^{-2} \text{MHz}^{-1}$
Solar Protons	5573*	1	1	10775*	2	2	2502*	4	1	1	13522*	1	1	9957*	1	1	(6)	Max.Hr.Value Protons cm^{-2} s^{-1} (> 10 Mev)
Magnetic Condition	D						(S)				S						(D)	
A _p	19*	6	3	2	4	4	(65*)	14	4	3	3	10*	8	4	6	7	(14*)	Daily avg.
D _{st}	-21*	-5	1	9	10	10	(68*)	-56	-35	-22	-9	3	-17*	-14	-9	-2	(-21*)	Max.Hr.Value
AE	329*	96	90	35	97*	69	(416*)	255	71	(75*)	47	116	186*	104	130*	98	(156*)	Daily Avg. Gammas
2-mb Zonal Temp(60-80°)	233	233	234	235	236	236	236	236	236	236	238	240	241	243	243	244	245	°K
10-mb Max. Temp.	233	238	238	238	238	238	238	238	243	243	243	243	243	243	243	243	243	°K

* Relative Maximum

TABLE 10

Indices vs. Date (25 December 1970 - 10 January 1971)

Date Index	25	26	27	28	29	30	31	1	2	3	4	5	6	7	8	9	10	Units
Solar Flare																		Importance
Daily Flare Index	85*	20*	1	0	4	12*	0	10	6	0	5	18*	10	10	1	65*	12	
SID	2																2	Importance
Solar X-rays (1-8A)	1	3*	1	0	1	1	1	1	1	1	1	1	2*	1	1	4	5*	Max. Hr. Value 10^{-3} ergs cm^{-2} s^{-1}
2800 MHz Solar Flux	124	122	120	117	123	129	133*	130	135	135	140	146	147	150*	149	153*	152	10^{-22} $\text{W m}^{-2} \text{MHz}^{-1}$
Solar Protons	8946*	3	2	4242*	1	1	6429*	1	1	1	9595*	1	1	13009*	1	1	15600*	Max. Hr. Value Protons cm^{-2} s^{-1} (>10 Mev)
Magnetic Condition			S	S	S			S	S	D								
A _p	4	4	8	18*	12	13*	2	6	19	33*	16	9	4	1	0	1	6	Daily avg.
D _{st}	-8	-5	-2	-20*	-17	-16	-1	5	7	-8*	-8*	-3	-2	3	9	17	19	Max. Hr. Value
AE	71	74	179	324*	159	143	25											Daily Avg., Gammas
N-S Wind, College (75-105 km)	+8	+8	+8	+5	-5	-20	-25	-40	-40	-38	-38	-35	-35	-35	+20	-20	+10	Avg. Daily Component, ms^{-1}
2-mb Zonal Temp(60-80°)	246	249	252*	252*	250	249	249	250	251	252	254	255	257	260	263	266	268*	°K
10-mb Max. Temp.	243	243	248*	248*	243	243	243	238	238	243	253*	243	243	253	258*	248	248	°K
E-W Wind, College (75-105 km)	+15	+10	0	+25	+35	+5	-15	-35	-35	-35	-35	-35	-35	-38	-40	+2	+15	Avg. Daily Component, ms^{-1}

* Relative maximum

TABLE 11

AE INDEX VS. ELAPSED DAYS FROM START OF WARMING

Start Date	Elapsed Days	0	-1	-2	-3	-4	Average
3 Jul 1969		97	169	294*	125	126*	162
1 Aug 1969		102	131	191*	67	108	120
11 Aug 1969		65	219*	203	210	215*	182
17 Dec 1969		78	190*	99	62	46	95
17 Dec 1970		75	71	255	416*	69	147
Average		83	156	208*	176	113	141

* Relative maximum

TABLE 12

RELATIVE VARIATION OF AE FROM AVERAGE VALUE OF EACH 5-DAY
PERIOD VS. ELAPSED DAYS FROM START OF WARMING

Start Date	Elapsed Days	0	-1	-2	-3	-4
3 Jul 1969		.60	1.04	1.81*	.77	.78
1 Aug 1969		.85	1.09	1.59*	.56	.90
11 Aug 1969		.36	1.20*	1.12	1.15	1.18
17 Dec 1969		.82	2.00*	1.04	.65	.48
17 Dec 1970		.51	.48	1.73	2.83*	.47
Average		.63	1.16	1.46*	1.19	.76

* Relative maximum

TABLE 13

AE VS. ELAPSED DAYS FROM DATE OF MAJOR WARMING PEAKS

Peak Date	Elapsed Days	0	-1	-2	-3	-4	Average
30 Apr 1969		421*	207	333*	216	158	267
5 May 1969		235*	191	380*	342	222	274
8 Jul 1969		139	146*	98	110	90	116
11 Jul 1969		208	235	299*	139	146	103
13 Jul 1969		278	291*	208	235	299*	262
6 Aug 1969		116	178	291	294*	93	194
8 Aug 1969		210	215*	116	178	291*	202
16 Aug 1969		121	50	192*	174	315*	170
26 Aug 1969		147	189*	155	236*	107	167
29 Aug 1969		65	66	145	147	189*	122
Average		194	177	222*	207	191	198

* Relative maximum

TABLE 14

AFC VS. ELAPSED DAYS FROM DATE OF MINOR WARMING PEAKS

Peak Date	Elapsed Days	0	-1	-2	-3	-4	Average
19 Apr 1969		124	271	464*	363	319	308
23 Apr 1969		100	115	88	174*	124	120
12 May 1969		157	157	211	218*	134	175
3 Jul 1969		97	169	294*	125	126	162
18 Jul 1969		132	120	229	129	246*	171
22 Jul 1969		149*	138	121	78	132	124
20 Aug 1969		205	346*	115	230	121	203
13 Dec 1969		46	88	140*	114	99	97
18 Dec 1969		47	78	190*	99	62	95
20 Dec 1969		32	39	47	78	190*	77
2 Jan 1970		403*	120	65	44	65	139
27 Dec 1970		179	74	71	156*	98	116
Average		139	143	170*	151	143	149

* Relative maximum

TABLE 15

Solar X-Rays (1-8A) (Max.Hr.Value, 10^{-3} ergs cm^{-2} s^{-1})

Vs. Elapsed Days From Start of Warming

Elapsed Days Start Date	0	-1	-2	-3	-4	Average
3 Jul 1969	3	3	2	4*	1	2.6
1 Aug 1969	7*	2	2	4*	2	3.4
11 Aug. 1969	10*	2	1	1	6*	4.0
17 Dec 1969	26*	2	3	9*	2	8.4*
17 Dec 1970	1	2	2	5	5	3.0
Average	9.4*	2.2	2.0	4.6	3.2	4.3

* Relative maximum

TABLE 16

Solar X-Rays (1-8A) (Max. Hr. Value, 10^{-3} ergs $\text{cm}^{-2} \text{s}^{-1}$)

Vs. Elapsed Days From Date of Major Warming Peaks

Peak Date	0	-1	-2	-3	-4	Average
30 Apr 1969	2	1	1	4*	2	2.0
5 May 1969	7*	2	2	7*	3	4.2
8 Jul 1969	2	1	1	6*	4	2.8
11 Jul 1969	1	3*	1	2	1	1.6
13 Jul 1969	3	7*	1	3	1	3.0
6 Aug 1969	1	3*	2	3*	6	3.0
8 Aug 1969	1	6*	1	3	2	2.6
16 Aug 1969	0	1	2	2	2	1.4
26 Aug 1969	7	5	5	8*	6	6.0*
29 Aug 1969	2	3	2	7*	5	3.8
4 Jan 1971	1	1	1	1	1	1.0
8 Jan 1971	1	1	2*	1	1	1.2
11 Jan 1971	1	5*	4	1	1	2.4
Average	2.2	2.9	1.9	3.7*	2.7	2.7

* Relative maximum

TABLE 17

Solar X-Rays (1-8A) (Max. Hr. Value, 10^{-3} ergs $\text{cm}^{-2} \text{s}^{-1}$)

Vs. Elapsed Days From Date of Minor Warming Peaks

Peak Date	0	-1	-2	-3	-4	Average
19 Apr 1969	5	4	1	9	10*	5.8
23 Apr 1969	9	4	20*	5	5	8.8
12 May 1969	8*	1	1	1	1	2.4
3 Jul 1969	3	3	2	4*	1	2.6
18 Jul 1969	0	1	2	3	3	1.8
22 Jul 1969	1	1	1	1	0	0.8
20 Aug 1969	6*	0	2	0	0	1.6
13 Dec. 1969	2	9*	4	1	1	3.4
18 Dec 1969	2	26*	2	3	9	8.4
20 Dec 1969	2	10	2	26*	2	8.4
2 Jan 1970	1	3*	1	1	2	6.6
27 Dec 1970	1	3*	1	1	2	1.6
18 Jan 1971	3	2	68*	6	19	19.6*
Average	3.5	5.0	8.6*	6.2	4.2	5.5

* Relative maximum

TABLE 18
Solar Flare Importance (≥ 2) Vs. Elapsed Days
From Start of Warming

Start Date	Elapsed Days	0	-1	-2	-3	-4	-5
3 Jul 1969		2		2			
1 Aug 1969					3		
11 Aug 1969		2				2	
17 Dec 1969		2			3		
17 Dec 1970							

TABLE 19

Solar Flare Importance (≥ 2) Vs. Elapsed Days
From Date of Major Warming Peaks

Peak Date	Elapsed Days	0	-1	-2	-3	-4	-5
30 Apr 1969		2				2	
5 May 1969		2	2	2	2	2	2
8 Jul 1969			2	2	3	2	2
11 Jul 1969						2	2
13 Jul 1969							
6 Aug 1969			2				
8 Aug 1969			2		2		
16 Aug 1969							2
26 Dec 1969							2
29 Dec 1969							
4 Jan 1961					2		
8 Jan 1971							
11 Jan 1971							

TABLE 20

Solar Flare Importance (≥ 2) Vs. Elapsed Days
From Date of Minor Warming Peaks

Peak Date	Elapsed Days	0	-1	-2	-3	-4	-5
19 Apr 1969		2	2				
23 Apr 1969		2		3	2	2	2
12 May 1969		3					
3 Jul 1969		2		2			
18 Jul 1969		2					
22 Jul 1969						2	
20 Aug 1969							
13 Dec 1969							
18 Dec 1969			2			3	
20 Dec 1969			2		2		
2 Jan 1970		3					
27 Dec 1970							
18 Jan 1971							

TABLE 21

A_p Index Vs. Elapsed Days From Start of Warmings

Elapsed Days Start Date	0	-1	-2	-3	-4	Average
3 Jul 1969	3	6	17*	5	4	7.0
1 Aug 1969	3	6	13*	2	4	5.6
11 Aug 1969	4	6	11*	9	8	7.6
17 Dec 1969	4	11*	5	4	3	5.4
17 Dec 1970	3	4	14	65*	4	18.0*
Average	3.4	6.6	12.0	17.0*	4.6	8.7

* Relative maximum

TABLE 22

A_p Vs. Elapsed Days From Date of Major Warming Peaks

Peak Date	0	-1	-2	-3	-4	Average
30 Apr 1969	27	12	60*	11	6	23.2*
5 May 1969	10	8	15	28*	8	13.8
8 Jul 1969	5	6*	4	2	3	4.0
11 Jul 1969	6	7*	7*	5	6	6.2
13 Jul 1969	14*	12	6	7	7	9.2
6 Aug. 1969	5	7	13	14*	5	8.8
8 Aug 1969	9	8	5	7	13*	8.4
16 Aug 1969	4	4	6	7	21*	8.4
26 Aug 1969	15	4	6	11*	5	8.2
29 Aug 1969	4	6	21*	15	4	9.8
4 Jan 1971	16	33*	19	6	2	9.2
8 Jan 1971	0	1	4	9	16*	6.0
11 Jan 1971	8*	6	1	0	1	3.2
Average	9.5	8.8	12.8*	9.4	7.3	9.1

* Relative maximum

TABLE 23

A_p Vs. Elapsed Days From Date of Minor Warming Peaks

Peak Date	0	-1	-2	-3	-4	Average
19 Apr 1969	5	15	21*	17	14	14.4*
23 Apr 1969	5	10*	6	8	5	6.8
12 May 1969	8	5	10	11*	5	7.8
3 Jul 1969	3	6	17*	5	4	7.0
18 Jul 1969	3	4	10	5	13*	7.0
22 Jul 1969	7*	4	3	2	3	3.8
20 Aug 1969	7	13*	7	6	4	7.4
13 Dec 1969	3	5	11	8	12*	7.8
18 Dec 1969	3	4	11*	5	4	5.4
20 Dec 1969	3	4	3	4	11*	5.0
2 Jan 1970	30*	8	3	2	4	9.4
27 Dec 1970	8	4	4	14*	7	7.4
18 Jan 1971	15*	6	7	8	9	9.0
Average	7.7	6.8	8.7*	7.3	5.9	7.3

TABLE 24

D_{st} Index Vs. Elapsed Days From Start of Warming

Elapsed Days Start Date	0	-1	-2	-3	-4	Average
3 Jul 1969	12	4*	7	18	18	11.8
1 Aug 1969	6	-1	12	-1	-18*	-0.4
11 Aug 1969	15	-6*	-1	4	16	5.6
17 Dec 1969	0	-6*	10	13	8	5.0
17 Dec 1970	-22	-35	-56	-68*	10	-34.2*
Average	+2.2	-8.8*	-5.6	-6.8	6.8	-2.4

* Relative maximum

TABLE 25

D_{st} Vs. Elapsed Days From Date of Major Warming Peaks

Peak Date	0	-1	-2	-3	-4	Average
30 Apr 1969	-39*	-31	-38	5	4	-19.8*
5 May 1969	-4	-9	-17	-12	-21*	-12.6
8 Jul 1969	19*	24	29	24	19*	23.0
11 Jul 1969	14	5*	8	19	24	14.0
13 Jul 1969	2*	7	14	5	8	7.2
6 Aug 1969	4	-4	-13*	9	21	3.4
8 Aug 1969	4	16	4	-4	-13*	1.4
16 Aug 1969	9	9	0	-4*	-3	2.2
26 Aug 1969	18	9	11	5*	12	10.0
29 Aug 1969	6	-12	-22*	18	9	0.0
4 Jan 1971	-8*	-8*	7	5	-1	-0.8
8 Jan 1971	9	3	-2	-3	-8*	-0.2
11 Jan 1971	8	19	17	9	3*	9.6
Average	3.2	2.2	-0.2*	5.8	4.2	3.0

* Relative maximum

TABLE 26

D_{st} Vs. Elapsed Days From Date of Minor Warming Peaks

Elapsed Date Peak Date	0	-1	-2	-3	-4	Average
19 Apr 1969	-10	-27	-33*	-18	-22	-22.0*
23 Apr 1969	4	15	-1	-6	-10*	-0.4
12 May 1969	14	3*	3*	3*	10	6.6
3 Jul 1969	12	4*	7	18	18	11.8
18 Jul 1969	10	6	6	6	0*	5.6
22 Jul 1969	6*	25	25	12	10	15.6
20 Aug 1969	-5*	2	11	-3	9	2.8
13 Dec 1969	8	-1	-5*	2	9	2.6
18 Dec 1969	10	0	-6*	10	13	5.4
20 Dec 1969	20	14	10	0	-6*	7.6
2 Jan 1970	-16*	9	13	8	6	4.0
27 Dec 1970	-2	-5	-8	-21*	-2	-7.6
18 Jan 1971	11	12	4	-5*	1	4.6
Average	4.8	4.4	2.0	0.5*	2.7	2.9

* Relative maximum

TABLE 27

He II Index Vs. Elapsed Days From Start of Warming

Elapsed Days Start Date	0	-1	-2	-3	-4	Average
3 Jul 1969	82*	77	77	77	77	78
1 Aug 1969	80*	70	71	71	75	73
11 Aug 1969	90	90	90	90	90	90*
Average	84*	79	79	79	81	80

* Relative maximum

TABLE 28

He II Index Vs. Elapsed Days From Date of Major Warming Peaks

Peak Date	0	-1	-2	-3	-4	Average
30 Apr 1969	83	86	88*	87	86	86
5 May 1969	85	84	84	85	86*	85
8 Jul 1969	88	83	86	90*	90*	87
11 Jul 1969	87	89	91*	88	83	88
13 Jul 1969	89	89	87	89	91*	89*
6 Aug 1969	88	88	93*	86	83	88
8 Aug 1969	90	88	88	88	93*	89*
16 Aug 1969	75	77	82	85	87*	81
26 Aug 1969	85	89*	83	70	70	79
29 Aug 1969	95*	86	86	86	85	88
Average	86	86	87*	85	84	86

* Relative maximum

TABLE 29

He II Index Vs. Elapsed Days From Date of Minor Warming Peaks

Peak Date	0	-1	-2	-3	-4	Average
19 Apr 1969	90	90	91	91	92*	91*
23 Apr 1969	85	89	92*	90	90	89
12 May 1969	93*	90	88	88	85	89
3 Jul 1969	90*	86	82	77	77	82
18 Jul 1969	84	84	85*	85*	85*	85
22 Jul 1969	77	81	82	82	84*	81
20 Aug 1969	69	71	72	73	75*	72
Average	84	84	84	84	84	84

* Relative maximum

TABLE 30

SID Index Vs. Elapsed Days from Start of Warming

Start Date	Elapsed Days	0	-1	-2	-3	-4
3 Jul 1969		3		2 ⁺		
1 Aug 1969			2		3	2 ⁺
11 Aug 1969		3 ⁻				
17 Dec 1969		2		2		
17 Dec 1970						

TABLE 31

SID Index Vs. Elapsed Days From Date of Major Warming Peaks

Peak Date	Elapsed Days	0	-1	-2	-3	-4
30 Apr 1969					2	2 ⁺
5 May 1969		2			2	
8 Jul 1969					2 ⁺	
11 Jul 1969						
13 Jul 1969						
6 Aug 1969						
8 Aug 1969						
16 Aug 1969						
26 Aug 1969						
29 Aug 1969						
4 Jan 1971						
8 Jan 1971						
11 Jan 1971			2			

TABLE 32

SID Index Vs. Elapsed Days From Date of Minor Warming Peaks

Peak Date	0	-1	-2	-3	-4
19 Apr 1969	2 ⁻	2 ⁺		2 ⁺	
23 Apr 1969			2 ⁺	2 ⁺	2 ⁻
12 May 1969					
3 Jul 1969	3		2 ⁺		
18 Jul 1969					
22 Jul 1969					
20 Aug 1969	2				
13 Dec 1969		2	3 ⁻		
18 Dec 1969		2		2	
20 Dec 1969				2	
2 Jan 1970				2	
27 Dec 1970			2		
18 Jan 1971			2 ⁺		2

TABLE 33

Magnetic Condition Index Vs. Elapsed Days From Start of Warmings

Elapsed Days Start Date	0	-1	-2	-3	-4
3 Jul 1969			S		
1 Aug 1969			S		
11 Aug 1969	S				S
17 Dec 1969					
17 Dec 1970					S

TABLE 34

Magnetic Condition Index Vs. Elapsed Days from Date of Major Warming Peaks

Elapsed Days Peak Date	0	-1	-2	-3	-4
30 Apr 1969	D		S	S	
5 May 1969				S	
8 Jul 1969					
11 July 1969					
13 July 1969		S			
6 Aug 1969				D	
8 Aug 1969		S			
16 Aug 1969					S
26 Aug 1969	S				
29 Aug 1969			D	S	
4 Jan 1971					
8 Jan 1971					
11 Jan 1971					

D = Disturbed Day

S = Principal Magnetic Storm

TABLE 35

Magnetic Condition Vs. Elapsed Days From Date of Minor Warming Peaks

Elapsed Date Peak Date	0	-1	-2	-3	-4
19 Apr 1969			D		
23 Apr 1969		S	S		
12 May 1969	S				
3 Jul 1969			S		
18 Jul 1969					
22 Jul 1969					
20 Aug 1969		D			
13 Dec 1969					
18 Dec 1969					
20 Dec 1969					
2 Jan 1970	S	S			
27 Dec 1970	S			D	
18 Jan 1971	S				

TABLE 36

Average Value of Indices Vs. Warming Days, Nonwarming Days, Total Days, and For 0-4 Days Preceding Start of Warming, Major Warming Peaks, and Minor Warming Peaks

Index	Warming Days	Non-Warming Days	Total Days	Start of Warming	Major Warming Peaks	Minor Warming Peaks
AE	170(N)*	178(N)	175	141(B)	198(A)	149(B)
A _p	9.0(B)	10.8(A)	10.0	8.7(B)	9.1(B)	7.3(B)
D _{st}	+0.7(B)	-2.2(A)	-0.6	-2.4(A)	3.0(B)	2.9(B)

* N = Normal value

B = Below-normal value

A = Above-normal value

REFERENCES CITED IN PART II

References

- Akasofu, S., S. Chapman, and C. Meng; "The polar electrojet," J. Atmos. Terr. Phys. 27, 1275-1305, 1965.
- Anderson, A. D.; "Long-term (solar cycle) variation of the extreme ultraviolet radiation and 10.7-centimeter flux from the sun," J. Geophys. Res. 70, 3231, 1965.
- Anderson, A.D.; "The correlation between low-altitude neutral density variations near 400 km and magnetic activity indices," Planet Sp. Sci. 21, 2049, 1973.
- Barnett, J.J., et al.; "Stratospheric Warming Observed by Nimbus 4," Nature, 230, 47, 1971.
- Coffey, H.E., and J. V. Lincoln; Report UAG-26, World Data Center A for Solar-Terrestrial Physics, 1973.
- Cole, K.D.; "Joule heating of the upper atmosphere," Australian J. Phys. 15, 223, 1962.
- Dickinson, R.E.; "Planetary rossby waves propagating vertically through weak westerly wind wave guides," J. Atmos. Sci., 25, 984, 1968.
- Ellis, P.J., et al.; "First results from the selective chopper radiometer on Nimbus 4," Nature, 228, 139, 1970.
- Finger, F.G., and R.W. McInturff; "Needs and uses of stratospheric observations in the Stratwarm Programme," Proc. WMO Tech. Conf., Paris, 8-12 Sept. 1969
- Finger, F.G., and R.M. McInturff; "Meteorology and the supersonic transport," Science, 167, 16, 1970
- Fritz, S.; "Earth's radiation to space at 15 microns: stratospheric temperature variations," J. Appl Meteor., 9, 815, 1970.
- Fritz, S., and S.D. Soules; "Large-scale temperature changes in the stratosphere observed from NIMBUS III," J. Atmos. Sci., 27, 1091, 1970.
- Gelman, M.E.; "The stratospheric warming of December 1969-January 1970," paper presented at the AMS/AGU Meeting, Washington, D.C., April 20-24, 1970

- Groves, G.V.; "Seasonal and latitudinal models of atmospheric temperature, pressure, and density, 25 to 100 km," AFCRL-70-0261, 1970.
- Hines, C.O.; Comments on "A test of an apparent response of the lower atmosphere to solar corpuscular radiation," J. Atmos. Sci., 30, 739, 1973.
- Hirota, I.; "The vertical structure of the stratospheric sudden warming," J. Meteor. Soc. Japan, 45, 422, 1967.
- Hook, J.L.; "Wind patterns at meteor altitudes (75-105 km) above College, Alaska, associated with midwinter stratospheric warmings," J. Geophys. Res., 77, 3856, 1972.
- Houghton, J.T., and S.D. Smith; "Remote sounding of atmospheric temperature from satellites," Proc. R. Soc. London A, 320, 23, 1970.
- Johnson, J.W., A.J. Miller, and M.E. Gelman; "Proposed indices characterizing stratospheric circulation and temperature fields," Mon. Weather Rev. 97, 565, 1969.
- King, J.W.; "Weather and the Earth's magnetic field," Nature, 247, 131, 1974.
- Labitzke, K.; "Midwinter warmings in the upper stratosphere in 1966," A. J. Royal. Met. Soc., 94, 279, 1968.
- Labitzke, K.; "Temperature changes in the mesosphere and stratosphere connected with circulation changes in winter," J. Atmos. Sci., 29, 756, 1972.
- Labitzke, J. and J.J. Barnett, "Global time and space changes of satellite radiances received from the stratosphere and lower mesosphere," J. Geophys. Res., 78, 483, 1973.
- Matsuno, T.; "A dynamical model of the stratospheric sudden warming," J. Atmos. Sci. 28, 1479, 1971.
- Miller, A.J., F.G. Finger, and M.E. Gelman; "30-mb synoptic analyses for 1969 Southern Hemisphere winter derived with the aid of Nimbus III (SIRS) data," NASA TM-X-2109, December 1970.

Miller, A., J. Brown and J. Campana; "A study of the energetics of an upper stratosphere warming (1969-1970)," Quart. J. Roy. Met. Soc., 98, 730, 1972.

Quiroz, R.S., "The determination of the amplitude and altitude of stratospheric warmings from satellite-measured radiance changes," J. Appl. Met., 10, 555, 1971.

Roberts, W.O., and R.H. Olson; "Geomagnetic storms and wintertime 300-mb trough development in the North Pacific-North America area," J. Atmos. Sci., 30, 135, 1973.

Shapiro, R., "A test of apparent response of the lower atmosphere to solar corpuscular radiation," J. Atmos. Sci., 29, 1213, 1972.

Smith, W.L., H.M. Woolf, and W.J. Jacob, "A regression method for obtaining real time temperature and geopotential height profiles from satellite spectrometer measurements and its application to Nimbus 3 SIRS observations," Mon. Weather Rev., 98, 1970.

Trenberth, J.E.; "Dynamical coupling of the stratosphere with the troposphere and sudden warmings," MIT, Dept. Meteorology, Ph.D. Thesis, Jan. 1972.

Wark, D.Q.; "SIRS: an experiment to measure the free air temperature from a satellite," Applied Optics, 9, 1761, 1970.

Wilcox, J., P. Scherrer, L. Svalgaard, W. Roberts, and R. Olson; "Solar magnetic sector structure: relation to circulation of the Earth's atmosphere," Science, 180, 185, 1973.

Willett, H.C.; "Remarks on the seasonal changes of temperature and ozone in the Arctic and the Antarctic stratospheres," J. Atmos. Sci., 25, 341, 1968.

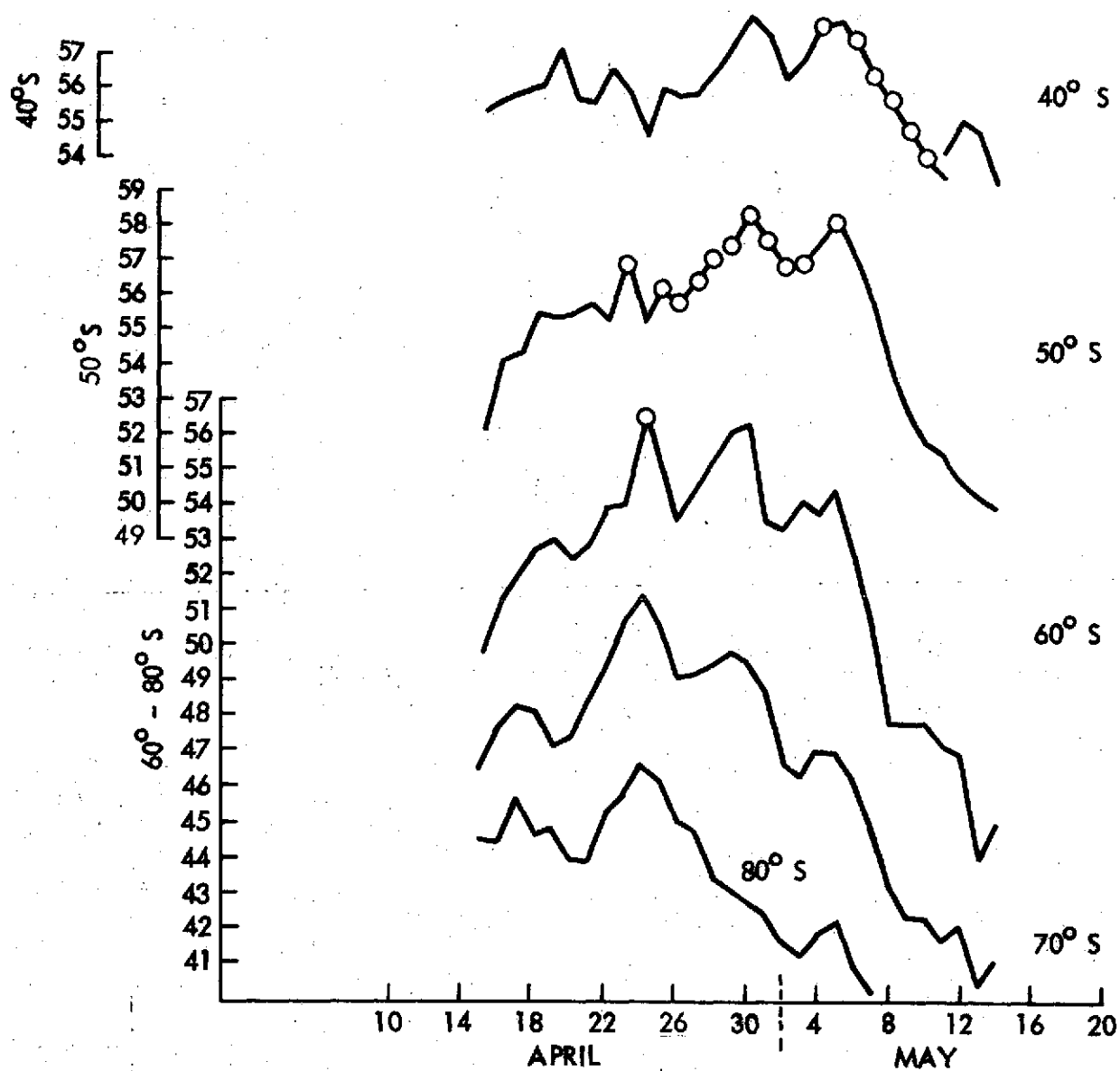


Fig. 1 March of Maximum Zonal Radiance, SIRS
Channel 8, April 15-May 14, 1969
(Circled points are hemispheric maxima)

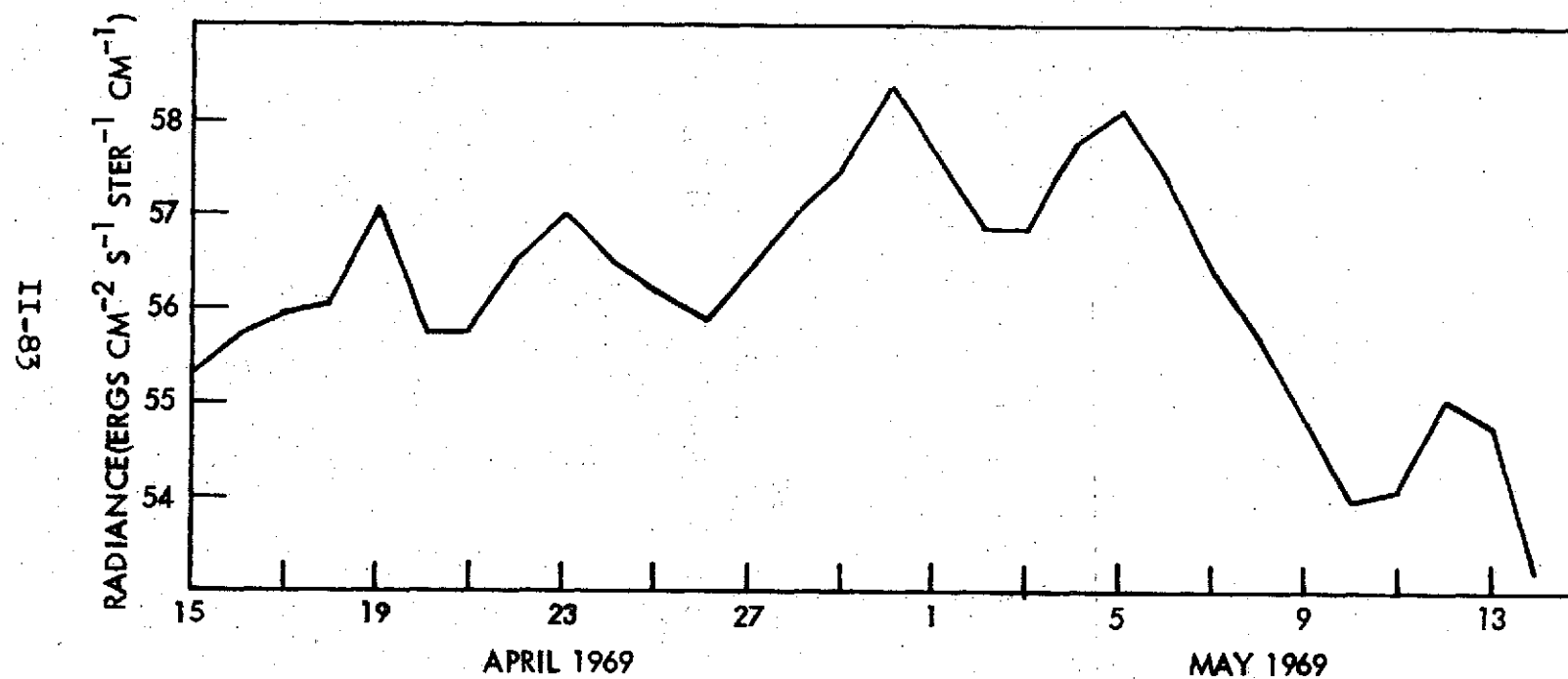


Fig. 2 March of Maximum Radiance, SIRS A Channel 8
April 15-May 14, 1969

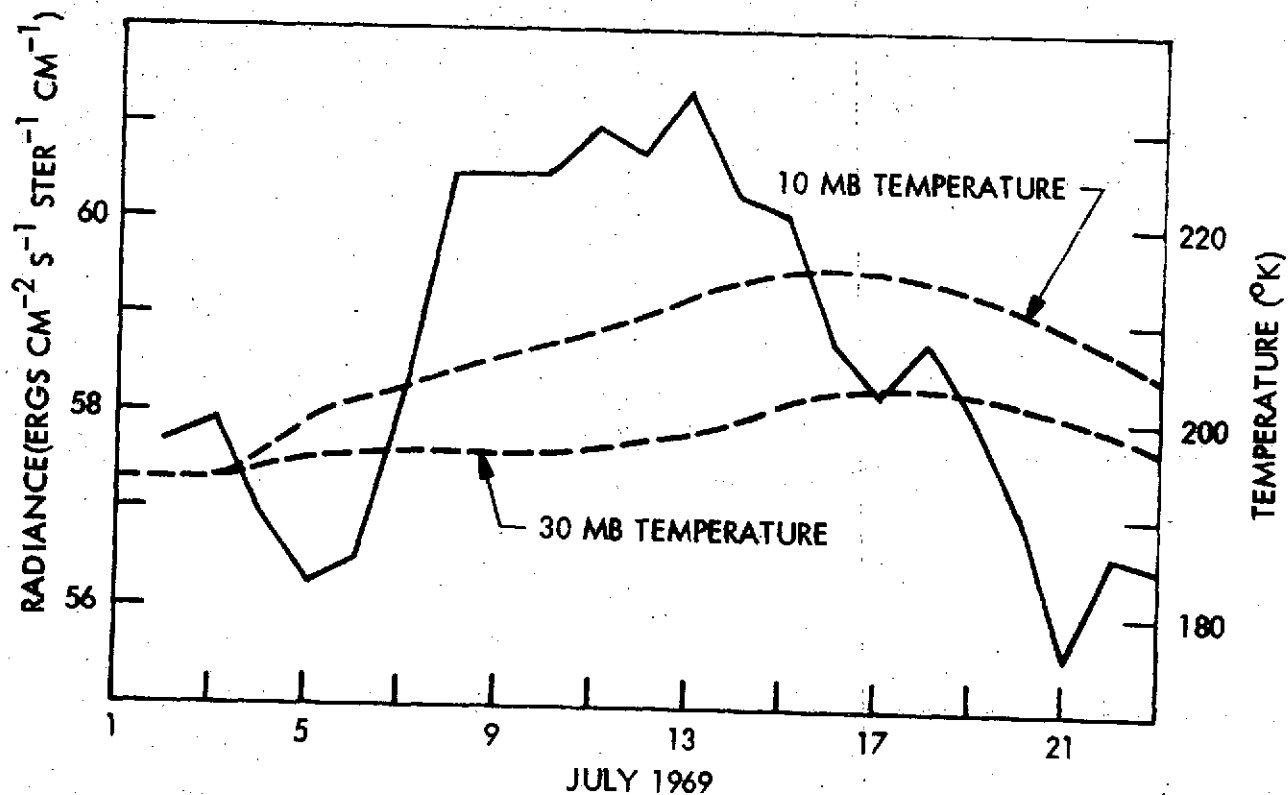


Fig. 3 March of Maximum SIRS A Channel 8 Radiance, July 1969 Southern Hemisphere.

Solid curve is maximum radiance
Dashed curves are 10- and 30-mb temperatures from
Mirny, Antarctica (Finger and McInturff, 1969;
Smith, et al, 1970)

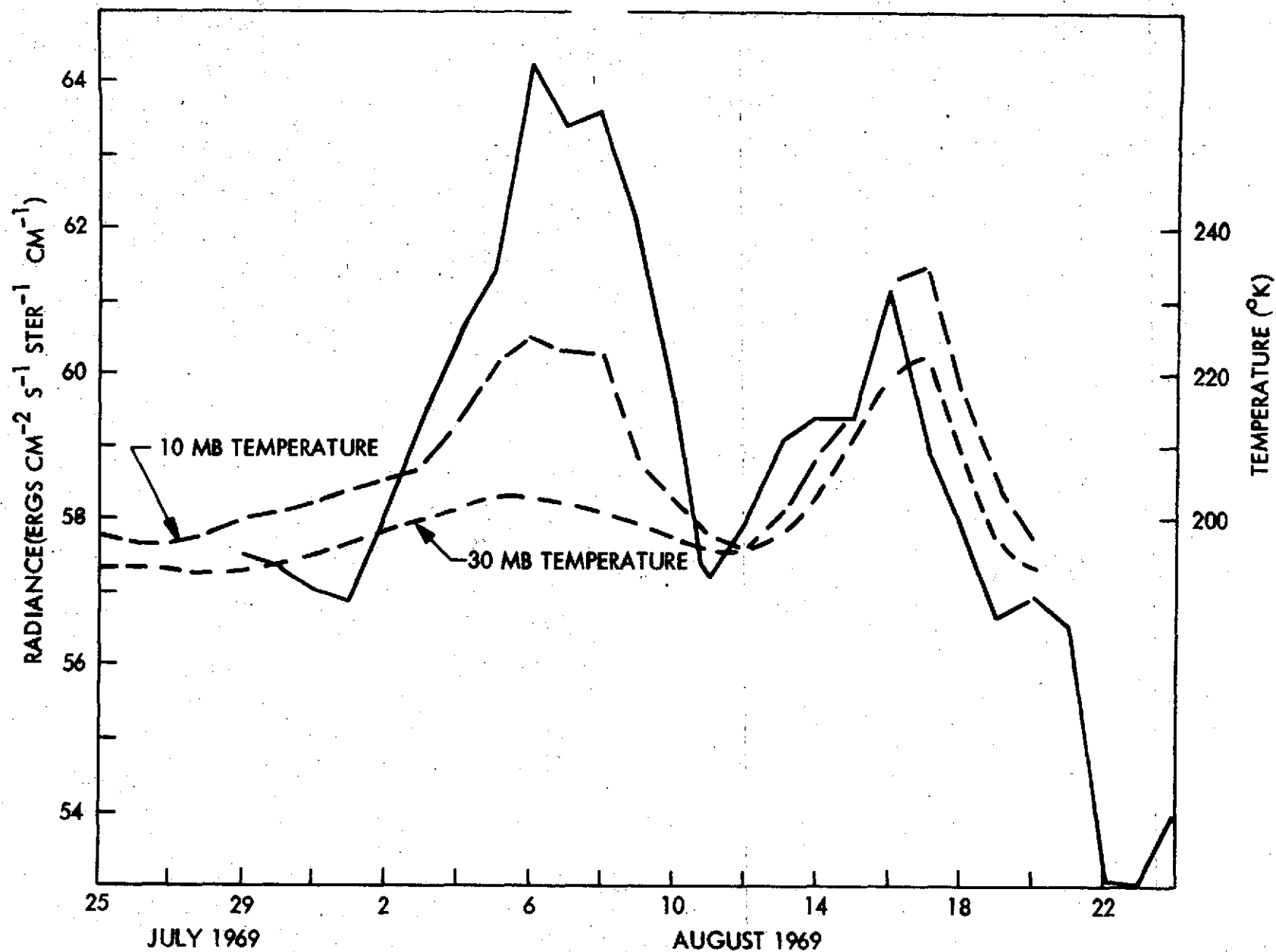


Fig. 4 March of Maximum SIRS A Channel 8 Radiance, July 25-August 24, 1969 Southern Hemisphere

Solid curve is maximum radiance.

Dashed curves are 10- and 30-mb temperatures from Mirny, Antarctica (Finger and McInturff, 1969, Smith, et al, 1970)

REPRODUCIBILITY OF THE
ORIGINAL PAGE IS POOR

REPRODUCIBILITY OF THE
ORIGINAL PAGE IS POOR

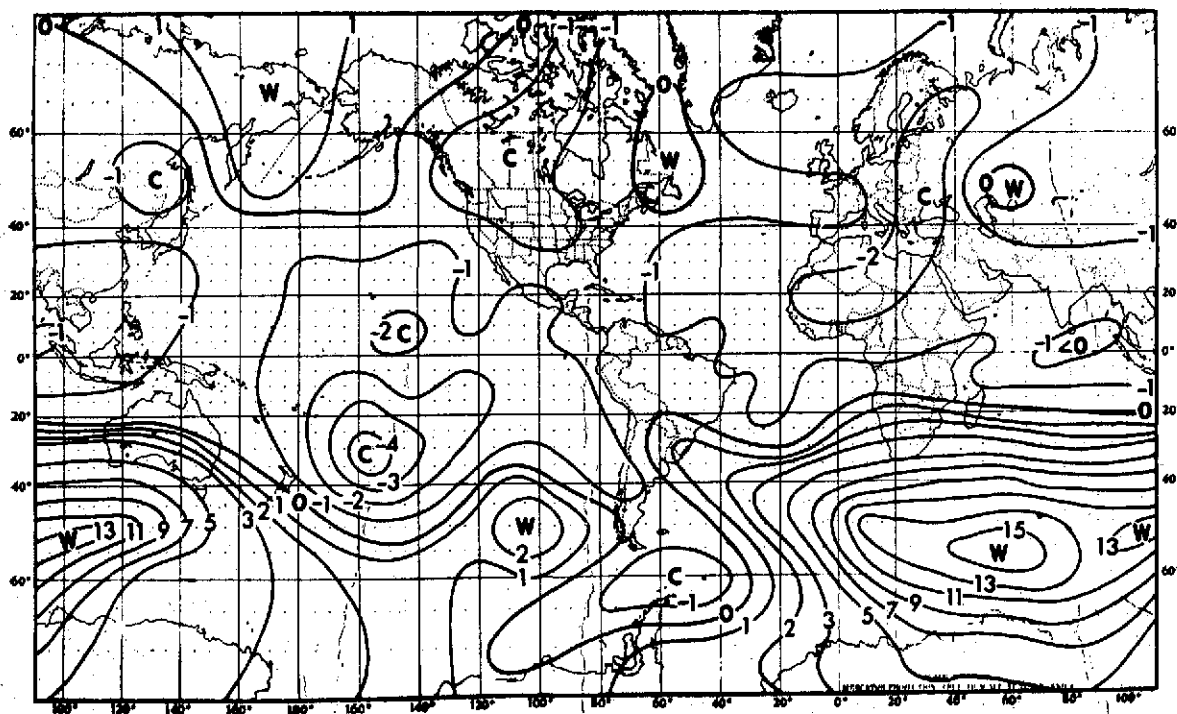


Fig. 5. Change in radiances(ergs/cm²) NIMBUS 3 SIRS(669.3 cm⁻¹) from 25 June 1969 to 10 July 1969. (Fritz and Soules, 1970)

REPRODUCIBILITY OF THE
ORIGINAL PAGE IS POOR

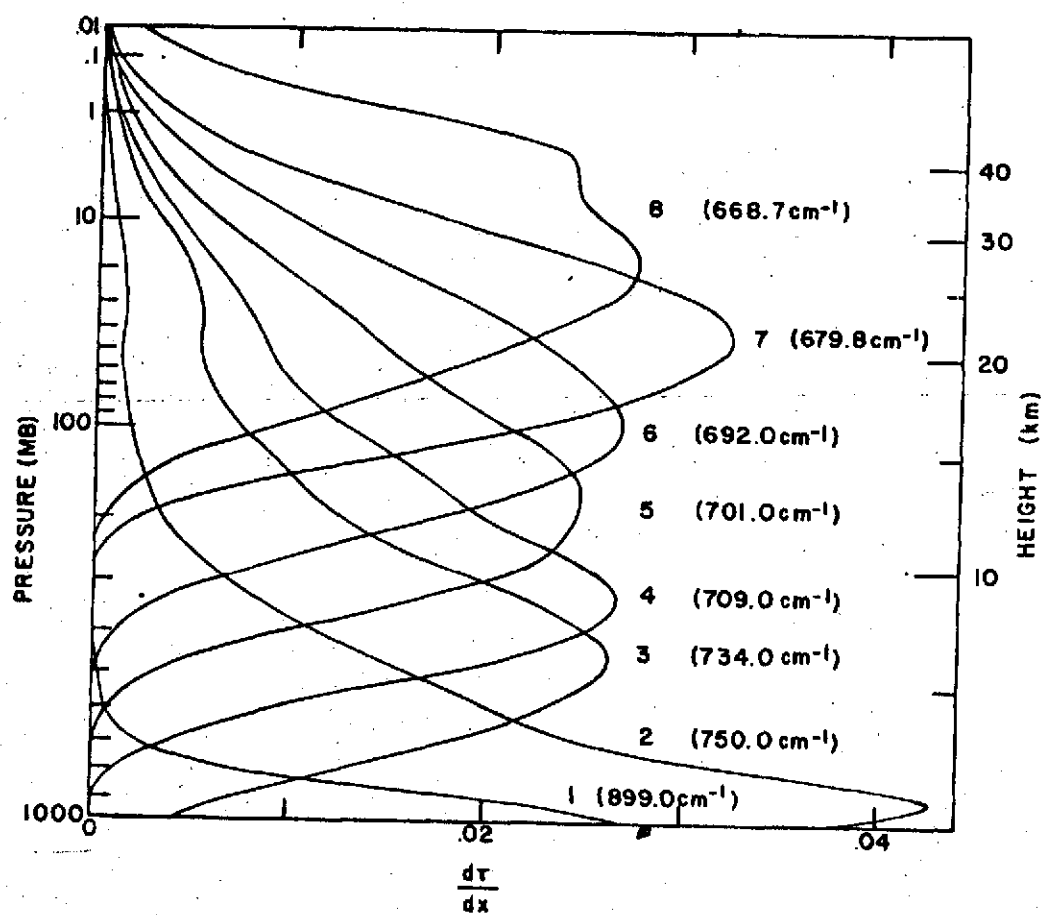


Fig.6. Weighting functions for SIRS channels (Wark, 1970)

REPRODUCIBILITY OF THE
ORIGINAL PAGE IS POOR

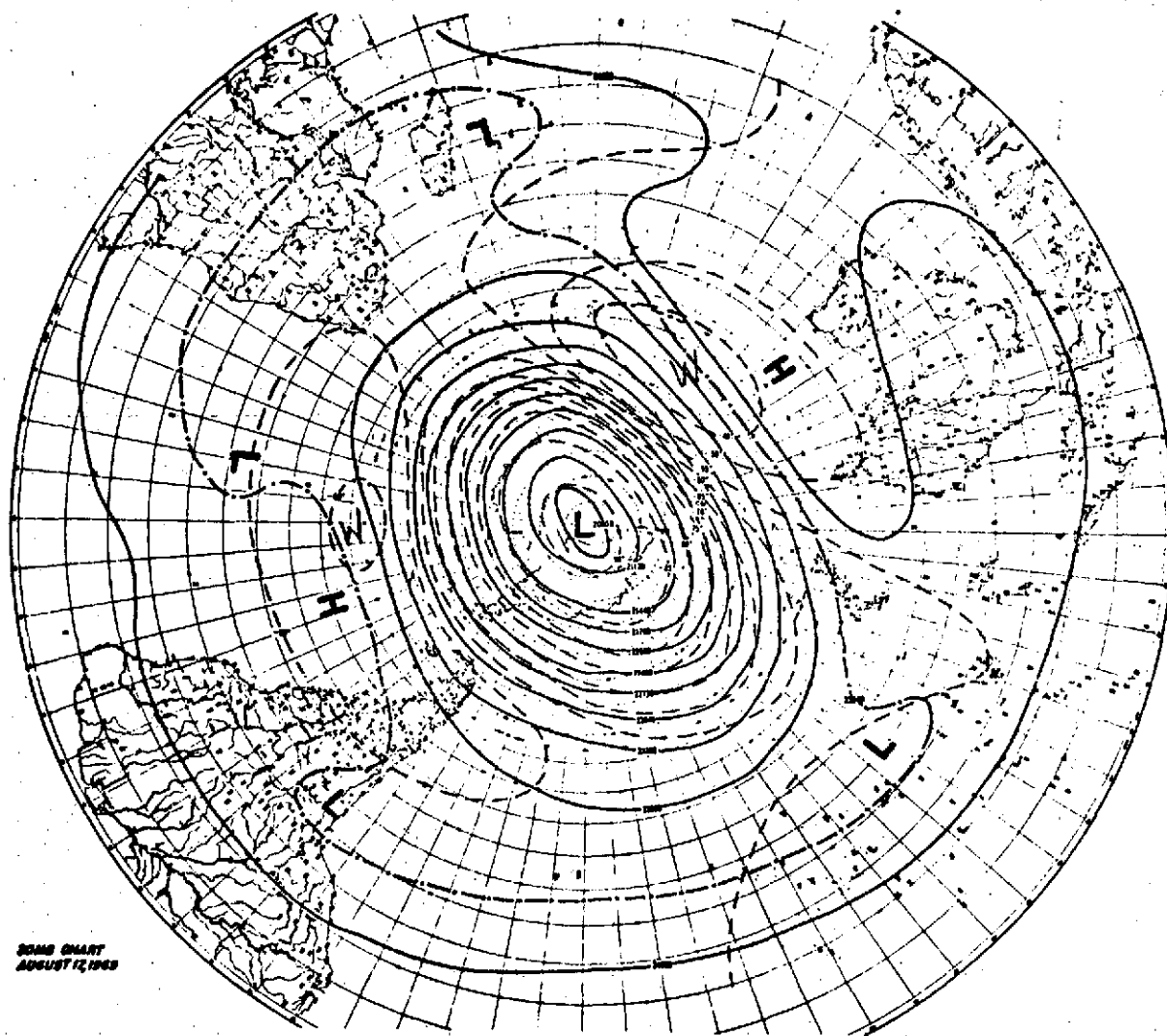


Fig. 7 30-mb analysis for 17 August, 1969. Units: geo-potential meters and degrees Celsius. (Miller, et al, 1970)

REPRODUCIBILITY OF THE
ORIGINAL PAGE IS POOR

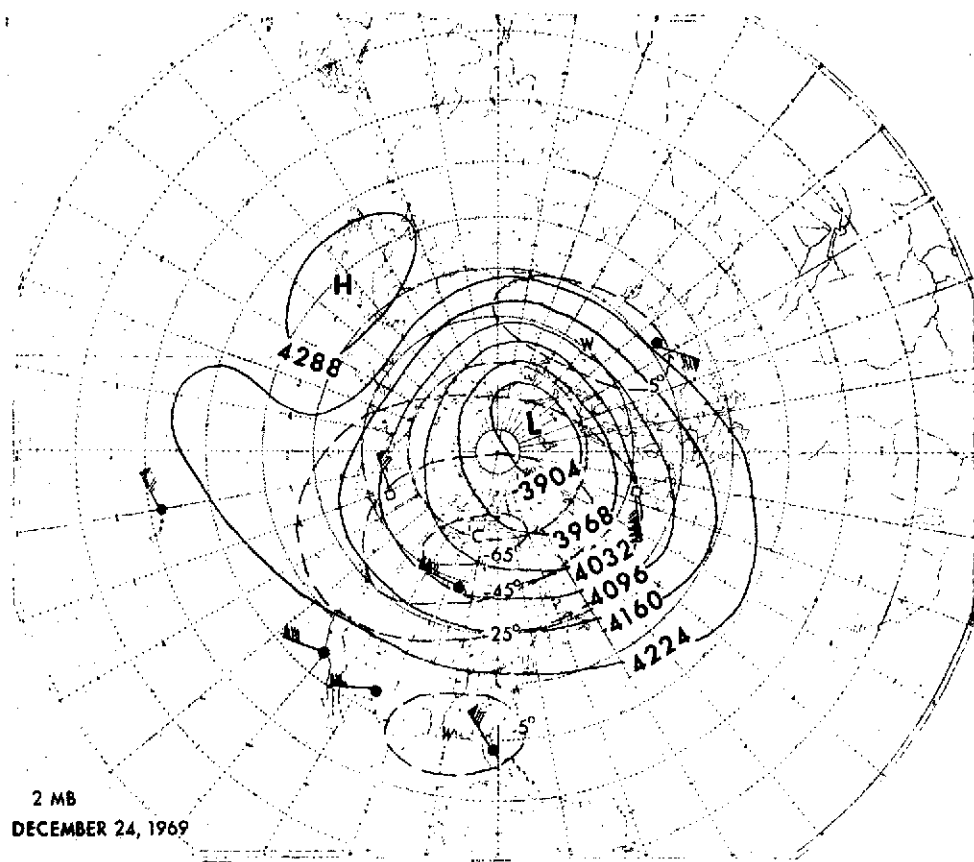


Figure 8. 2 mb analysis for 24 December 1969. Filled circle represents an observation for the analysis day, an open square one that is up to two days from analysis day. A barb on the wind vector represents 10 kt, a filled pennant 50 kt. Height is presented in geopotential decameters, temperature in °C.
(Miller, et al, 1972)

REPRODUCIBILITY OF THE
ORIGINAL PAGE IS POOR

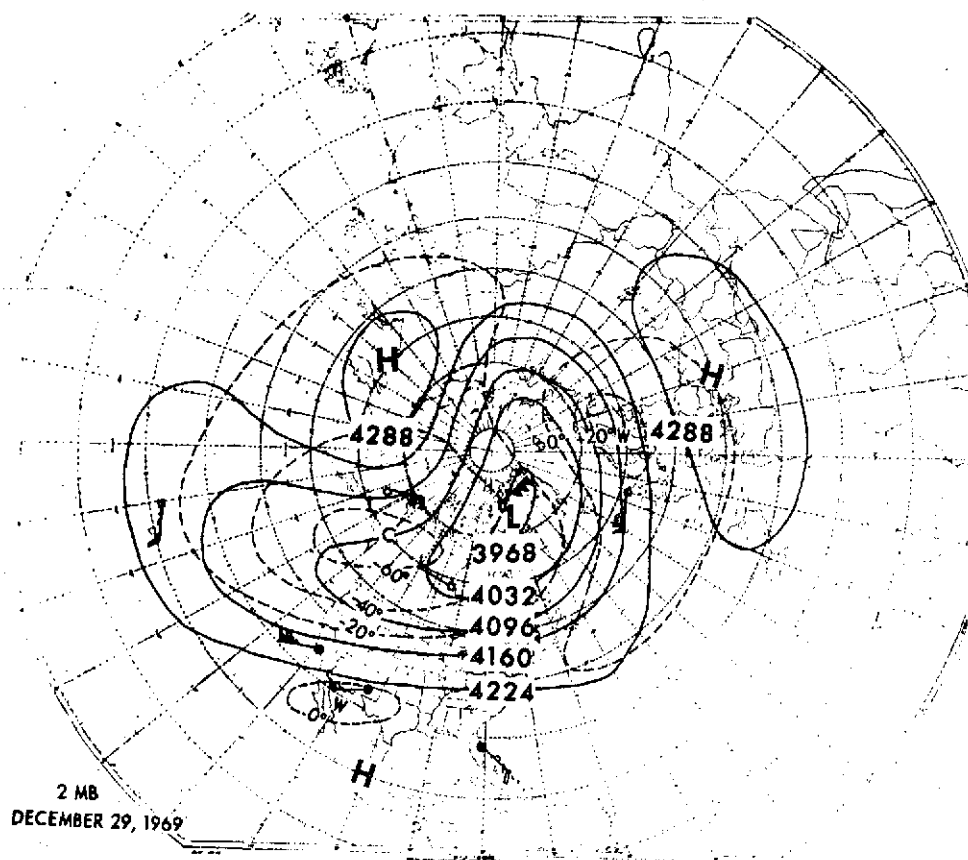


Figure 9 Same as Fig. 8 for 29 December 1969.

REPRODUCIBILITY OF THE
ORIGINAL PAGE IS POOR

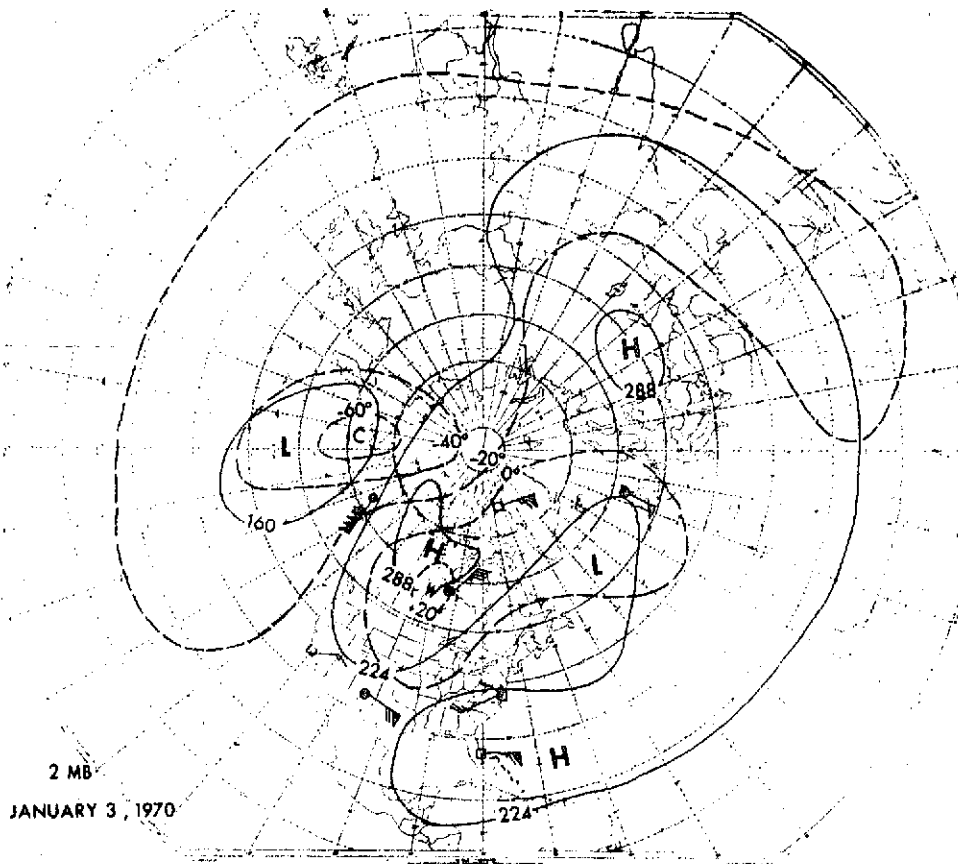


Figure 10 Same as Fig. 8 for 3 January 1970.

REPRODUCIBILITY OF THE
ORIGINAL PAGE IS POOR

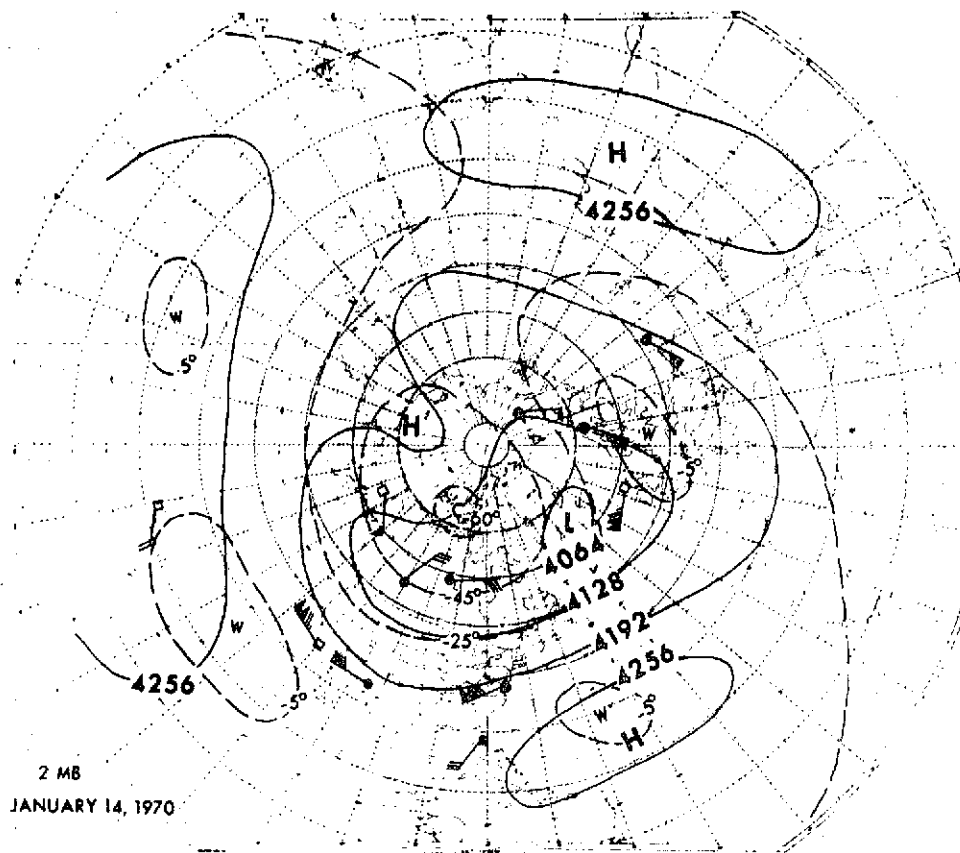


Figure 11 Same as Fig 8 for 14 January 1970.

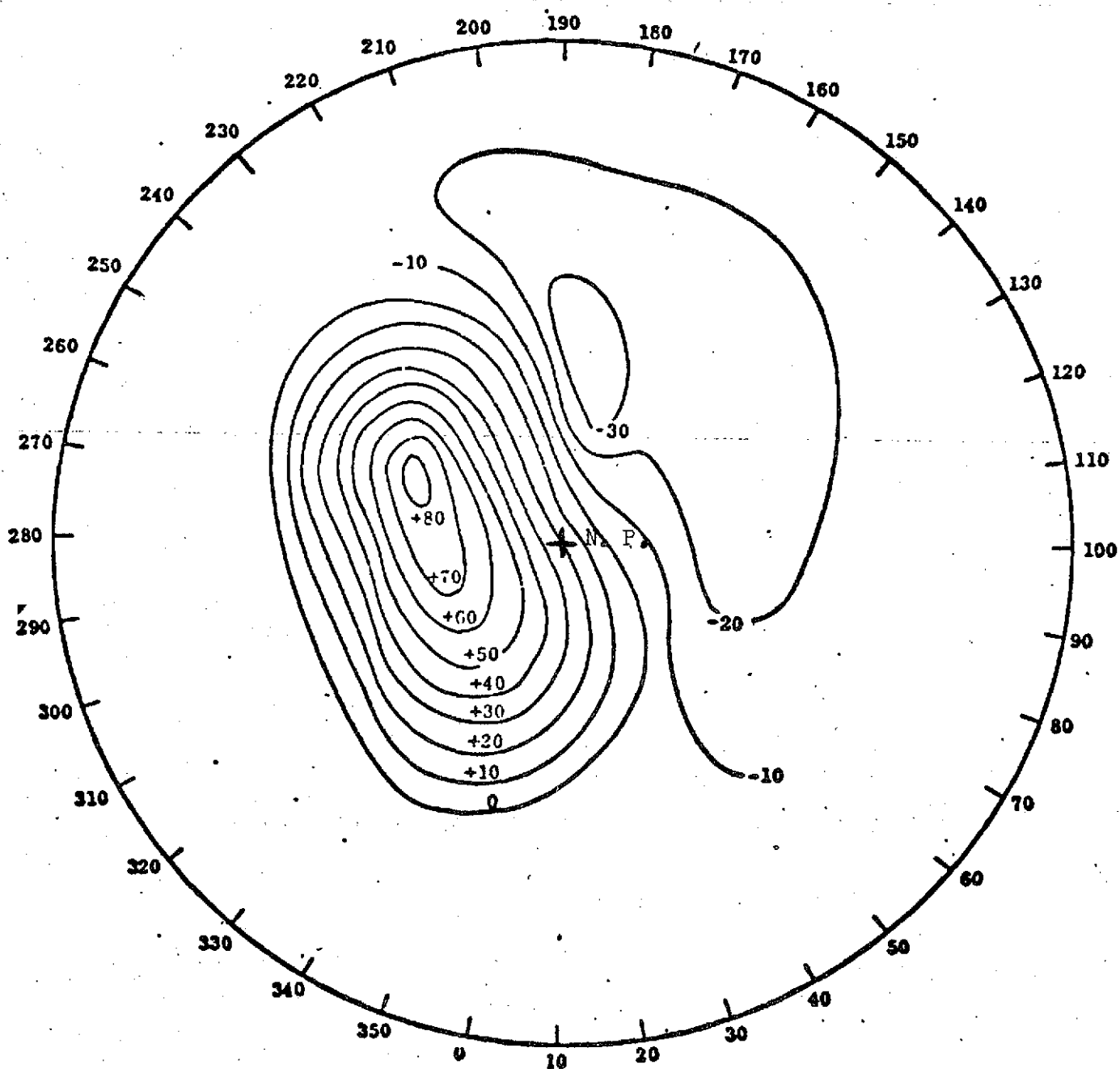


Fig. 12. Change in 2-mb Temperature between December 24, 1969 and January 3, 1970. (Derived by subtracting the temperature field in Fig. 8 from that in Fig. 10)

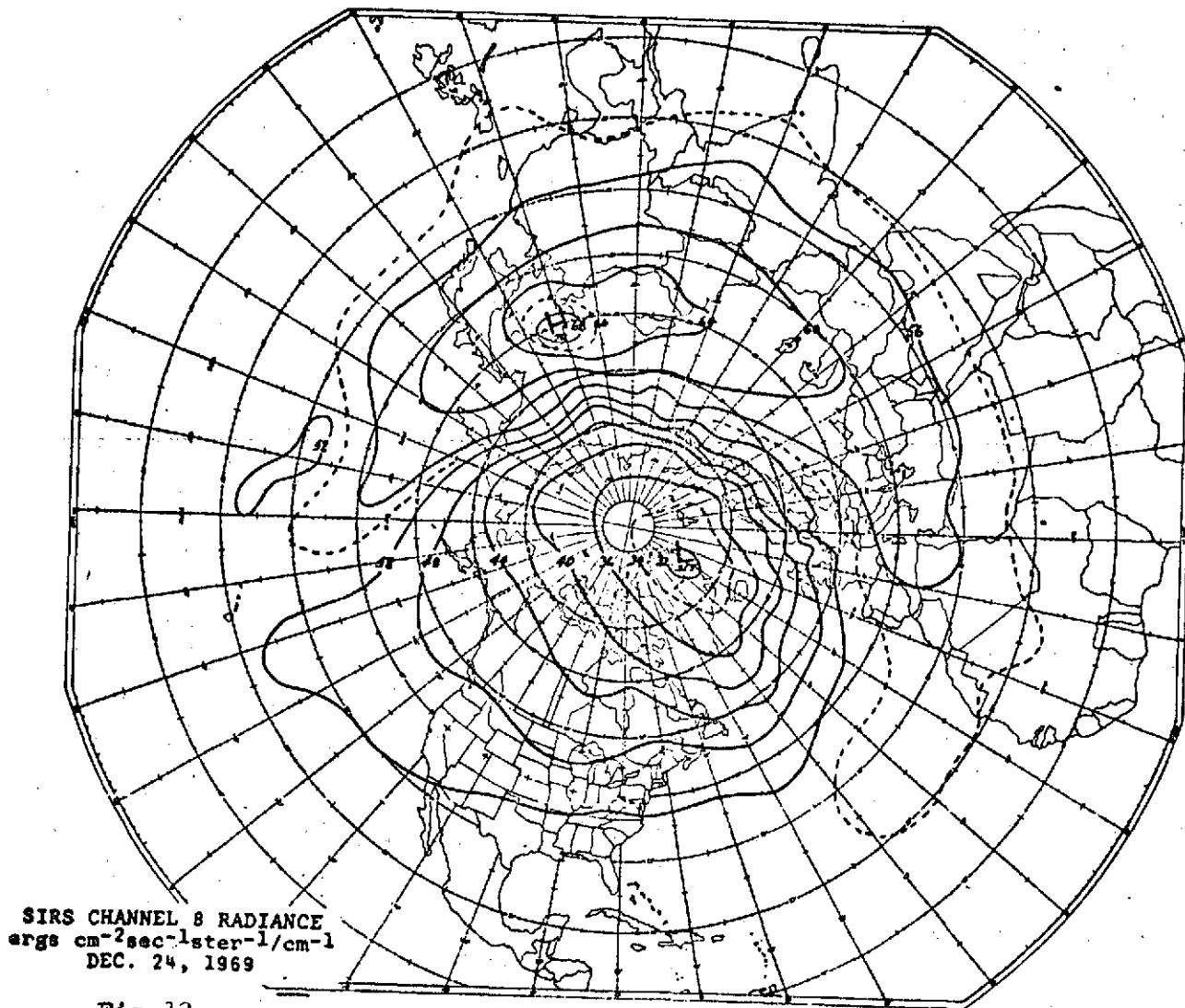


Fig. 13. Channel 8 radiance map for 24 December 1969. Maximum value in eastern Siberia is 70 ergs/, minimum near pole is 31.5 ergs/.
 (Quiroz, 1971)

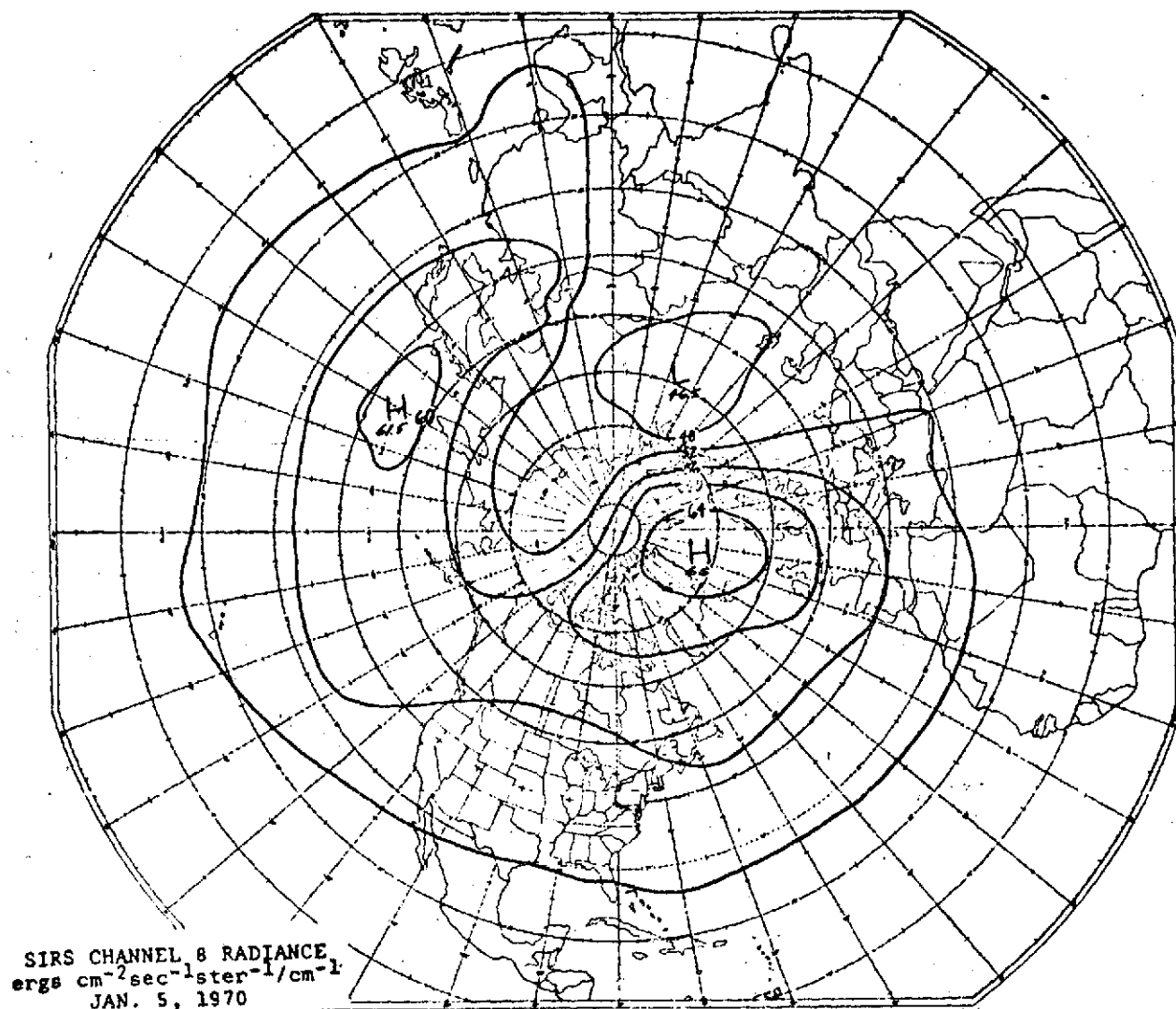


Fig 14. Channel 8 radiance map for 5 January 1970. Principal high-radiance center (66 ergs/) is located over NE Greenland coast. A secondary high (61.5 ergs/) was generated from main system in polar area, travelling westward to Far East (Quiroz, 1971)

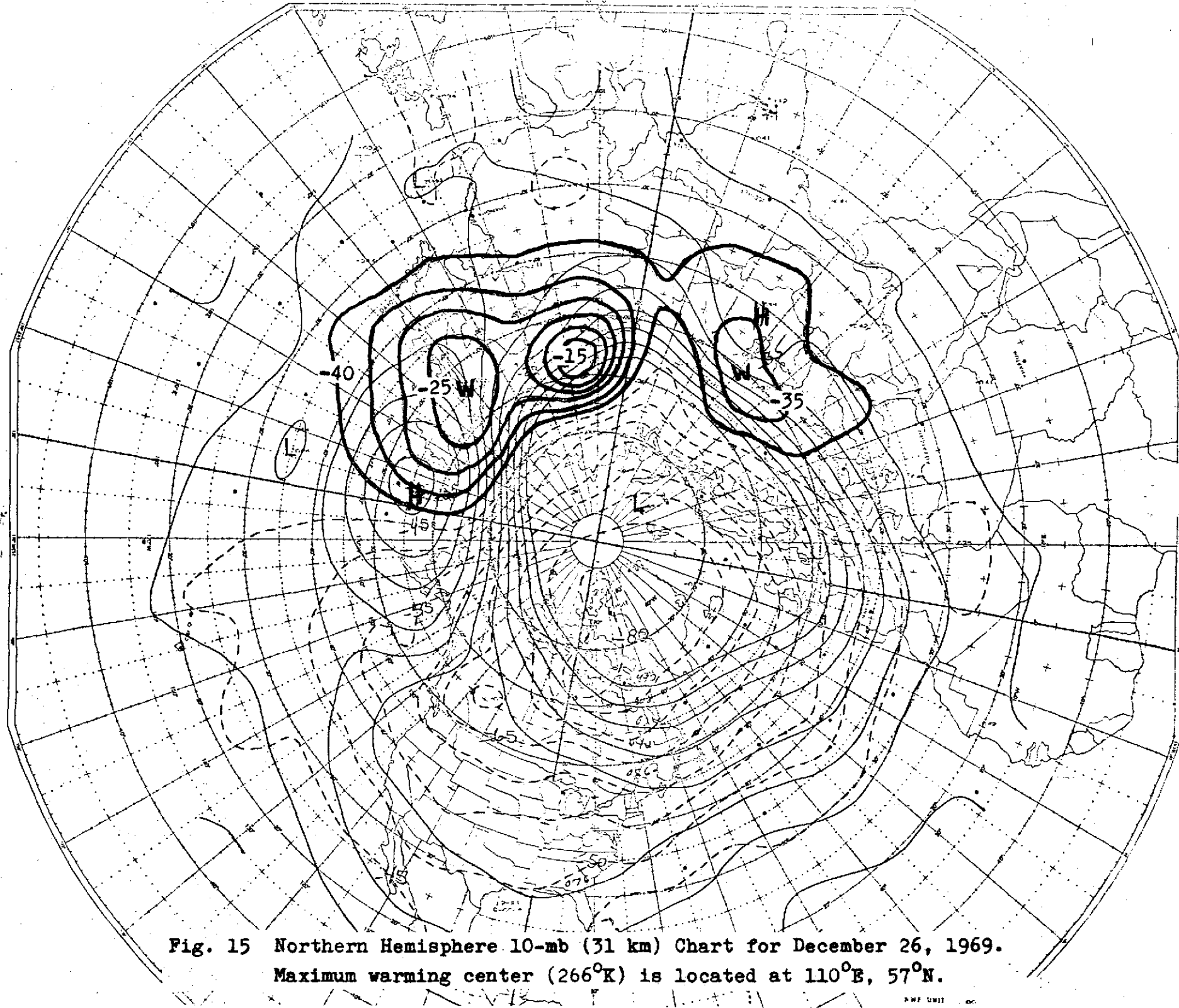


Fig. 15 Northern Hemisphere 10-mb (31 km) Chart for December 26, 1969.
Maximum warming center (266°K) is located at 110°E, 57°N.

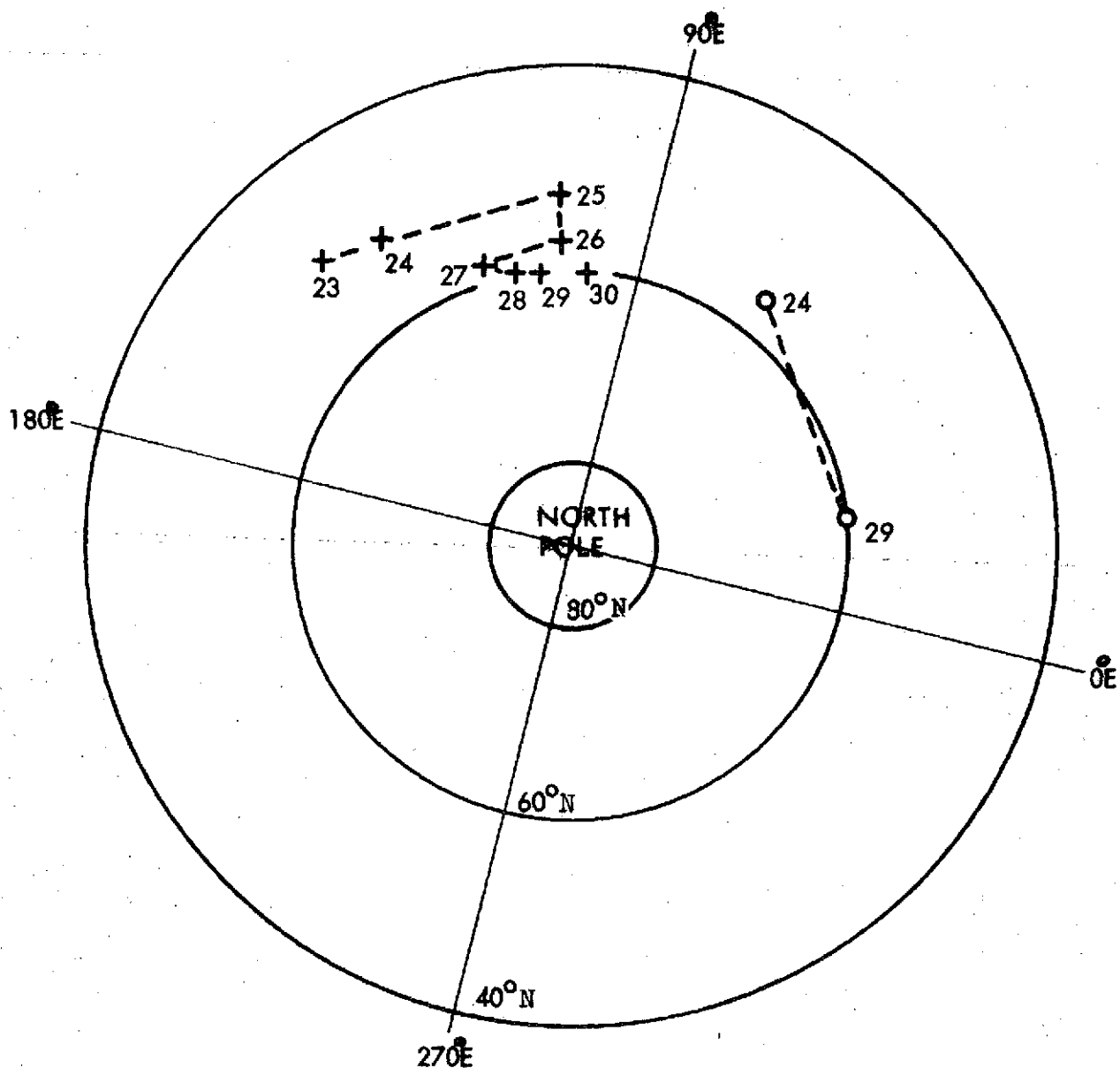


Fig. 16 Movement of Warming Center at 10 mb from 23 to 30 December 1969
 Date is beneath locating cross.
 Circles locate warming center at 2 mb (43 km)

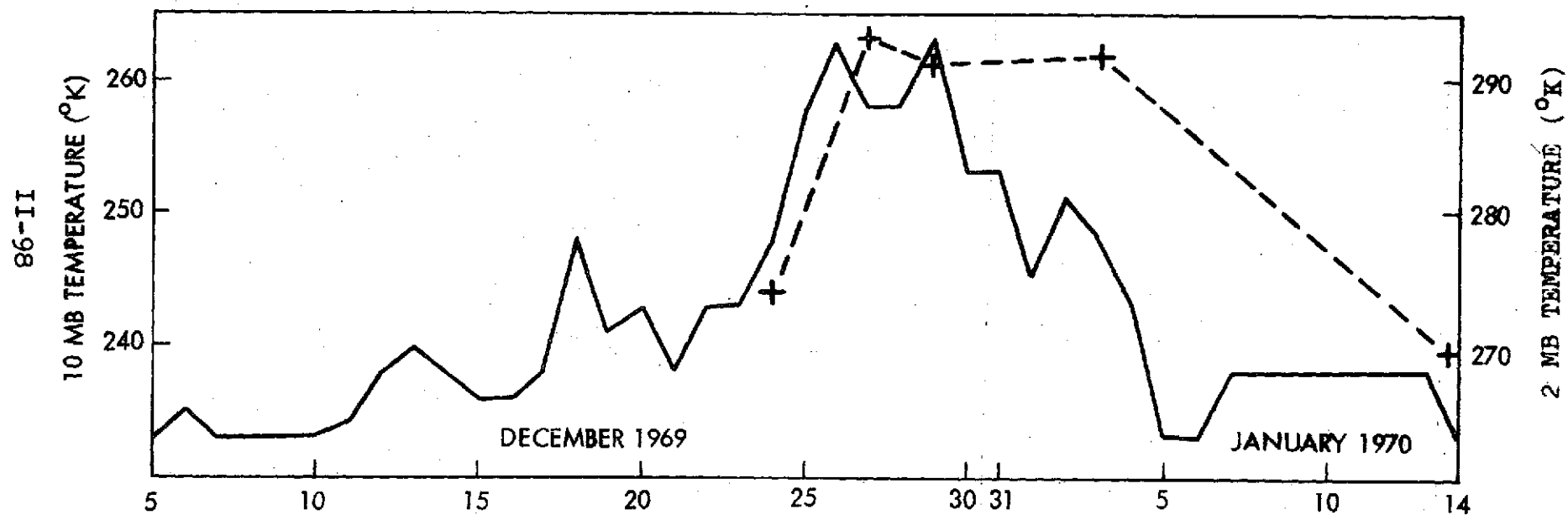
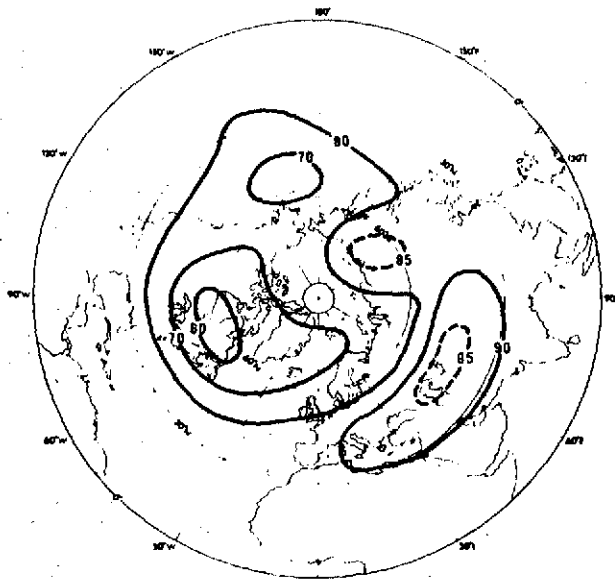


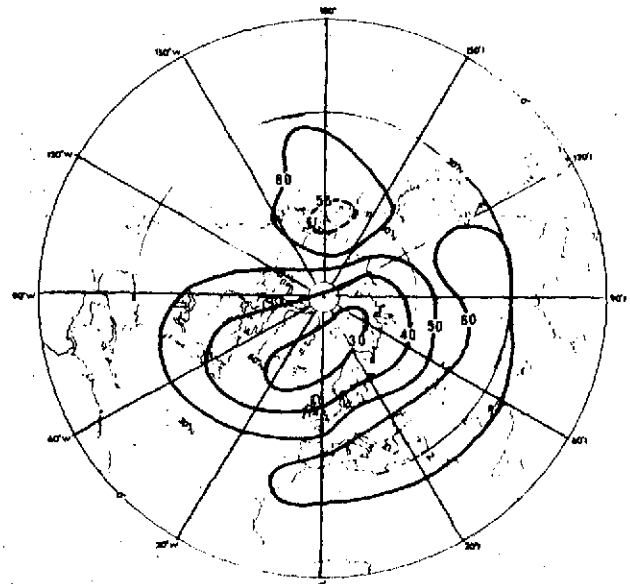
Fig. 17 March of Maximum Daily 10-mb Temperature at Latitudes Above 40°N
Between December 5, 1969 and January 14, 1970

Dashed curve indicates march of 2-mb (43 km) Temperature



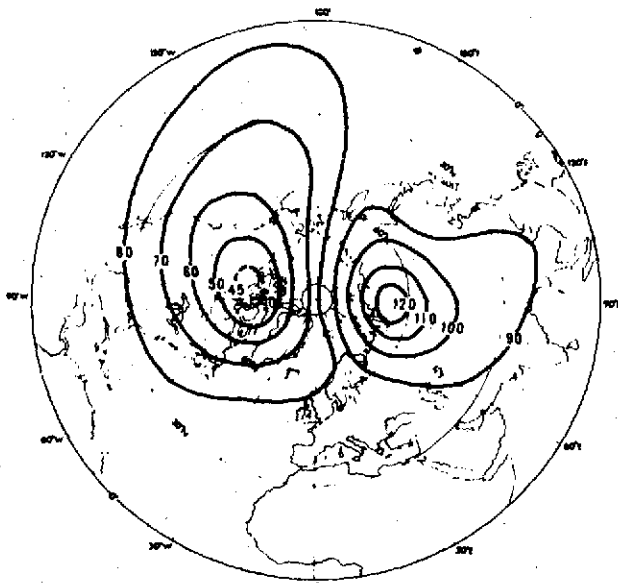
(a)

Channel A (~ 2 mb) Dec 30, 1970



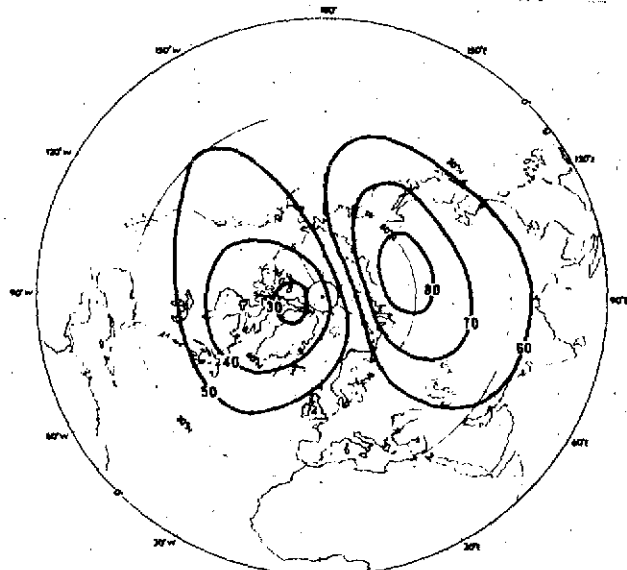
(b)

Channel B (~ 20 mb) Dec 30, 1970



(c)

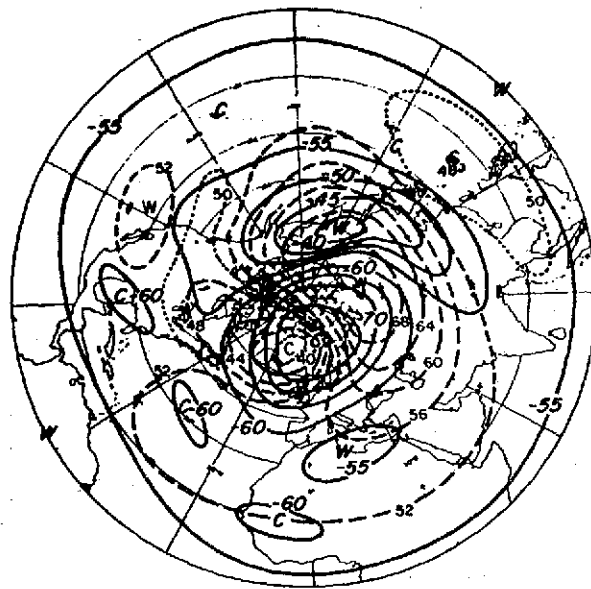
Channel A (~ 2 mb) Jan 4, 1971



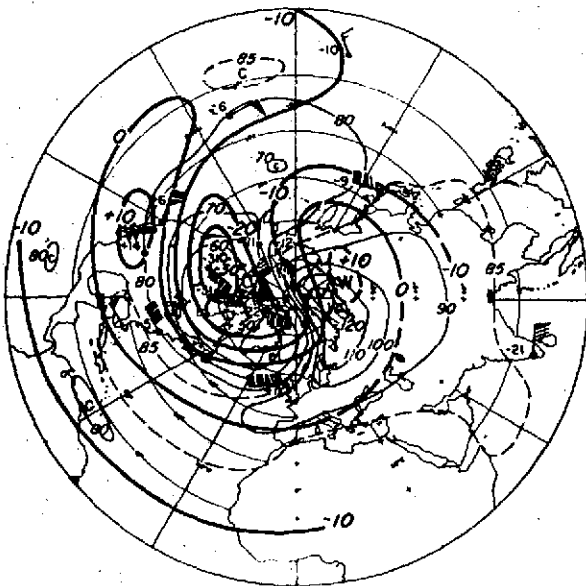
(d)

Channel B (~ 20 mb) Jan 4, 1971

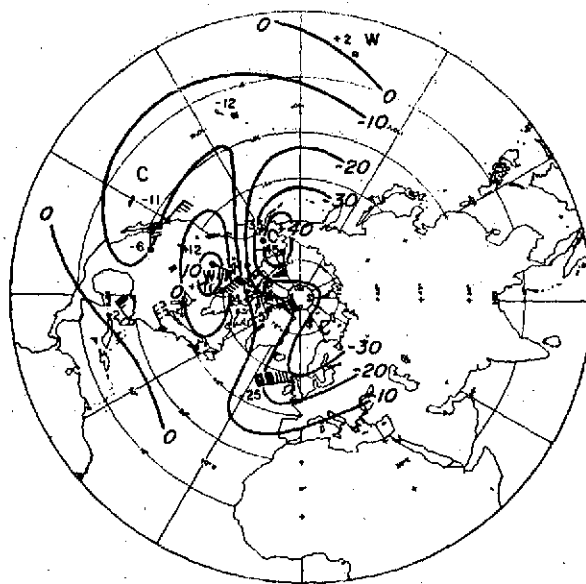
Fig. 18. North Polar stereographic maps showing isopleths of radiance in $\text{mW/m}^2\text{sr cm}^{-1}$ from SCR Channels A and B. (Barnett, et al, 1971)



a



b



c

Fig. 19. a, Temperatures at 30 mb (solid lines) and radiances of SIRS channel 8 (dashed lines) for 7 Jan. 1971. b, Temperatures at 45 km (heavy lines) and radiances (thin lines) of channel A of SCR for 6 Jan. 1971, based on all rocket observations available within 3 days before and after map date. c, temperatures at 60 km for 6 Jan. 1971 (with the notation of Fig. b). (Labitzke, 1972)

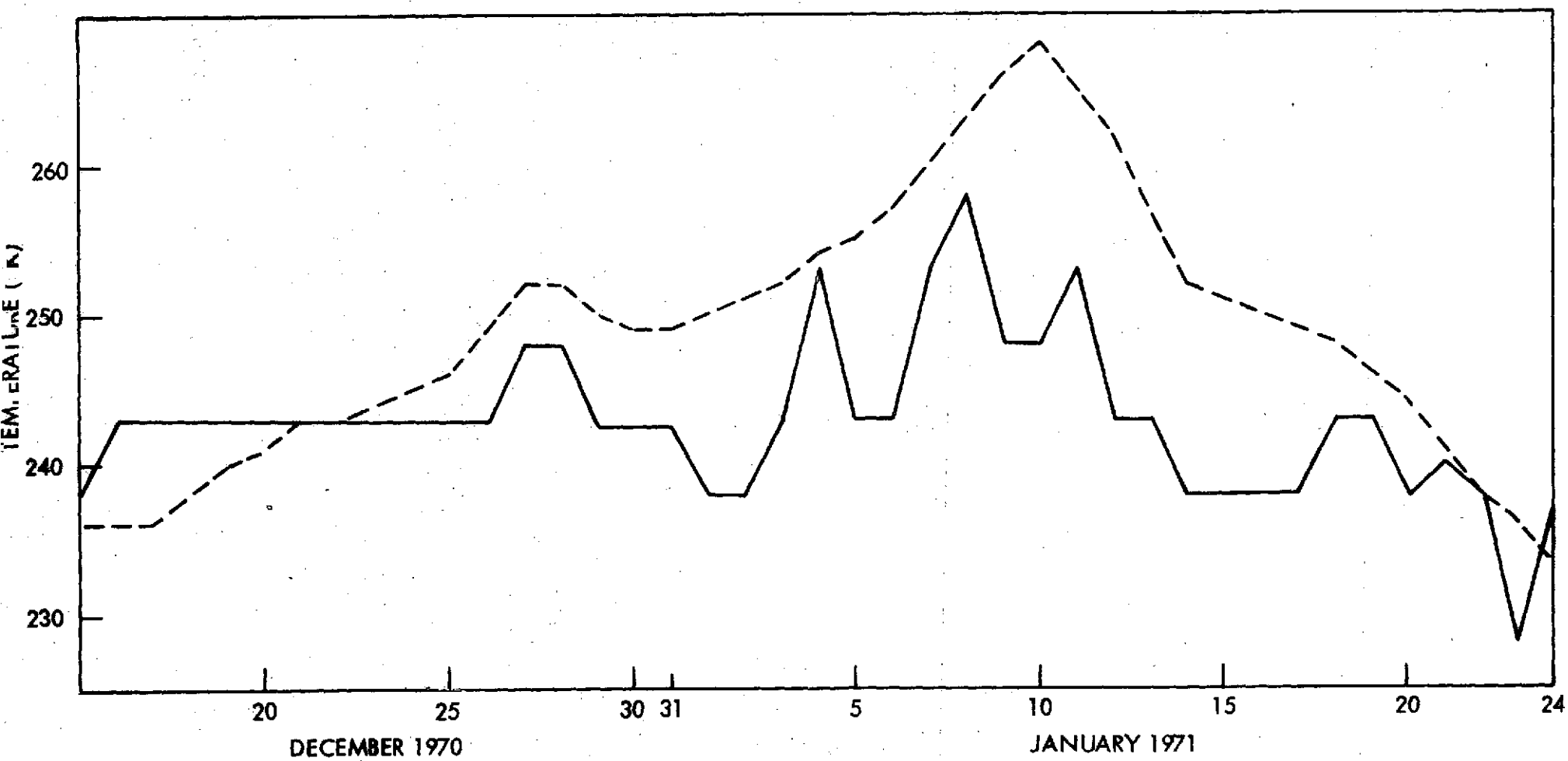


Fig. 20 March of Maximum Daily 10-mb Temperature Above 40°N Latitude From December 15, 1970 to January 24, 1971.

Dashed curve indicates the march of 2-mb (43 km) high-latitude zonal average temperature.

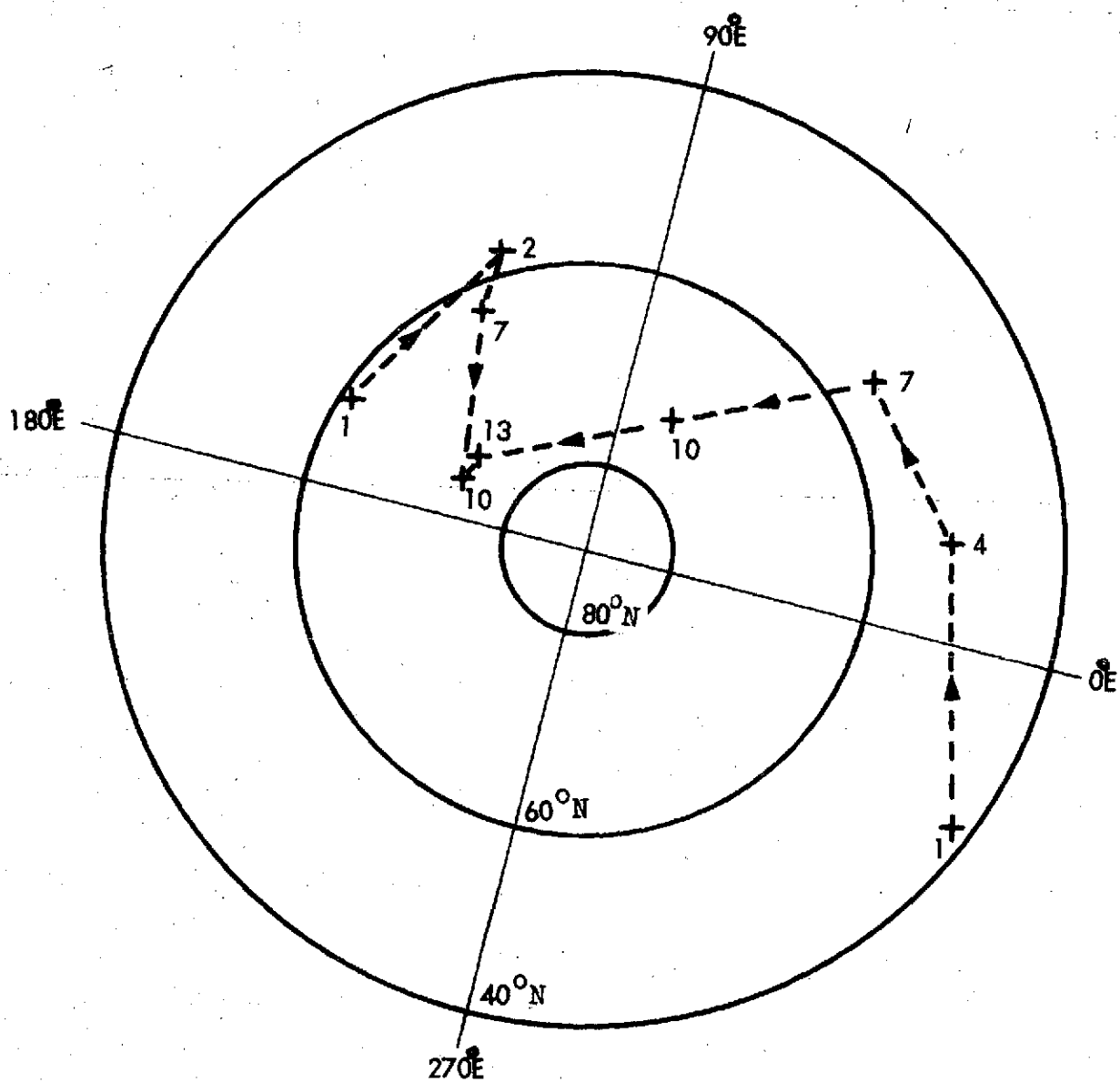


Fig. 21 Global March of Warming Centers at 10 mb in January 1971.

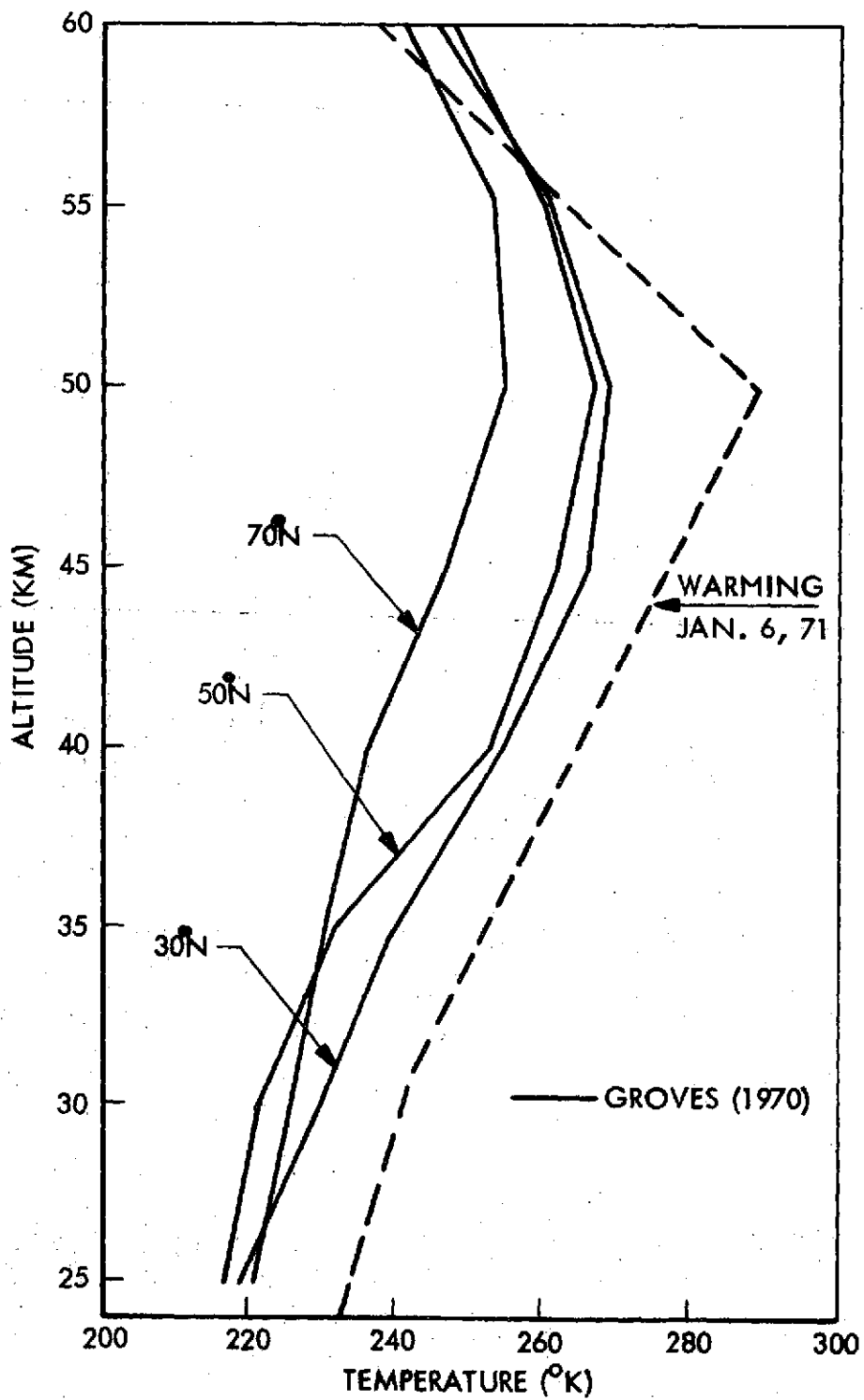


Fig. 22 Temperature-Height Profile in the Vicinity of a Warming, Derived from Constant Pressure Charts

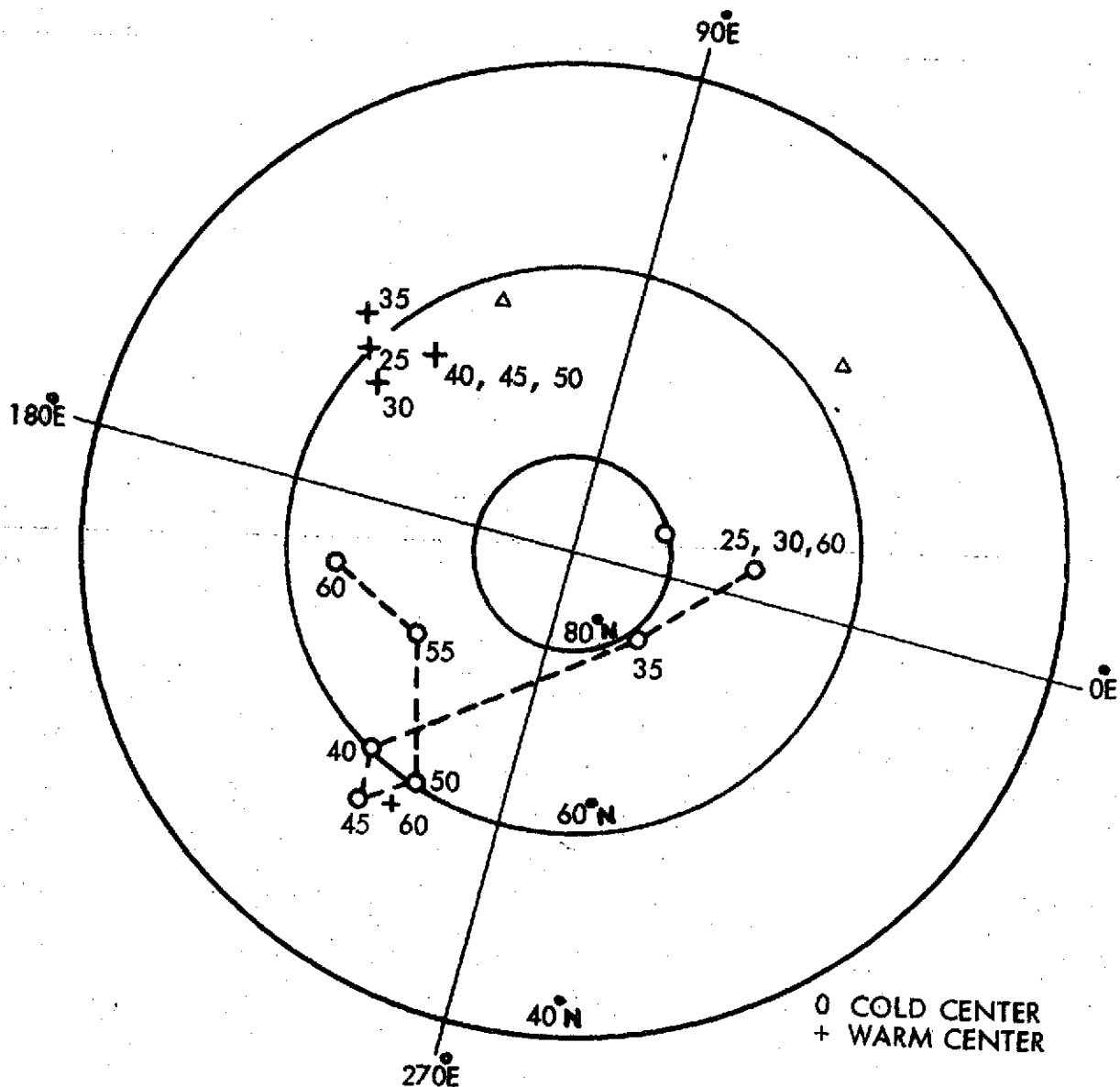


Fig. 23 Locations of Warm and Cold Centers from 25 to 60 km on January 6, 1971 in the Northern Hemisphere
Altitude in kilometers is indicated below locations.
Triangles indicate positions of warm centers at 31 km.
Square indicates position of low.

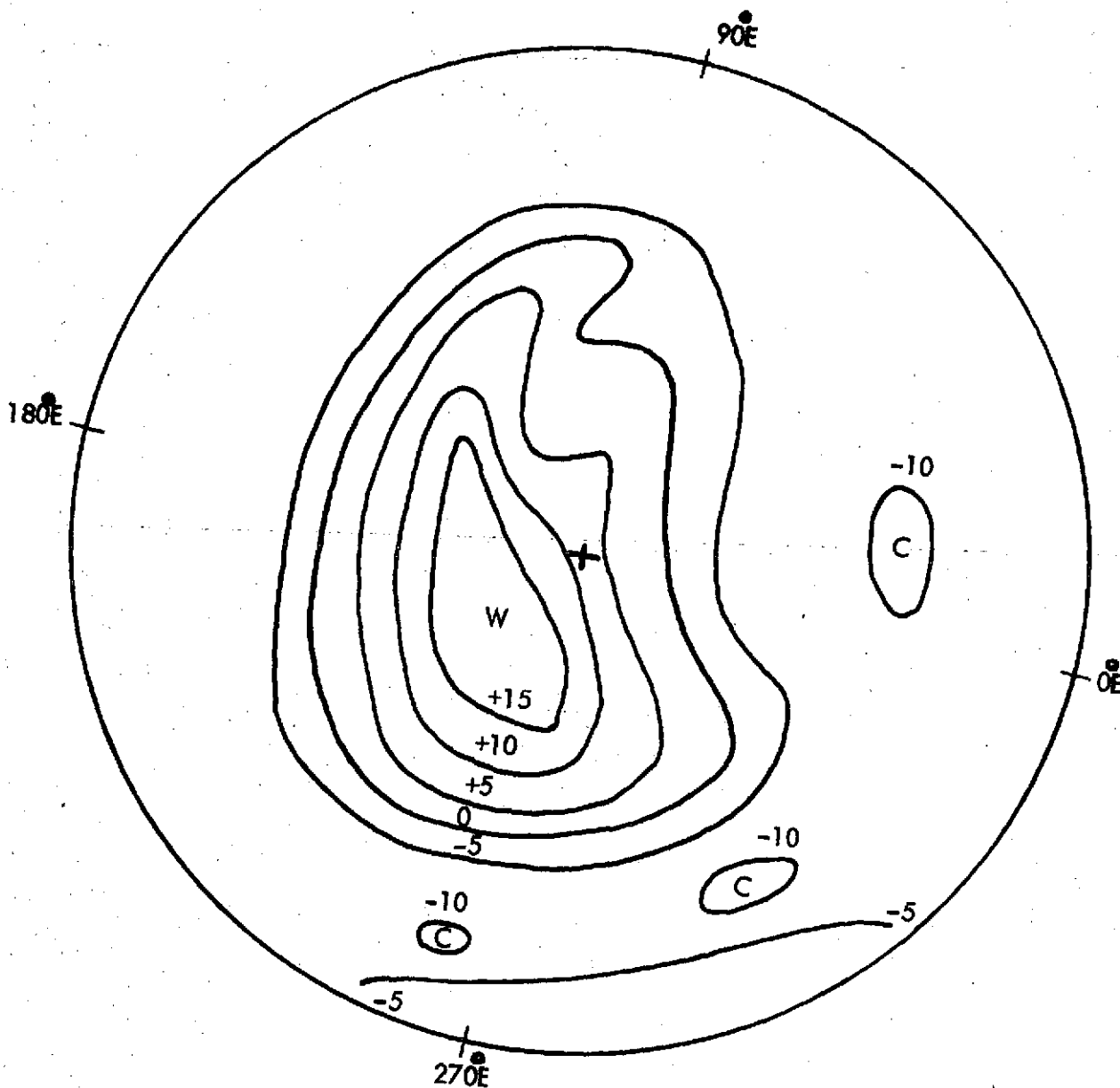


Fig. 24 Temperature Change from Unwarmed Condition
at 25 km on January 6, 1971
Temperature change is in $^{\circ}\text{K}$.

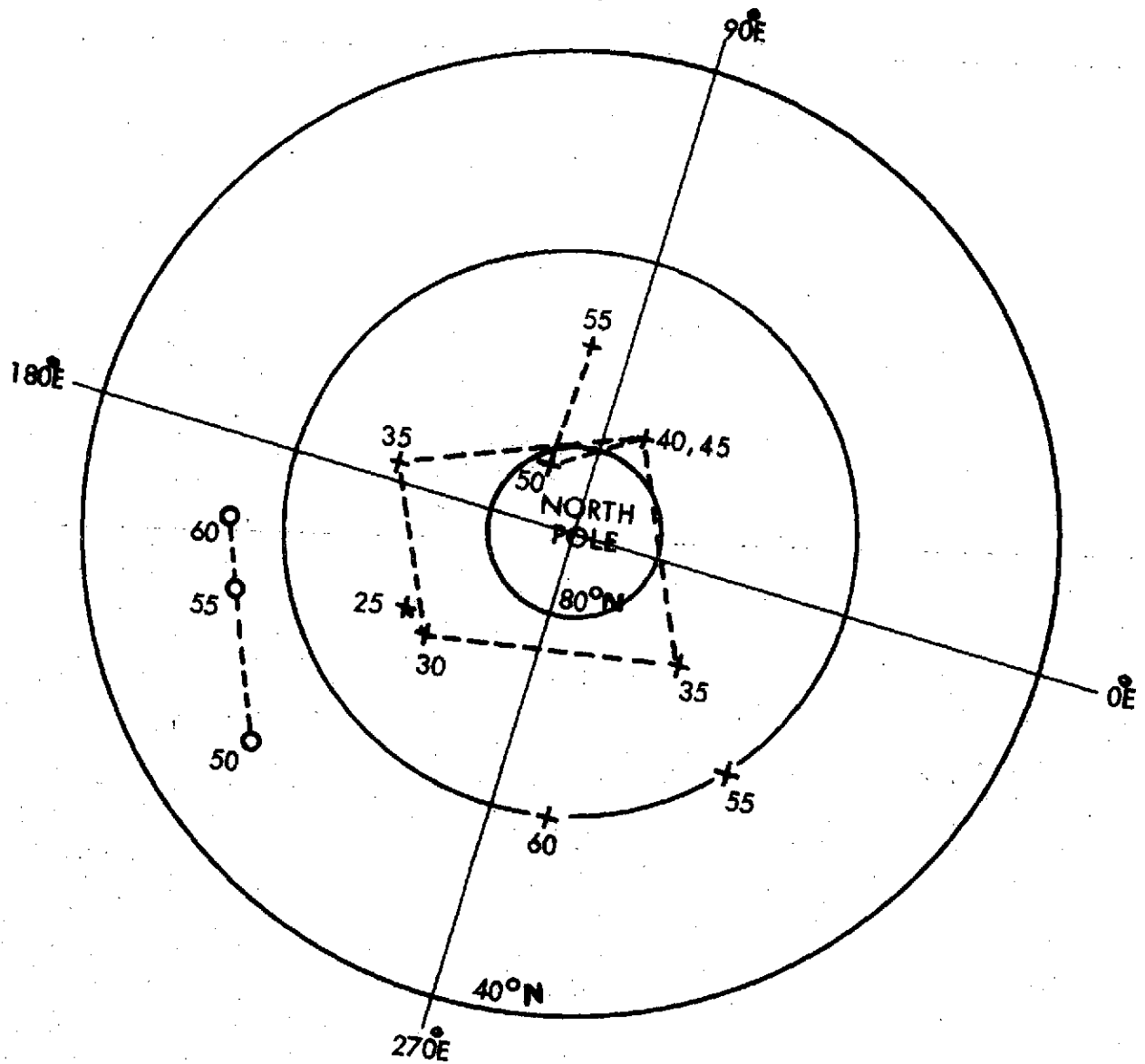


Fig. 25 Locations of Temperature Change Centers from 25 to 60 km January 6, 1971.

Temperature increase centers indicated by crosses.
 Temperature decrease centers indicated by circles.
 Altitude in kilometers shown below circle or cross.

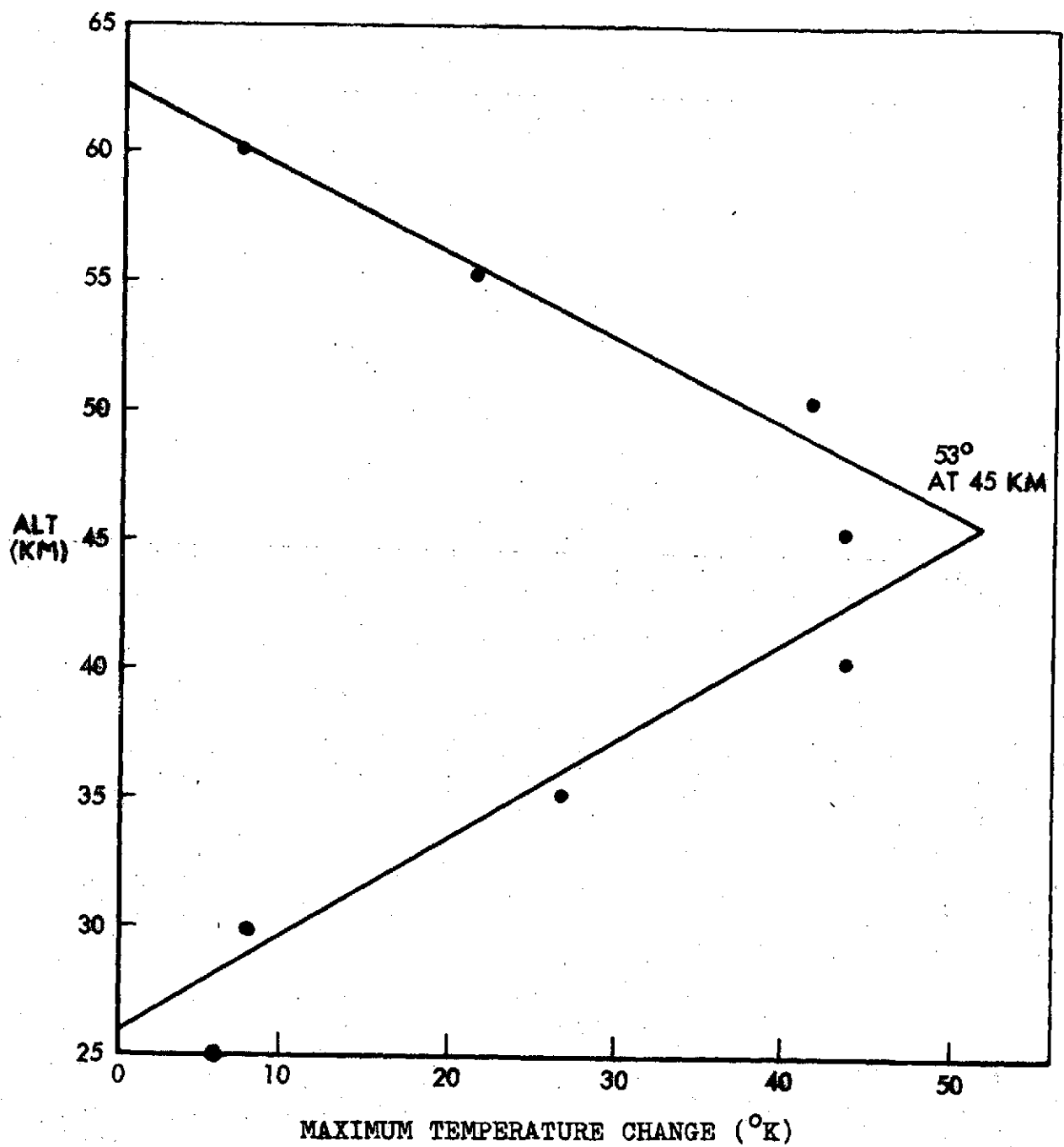


Fig. 26 Maximum Temperature Increase at Altitudes Between 25 and 60 Kilometers at 78°N, 70°E During 1970-71 Warming.

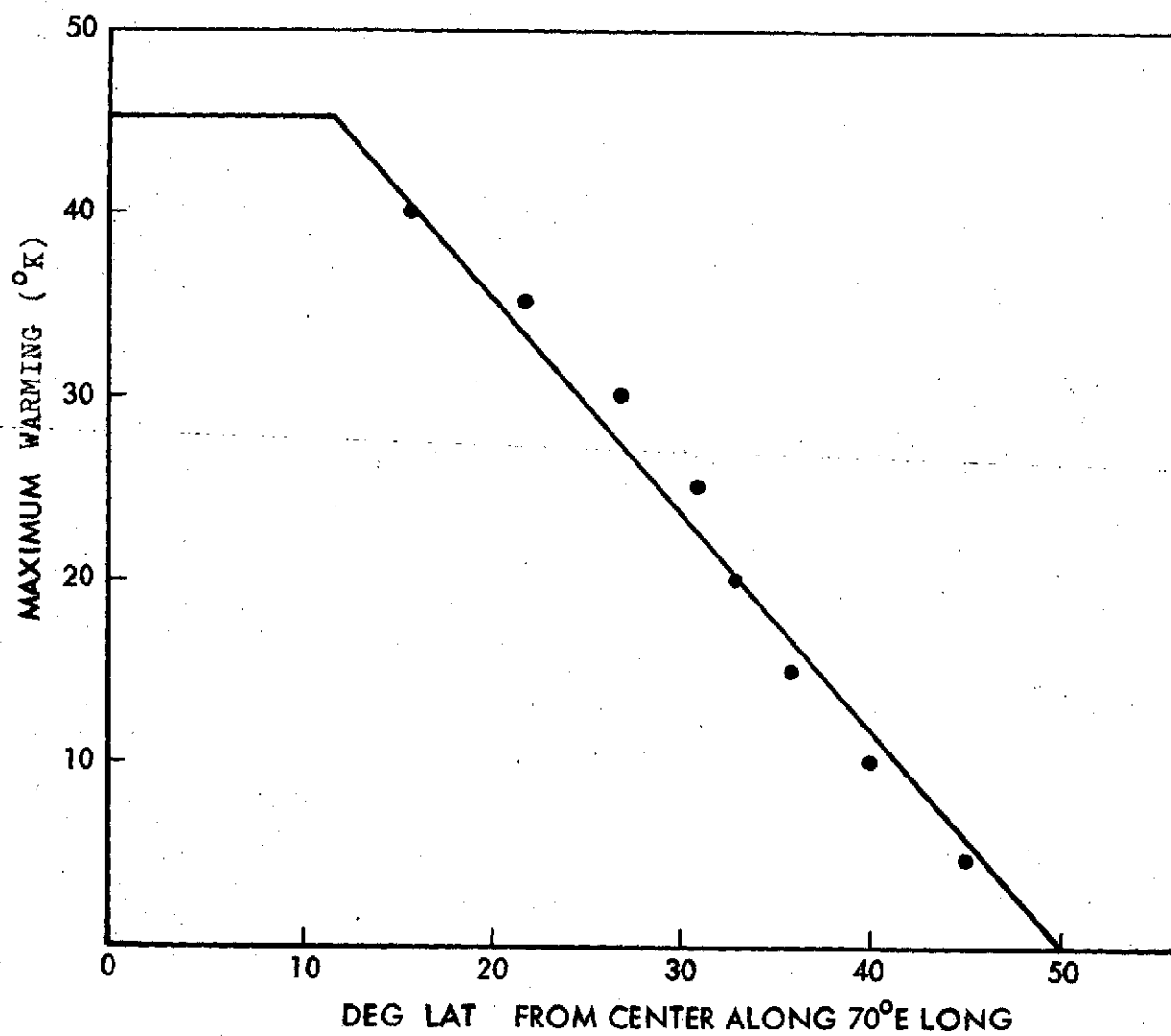


Fig. 27 Decrease in Warming Magnitude with Distance from Warming Center

PART III

ANALYSIS OF DATA FROM SPACECRAFT - STRATOSPHERIC WARMINGS

AN HYPOTHESIS FOR THE RELATION BETWEEN
AURORAL ELECTROJETS AND STRATOSPHERIC WARMINGS

Albert D. Anderson

TABLE OF CONTENTS

PART III

THE AURORAL ELECTROJETS	III-1
WINTER CIRCUMPOLAR VORTEX	III-2
PLANETARY WAVES AND THE CRITICAL LEVEL	III-2
AN HYPOTHESIS FOR THERMOSPHERIC-STRATOSPHERIC INTERACTION (WARMINGS)	III-3
IMPLICATIONS FOR OTHER ATMOSPHERIC PHENOMENA	III-7
REFERENCES TO PART III	III-8
FIGURES	III-11

AN HYPOTHESIS FOR THE RELATION BETWEEN AURORAL ELECTROJETS AND STRATOSPHERIC WARMINGS

Albert D. Anderson

The following explanation is presented to show how warming events at 10 mb may be related to magnetic activity, especially AE, with a time delay of about two days. First, the properties of auroral electrojets, the winter circumpolar vortex and planetary waves will be discussed.

The Auroral Electrojets (AEJ)

Thermospheric heating is definitely correlated with magnetic activity as indicated by A_p and Dst (Anderson, 1973). Cole (1971) indicates that the heating mechanism is joule dissipation associated with auroral electrojets (AEJ) that results in a global input of heat into the lower thermosphere during strong geomagnetic disturbances that is larger than that due to solar extreme ultraviolet radiation. The marked correlation exhibited between the magnetic indices, especially the AE index, and stratospheric warmings suggests that AEJ heating strongly influences the lower atmosphere also, with a time delay of about 2 days.

AEJ are intense electric currents, associated with polar magnetic disturbances, that flow in the auroral oval in the lower thermosphere (Akasofu et al., 1965). The westward AEJ grows to approximately 10^6 amperes during a magnetic substorm due to an increase in the conductivity of the E-layer of the ionosphere in the midnight to dawn sector of the auroral oval. The eastward flowing AEJ has a strength of about 10^3 amperes in the late evening sector. Cole (1962) has estimated that $5 \text{ ergs cm}^{-2} \text{ s}^{-1}$ could be deposited in the auroral zone by means of joule heating associated with the AEJ at moderately disturbed times and an order of magnitude more during

large geomagnetic storms. The height of maximum joule heating lies between 100-150 km (Blumen and Hendl, 1969). Cole (1971a) indicates that major AEJ heating of the thermosphere during strong geomagnetic disturbances could perturb the atmosphere down to 100 km.

Winter Circumpolar Vortex

It is well known that the winter circulation in the troposphere is dominated by a cold low centered near the pole that becomes more pronounced at higher altitudes and is surrounded by a band of strong westerly winds (Labitzke, 1972). Evidently, this vortex extends up through the stratosphere and mesosphere to the base of the thermosphere near 100 km. The normal westerly zonal flow in the meteor region (75-105 km) is consistent with a large-scale cyclonic system centered near the pole (Hook, 1972). However, during warmings there is evidence indicating substantial circulation and temperature changes in the mesosphere (Quiroz, 1969; Hook, 1970). During the midwinter stratospheric warmings for 1967-68 and 1970-71, both the meridional and zonal winds at College, Alaska at 75-100 km reversed (Hook, 1972). The reversal of the zonal flow during the warmings is consistent with an anticyclonic system. During the warming of 1970-71, the prevailing flow reversed from about 31 December 1970 to 7 January 1971. Hook (1972) concludes that the warming in the upper mesosphere started approximately 10 days before the warming at the 10 mb level. From this, he states that the circulation breakdown during this warming affected the upper mesosphere before it affected the mid-stratospheric level.

Planetary Waves and the Critical Level (CL)

Planetary-scale disturbances can propagate upward from the troposphere into the higher atmosphere if the prevailing winds are moderate westerlies (Charney and Drazin, 1961). Planetary waves occur in the stratosphere (Finger *et al.*, 1966), reaching as high as the thermosphere (Newell and Dickinson, 1967). The waves cannot propagate upward in easterly winds so that when the waves reach a critical level (CL), the level at which the

zonal velocity is zero, the wave amplitude decreases rapidly and the wave energy flow vanishes (Dickinson, 1968). If the level is horizontal, meridional heat transfer by the waves is constant in the westerly layer and jumps to zero at the CL. Hence, the temperature disturbance amplitude is very large near the CL. The easterly winds near the CL are accelerated by the waves, thereby lowering the level (Matsuno, 1971). Thus, the warming and wind reversal shift downward. The easterly layer spreads downward first very rapidly, then slowly, because the air density increases as the layer lowers. The warmest layer moves down with the descent of the CL. Since the waves transport heat from lower to higher latitudes, the temperatures at the high latitudes is always higher than at the lower latitudes, except initially. Intense warming of the polar region is expected to occur just below the CL, while the temperature may fall in the low-latitude region.

An Hypothesis for Thermospheric-Stratospheric Interaction (Warmings)

Taking into account the information concerning the AEJ, Cold Low, Planetary Waves and CL, an attempt will now be made to outline the dynamics of a stratospheric warming:

Strong AEJ heating occurring in the auroral zone near 100 km is conducted down into the mesosphere, destroying the cold low from above and replacing it with a warm anticyclone. This results in the formation of the CL in the upper mesosphere. Johnson and Gottlieb (1970) have shown the important role played by the eddy transfer of heat in the 60-120 km region; at higher altitudes heat transfer between levels is dominated by molecular conduction, and at lower levels by radiation exchange. Downward motion in the upper mesosphere will be accompanied by compressional heating, thus enhancing the AEJ heating. Normally, a strong planetary wave propagated upward from the troposphere would be dissipated in the thermosphere. However, once the CL is formed, the wave interacts with the easterly winds at the CL in the upper mesosphere, heats the air there, enhances the CL and lowers it. Once this process is started, the lowering of the CL will continue, as long as the strong wave exists. If the wave is strong enough and persists long

enough, the CL will lower down into the stratosphere, even though the AEJ is no longer heating the upper mesosphere and cooling is taking place there (Labitzke, 1972). When the critical level descends to near 45 km, "explosive" warming starts, probably because the wave energy density attains a maximum in the middle and low stratosphere (Matsuno, 1970). The length of time it takes for a strong CL to descend from the upper atmosphere into the stratosphere is unknown. It could take anywhere from a day to a week or more.

Apparently, AEJ heating is not continuous during warmings. Evidently, there is no significant difference between the average AE index for warming days and nonwarming days. The AE index varies greatly from hour to hour. Therefore, in order for the CL to form, the strongly fluctuating AEJ heating must proceed in such a fashion as to progressively destroy from above the cold low in the upper mesosphere. Once the CL is established, the interplay among the amount and duration of AEJ heating and amplitude of waves from the troposphere determines its initial strength and altitude, and this in turn determines the starting altitude and initial extent of the warming.

Although the existence of a strong CL descending in the mesosphere can explain some features of the warmings occurring there, a strong CL cannot explain most of the characteristics of the warmings in the stratosphere. For example, the warming in 1969-1970 started about December 17, 1969 and ended about January 5, 1970. Hence, it affected the 10 mb altitude for several weeks, a time interval typical of major warmings. Yet the start of warmings and many of the major and minor peaks appear at 10 mb many days before the "explosive" warming in the stratosphere. Apparently, pulsations of warming in the stratosphere precede a major warming event (Hook, 1972).

During the December 1969 - January 1970 and December 1970 - January 1971 Northern-Hemisphere warmings many small eastward-moving warm (closed isotherm) centers appeared before the major warmings at midlatitudes (30°N to 50°N) on the periphery of the low circulation. Evidently, the warming builds up in the stratosphere, at least in part, by successive heat pulses. Although heat pulses are usually observed before a major warming, they do not appear to constitute a necessary condition for the development of a major warming (Quiroz, 1973). The generation of these pulses appear to start at high mesospheric levels in early winter (Theon and Smith, 1970). It has already been noted that the major fluctuations in the AE index indicates that the AEJ heating is not a continuous process. Also, the fact that there is roughly the same time delay (about two days) between the maximum AE index and start of warmings, and major and minor peaks at 10 mb indicates that the AEJ heating near 100 km could be responsible for the warming phenomena at 10 mb.

The following tentative explanation is offered for the pulsations of warming at 10 mb: It is assumed that (a) a weak CL exists in the upper mesosphere only when AEJ heating is above a certain intensity, and (b) waves are reflected (Hines, 1972) by the weak CL down into the stratosphere where they interact with upward propagating waves to release heat in the region where the wave energy density attains a maximum. A weak CL implies the absence of very strong waves, although weak waves may be present. Since the AEJ heating is fluctuating, the weak CL probably would have a sporadic existence in the upper mesosphere. Thus, even though the waves are persistent, the reflection of waves from the upper mesosphere fluctuates directly with AEJ heating. The reflected waves take roughly two days to descend to 10 mb.

Some of the heating characteristics that appear at 10 mb may depend also on the horizontal shape of the CL. Initially, the CL should form in the auroral zone. However, the shape of the CL probably is not symmetric with the auroral zone. The initial CL shape will depend on the interaction between the newly-developing anticyclonic circulation resulting from CL

heating with the strong westerly winds around the cold polar low. Some of the heat created at the CL probably will not remain there; a portion may be transported vertically and some may be ducted horizontally (Friedman, 1966; Cowling et al., 1971).

The horizontal extent of the CL in the upper mesosphere cannot be determined at present because of lack of data. Perhaps, some idea of its distribution in the stratosphere can be obtained by examining available Northern Hemisphere stratospheric isotherm patterns on a date when a major warming appeared there. Figure 1 displays a disturbed temperature map for the Northern Hemisphere at 50 km, January 6, 1971, a major warming date. The level of maximum warming was between 40 and 50 km on this date. Cooling took place above the warming area (Labitzke, 1972). Hence, Figure 1 may represent heating near the altitude of the CL. The heating pattern in Figure 1 appears quite similar to the theoretical disturbed geopotential height distribution at 45 km computed by Matsuno (1970) for the January 1967 warming. Yet there is one marked difference. In Figure 1 the zone of maximum warming closely parallels the auroral zone for over half of its perimeter on the east. This is not true for the disturbed geopotential height distribution. During a geomagnetic storm, the auroral zone would expand to approach even more closely to the zone of maximum heating in Figure 1.

The close association of the zone of maximum heating with the auroral zone in Figure 1 indicates that at least part of the original heating pattern established at the CL in the upper mesosphere has persisted down to 50 km. Willett (1968) has pointed out the existence of a circumpolar zone of maximum warmth in the arctic winter stratosphere, centered on the geomagnetic pole. All of the observed stratospheric warmings from 1951 to 1966 developed in the equatorward dip of the auroral zone. In Figure 1, the heating extends to midlatitudes at longitudes near the equatorward dip of the auroral zone; at 45°N the zone of maximum heating is at the same longitude (290°E) as the dip. It was

pointed out that many small warming centers appear initially at 10 mb at midlatitudes (30°N to 50°N) and move east on the periphery of the low circulation. Also, it is observed that many of the centers initially appear at longitudes east of the auroral trough (290°E) in the 300°E to 360°E sector. Although the zone of maximum warming in Figure 1 extends from high to mid-latitudes, the heat at midlatitude may be noticeable because it appears as local temperature maxima at 10 mb. No small, closed warm isotherm patterns develop at higher latitudes because the heat is mixed with the cold ascending currents of the low. This explanation is based on the assumption that the heat pattern in Figure 1 is representative of a weak CL pattern in the upper mesosphere. Consequently, the heat at mid-latitudes results from the interaction of the reflected wave with the upward wave in the mid-stratosphere.

Implications for Other Atmospheric Phenomena

The magnetic indices are correlated somewhat with each other. A_p contains contributions from at least two major sources; the auroral electrojet (AE) and the ring current (Dst). Therefore, AEJ heating may be the key to explaining other puzzling correlations between magnetic activity and lower atmosphere behavior. Studies (Levine et al., 1974) have indicated that meteorological responses in the lower atmosphere occur within 2 or 3 days after geomagnetic activity and that these responses are most pronounced in winter. If AEJ heating affects the circulation in the mesosphere and stratosphere, undoubtedly it will influence conditions in the troposphere too. In other words, during a major warming, the whole circulation in the winter atmosphere, extending from the troposphere to the thermosphere, probably is affected. If AEJ activity affects the lower atmosphere, then, inasmuch as AEJ heating is controlled by solar (plasma) activity, it follows that variations in solar activity affect the weather. Consequently, a new link between solar activity and the lower atmosphere may have been uncovered.

References

- Akasofu, S., S. Chapman, and C. Meng, The polar electrojet, J. Atmos. Terr. Phys., 27, 1275-1305, 1965.
- Anderson, A. D., The correlation between low-latitude neutral density variations near 400 km and magnetic activity indices, Planet. Space Sci., 21, 2049-2060, 1973.
- Blumen, W. and R. G. Hendl, On the role of joule heating as a source of gravity-wave energy above 100 km. J. Atmos. Sci., 26, 210-217, 1969.
- Charney, J. G. and P. G. Drazin, Propagation of planetary-scale disturbances from the lower into the upper atmosphere, J. Geophys. Res., 66, 83-110, 1961.
- Cole, K. D., Joule heating of the upper atmosphere, Australian J. Phys., 15, 223-235, 1962.
- Cole, K. D., Electrodynamic heating and movement of the thermosphere, Planet. Space Sci., 19, 59-75, 1971.
- Cole, K. D., Thermospheric winds induced by auroral electrojet heating, Planet. Space Sci., 19, 1010-1012, 1971a.
- Cowling, D., H. Webb, and K. Yeh, Group rays of internal gravity waves in a wind-stratified atmosphere, J. Geophys. Res., 76, 213-220, 1971.
- Dickinson, R. E., Planetary Rossby waves propagating vertically through weak westerly wind wave guides, J. Atmos. Sci., 25, 984-1002, 1968.
- Finger, F., H. Woolf, and C. Anderson, Synoptic analyses of the 5, 2, and 0.4 millibar surfaces for the IQSY period, Mon. Weather Rev. 94, 651-661, 1966.

- Friedman, J. P., Propagation of internal gravity waves in a thermally stratified atmosphere, J. Geophys. Res., 71, 1033-1054, 1966.
- Hines, C. O., Motions in the ionospheric D and E regions, Phil. Trans. R. Soc. Lond. A, 457-471, 1972.
- Hook, J. L., Winds at the 75-110 km level at College, Alaska, Planet. Space Sci., 18, 1623-1638, 1970.
- Hook, J. L., Wind patterns at meteor altitudes (75-105 km) above College, Alaska, associated with midwinter stratospheric warmings, J. Geophys. Res., 77, 3856-3868, 1972.
- Johnson, F. S., and B. Gottlieb, Eddy mixing and circulation at ionospheric levels, Planet. Space Sci., 18, 1707-1718, 1970.
- Labitzke, K., Temperature changes in the mesosphere and stratosphere connected with circulation changes in winter, J. Atmos. Sci., 29, 756-766, 1972.
- Levine, J. S. et al, Possible relationships between solar activity and meteorological phenomena, Trans. A. G. U., 55, 524-527, 1974.
- Matsuno, T., Vertical propagation of stationary planetary waves in the winter Northern Hemisphere, J. Atmos. Sci., 27, 871-883, 1970.
- Matsuno, T., A dynamical model of the stratospheric sudden warming, J. Atmos. Sci., 28, 1479-1494, 1971.
- Newell, R., and R. Dickinson, On the applications of a proposed global system for measuring meteor winds, Pure Appl. Geophys., 68, 162-172, 1967.
- Quiroz, R. S., The warming of the upper stratosphere in February 1966 and the associated structure of the mesosphere, Mon. Weather Rev., 97, 541-552, 1969.
- Quiroz, R. S., The abnormal stratosphere studied with the aid of satellite radiation measurements, Amer. Inst. Aero. and Astro. Paper No. 73-493, 1973.

Theon, J. S., and W. S. Smith, Seasonal transitions in the thermal structure of the mesosphere at high latitudes, J. Atmos. Sci., 27, 173-176, 1970.

Willett, H. C. Remarks on the seasonal changes of temperature and ozone in the Arctic and Antarctic stratosphere, J. Atmos. Sci., 25, 341-360, 1968.

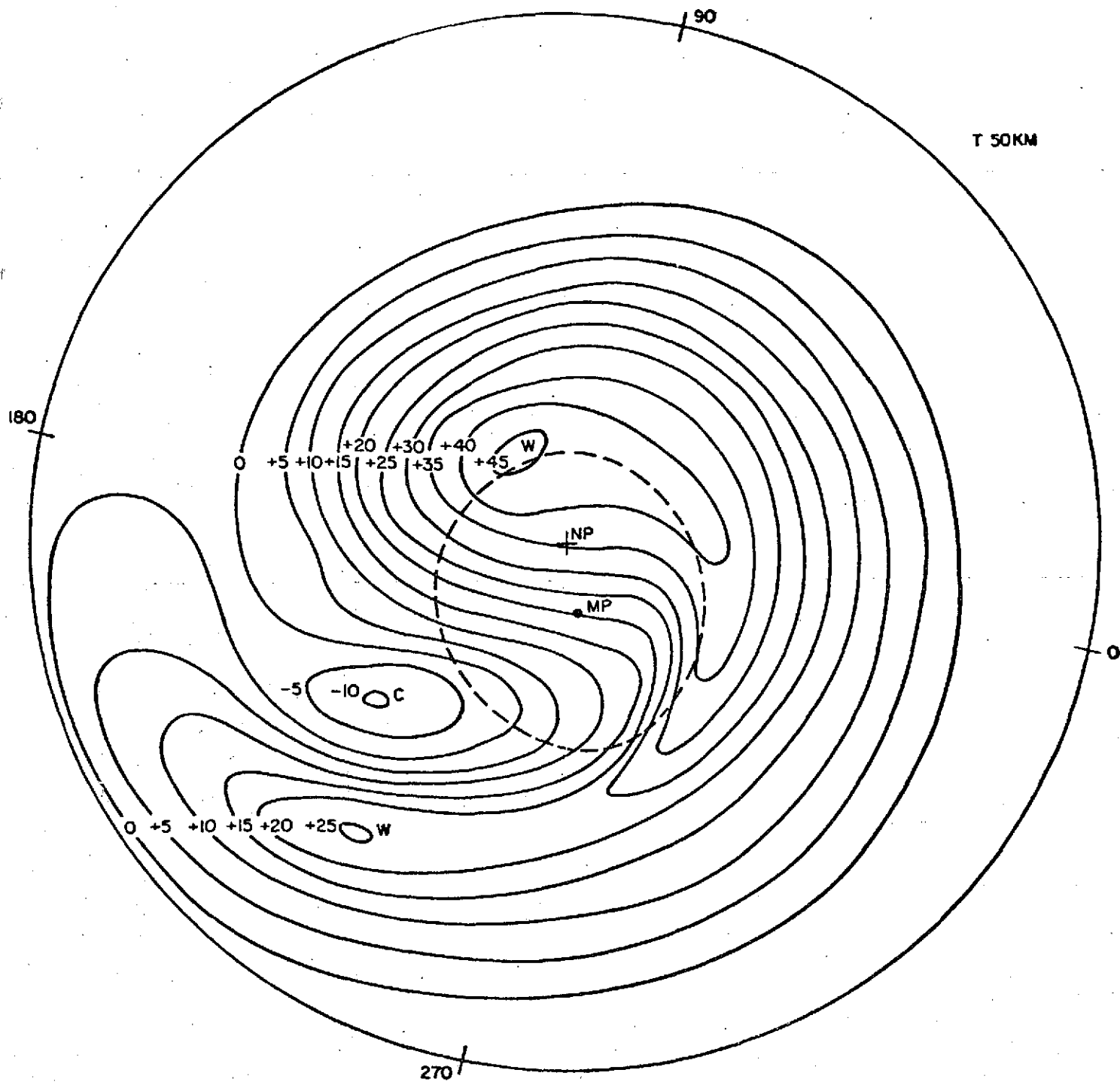


Fig. 1

Disturbed temperature map, 50 km,
January 6, 1971. Dashed oval curve
is auroral zone. Large cross is at
North Pole (NP). Black dot is geo-
magnetic pole (MP).